

DASA 1917-5
3-27-67-1 Vol. 5
November 1967

THERMAL RADIATION PHENOMENA

Radiation Hydrodynamics
of High Temperature Air

Edited by

R. K. M. Landshoff

Work performed under contract

DA-49-146-XZ-198

DASA Subtask RLN5015

ABSTRACT

This report introduces the reader to radiation hydrodynamics (RH) and discusses its application to fireballs in the atmosphere. After formulating the basic equations of RH, special attention is given to the radiative transfer problem. Several methods for solving the equations of transfer are touched upon but special emphasis is placed on the two stream method with a frequency averaging procedure, which is specifically designed for use with finite zone sizes. A version of the FIREBALL code which utilizes this approach is described. The physics of fireballs is illustrated with the example of a one kiloton detonation at sea level density and without interference from the ground. Some remarks are made on scaling procedures for extending the results to higher yields and altitudes. Estimates are made of the validity of the models.

FOREWORD

"Thermal radiation" is electromagnetic radiation emitted by matter in a state of thermal excitation. The energy density of such radiation in an enclosure at constant temperature is given by the well known Planck formula. The importance of thermal radiation in physical problems increases as the temperature is raised. At moderate temperatures (say, thousands of degrees Kelvin) its role is primarily one of transmitting energy; whereas at high temperatures (say, millions of degrees Kelvin) the energy density of the radiation field itself becomes important as well. If thermal radiation must be considered explicitly in a problem, the radiative properties of the matter must be known. In the simplest order of approximation, it can be assumed that the matter is in thermodynamic equilibrium "locally" (a condition called local thermodynamic equilibrium, or LTE), and all of the necessary radiative properties can be defined, at least in principle. Of course whenever thermal radiation must be considered, the medium which contains it inevitably has pressure and density gradients and the treatment requires the use of hydrodynamics. Hydrodynamics with explicit consideration of thermal radiation is called "radiation hydrodynamics".

In the past twenty years or so, many radiation hydrodynamic problems involving air have been studied. In this work a great deal of effort has gone into calculations of the equilibrium properties of air. Both thermodynamic and radiative properties have been calculated. It has been generally believed that the basic theory is well enough understood that such calculations yield valid results, and the limited experimental checks which are possible seem to support this hypothesis. The advantage of having sets of tables which are entirely calculated is evident: the calculated quantities are self-consistent on the basis of some set of assumptions, and they can later be improved if calculational techniques are improved, or if better assumptions can be made.

The origin of this set of books was in the desire of a number of persons interested in the radiation hydrodynamics of air to have a good source of reliable information on basic air properties. A series of books dealing with both theoretical and practical aspects was envisaged. As the series materialized, it was thought appropriate to devote the first three volumes to the equilibrium properties of air. They are:

The Equilibrium Thermodynamic Properties of Air,
by F. R. Gilmore

The Radiative Properties of Heated Air,
by B. H. Armstrong and R. W. Nicholls

Tables of Radiative Properties of Air,
by Lockheed Staff

The first volume contains a set of tables along with a detailed discussion of the basic models and techniques used for their computation. Because of the size of the related radiative tables and text, two volumes were considered necessary. The first contains the text, and the second the tables. It is hoped that these volumes will be widely useful, but because of the emphasis on very high temperatures it is clear that they will be most attractive to those concerned with nuclear weapons phenomenology, reentry vehicles, etc.

Our understanding of kinetic phenomena, long known to be important and at present in a state of rapid growth, is not as easy to assess as are equilibrium properties. Severe limitations had to be placed on choice of material. The fourth volume is devoted to general aspects of this topic. It is:

Excitation and Non Equilibrium Phenomena in Air,
by Landshoff, et al.

It provides material on the more important processes involved in the excitation of air, criteria for the validity of LTE and special radiative effects.

A discussion of radiation hydrodynamics was felt to be necessary and the fifth volume which deals with this topic is:

Radiation Hydrodynamics of High Temperature Air,
by Landshoff, Hillendahl, et al.

It reviews the basic theory of radiation hydrodynamics and discusses the application to fireballs in the atmosphere.

The choice of material for these last two volumes was made with an eye to the needs of the principal users of the other three volumes.

Most of the work on which these volumes are based was supported by the United States Government through various agencies of the Defense Department and the Atomic Energy Commission. The actual preparation of the volumes was largely supported by the Defense Atomic Support Agency.

We are indebted to many authors and organizations for assistance and we gratefully acknowledge their cooperation. We are particularly grateful to the RAND Corporation for permission to use works of F. R. Gilmore and H. L. Brode and to the IBM Corporation for permission to use some of the work of B. H. Armstrong. Most of the other authors are employed by the Lockheed Missiles and Space Company, in some cases as consultants.

Finally, we would like to acknowledge the key role of Dr. R. E. Meyerott of LMSC in all of this effort, from the initial conception to its realization. We are particularly grateful to him for his constant advice and encouragement.

Criticism and constructive suggestions are invited from all readers of these books. We understand that much remains to be done in this field, and we hope that the efforts represented by this work will be a stimulus to its development.

The Editors

J. L. Magee

H. Aroeste

R. K. M. Landshoff

Preface

This volume reviews the basic theory of radiation hydrodynamics and discusses the application to fireballs in the atmosphere. The first chapter starts with a formulation of the basic equations and goes on to discuss schemes for translating these impossibly difficult equations into manageable computing procedures. As a companion to this chapter we have added Appendix A with a version of Hillendahl's FIREBALL code, which runs without inputs of a classified nature.

Chapter 2 deals with the physics of fireballs. The main discussion is devoted to the description of a one kiloton detonation at sea level. That section has nearly all been written by H. L. Brode of the RAND Corporation but a few passages have been added by the editor. One of these deals with opaque precursors to shocks whose significance to the thermal output was noted by Hillendahl since the original version was written. The section on other yield and altitudes was also written by the editor.

The summary chapter examines the reliability of the results and how this is affected by approximations, incomplete basic information and other deficiencies in the present state of the art.

I would like to thank Dr. H. L. Brode for his contribution and the RAND Corporation for permission to include his work in this volume.

R. K. M. Landshoff

Contents

Chapter 1.	Radiation Hydrodynamics (R. W. Hillendahl, R. K. M. Landshoff)	1
1.1	Introduction	1
1.2	Basic equations of radiation hydrodynamics	3
1.3	Average absorption coefficients	8
1.4	Solution of the equation of transfer	10
1.5	Finite difference equations	15
Chapter 2.	The Physics of Fireballs (H. L. Brode, R. K. M. Landshoff)	36
2.1	Introduction	36
2.2	One kiloton at sea level	37
2.3	Other yields and altitudes	58
Chapter 3.	Summary (R. K. M. Landshoff)	74
3.1	Equation of state	74
3.2	Absorption coefficients	75
3.3	Radiation hydrodynamics codes	78
3.4	Deviations from LTE	80
Appendix A.	A Radiation-Hydrodynamics Code (R. W. Hillendahl)	83
A.1	Introduction	83
A.2	Reading FORTRAN	96
A.3	The computational scheme	101
A.4	Data printout routines	109

A.5	Variation of the number of zones in use	114
A.6	Hydrodynamics routine	117
A.7	Equation of state routine	120
A.8	Radiative properties routine	121
A.9	Radiative flux routine	126
A.10	Code listing	128

Chapter 1. RADIATION HYDRODYNAMICS

1.1 Introduction

A nuclear detonation deposits a large amount of heat energy in the air around it. The heating phase is of relatively short duration since the energy arrives in the form of X-rays which come either directly from the surface of the exploding bomb or from the shock heated air in the immediate vicinity of that surface.

Following the X-ray deposition the air approaches local thermodynamic equilibrium (LTE). The method of calculating the subsequent explosion history which is discussed in this chapter ignores this period where the air relaxes to LTE. Before we proceed we take a short look at the validity of that assumption.

The kinetics of relaxation processes has been discussed in Chapter 6, (4)^{*}. The relaxation time depends on the ambient air density and on the final temperature as shown in Fig. 6.1 (4).

For a detonation at sea level practically all the energy deposited by X-rays gets stuck in a relatively small volume and raises the temperature to very high values. Under these conditions relaxation times are very short. For a detonation at a high altitude a sizeable fraction of the X-ray energy is deposited at large distances and produces a lesser temperature rise because of the inverse square drop of the flux density. The lower air density and the lower temperature both contribute to increase the relaxation time.

* DASA-1917-4, from now on referred to as (4).

As an example, let us consider a detonation with an X-ray yield of 10^{20} ergs radiating like a blackbody with a temperature of 10^7 °K occurring at an altitude somewhat below 50 km where the air density is 10^{-3} times less than at sea level. A crude estimate, using the asymptotic theory of Section 4.4, (4) shows that about 10% of the X-ray energy is deposited at distances more than about 80 m where it produces temperatures less than $12,000$ °K. In Fig. 6.1 (4) one reads off that the relaxation time at that temperature and a density $\frac{\rho}{\rho_0} = 10^{-3}$ is 10^{-6} sec. Within that sphere it takes less time and on the outside more time to relax the air to its equilibrium temperature. Thus 10% of the energy relaxes at a relatively slow rate and the assumption that one can ignore the relaxation period is not entirely justified in that case.

The assumption of LTE is essential to the classical formulation of hydrodynamics. It means that the temperature is a well defined property of the fluid and that pressure and internal energy are known functions of density and temperature. Without LTE it would be much more difficult to formulate the conservation theorems for momentum and energy.

In the theory of radiative transfer (Chapter 2, (2)*) , which together with hydrodynamics accounts for the expansion of fireballs, LTE also is an assumption of major importance. Without it a quantitative prediction of the interaction between matter and radiation would be a hopelessly complicated problem.

Despite the very important role played by radiative transport radiation does not as a rule account for a significant fraction of the energy density and the pressure within a fireball. Even for blackbody radiation,

* DASA 1917-2, from now on referred to as (2).

which is not present unless the gas is opaque, this contribution is small unless the temperature exceeds values like 25 eV. Temperatures of that magnitude are only maintained during the very early stages of fireball histories. In this period the fireball cools down by radiative expansion and this goes so fast that there is essentially no hydrodynamical motion. In formulating the hydrodynamic equations one can therefore ignore the energy density and pressure of radiation because by the time they get into the act they are indeed negligible.

During the early period of fireball expansion (where radiative transfer of energy is important) the shape generally appears to be almost spherical, at least at low altitudes where the size is small compared to the scale height of the atmosphere. Asymmetries which are hidden by the opaque outer layers may possibly occur due to instabilities at the bomb air interface, but we shall ignore these. Not much is known about such phenomena in any case and adding the complication of asymmetry would compromise the already complicated problem of treating radiation flow. In line with the current state-of-the-art we shall therefore discuss only spherically symmetrical problems.

1.2 Basic equations of radiation hydrodynamics

The differential equations for calculating fireball histories are the conservation relations of ordinary hydrodynamics but with a rather complicated heating term in the energy equation. They can be written in either Eulerian or Lagrangian form. The two forms are characterized by a different choice of independent space variables. In the Eulerian system these are the coordinates in real space and in the

Lagrangian one they are coordinates which are tied to the particles of the fluid. In the Lagrangian system the coordinates in real space which describe the position of a specified particle are used as dependent variables. In the Eulerian system this is manifestly impossible and the motion is described in terms of the fluid velocity.

The other dependent variables which characterize the thermodynamic state of the fluid are the same in the two systems and can be chosen from a set which includes the density ρ or its reciprocal the specific volume V , the pressure p , the temperature T , the internal energy E , etc. It may be convenient to keep several of these variables in the equations but one must keep in mind that they are interrelated and that the thermodynamic state is specified by any two of them.

The Lagrangian method is especially useful in problems with a high degree of symmetry where one needs only one coordinate to specify the position. Having restricted ourselves to spherically symmetrical problems we shall therefore adopt the Lagrangian approach.

We define the Lagrangian radius r of a given particle as its radius at time zero, i.e. before it has started to move. The actual radius of the particle at any time is denoted by the capital letter R . The hydrodynamic problem is to find $R(r, t)$.

If ρ_0 stands for the initial density the specific volume at any instant is

$$V = \frac{1}{\rho_0} \left(\frac{R}{r} \right)^2 \frac{\partial R}{\partial r} \quad (\text{conservation of mass}) \quad (1.2-1)$$

Introducing the velocity

$$u = \frac{\partial R}{\partial t} \quad (1.2-2)$$

the other conservation equations are

$$\frac{\partial u}{\partial t} = - \frac{1}{\rho_0} \left(\frac{R}{r} \right)^2 \frac{\partial p}{\partial r} \quad (\text{conservation of momentum}) \quad (1.2-3)$$

$$\frac{\partial E}{\partial t} + p \frac{\partial V}{\partial t} = V \dot{Q} \quad (\text{conservation of energy}) \quad (1.2-4)$$

where the rate of heating per unit volume \dot{Q} still needs to be worked out.

As it stands the energy equation has a serious defect because it does not allow for the entropy raise produced by a shock. To get around this we adopt the method of Von Neumann and Richtmyer (1950) and add a pseudo-viscous pressure

$$q = \begin{cases} (\ell^2/V) (\partial u / \partial r) & \text{if } \frac{\partial u}{\partial r} < 0 \\ 0 & \text{if } \frac{\partial u}{\partial r} > 0 \end{cases} \quad (1.2-5)$$

to the regular pressure in Eqs. (1.2-3) and (1.2-4). The constant ℓ has the dimensions of a length; it will be further specified when we go to finite difference equations.

The radiative heating rate \dot{Q} at some point is the difference between absorbed and emitted power per unit volume

$$\dot{Q} = \iint \mu'_v (I_v - B_v) dv d\Omega \quad (1.2-6)$$

The emitted power presents no problem because the blackbody intensity B_ν is a known function of temperature. There is no angular dependence and the integral over frequency can be expressed in terms of the Planck mean, Eq. (2.4-15), (2). One obtains:

$$\dot{Q}_{em} = 4\bar{\mu}_p \sigma T^4 \quad (1.2-7)$$

where σ is the Stefan Boltzmann constant.

The absorbed power is much more difficult to evaluate because the calculation of the intensity I_ν is a major task. To carry this out one should in principle solve the equation of transfer (Eq. (1.3-1)) along every ray passing through the point in question and for all values of the frequency. One of the major difficulties of such a program arises from the fact that the optical properties of air in a large part of the relevant temperature range result mainly from transitions between molecular levels. The spectrum associated with the major band systems consists of an enormous number of lines and the absorption coefficient fluctuates from large values at the line centers to small ones between the lines. Because of these "windows" the radiation at some point generally comes from points along the ray which are an appreciable distance further back. This distance varies just as strongly with frequency as μ_ν' itself and it is therefore not proper to use local averages of μ_ν' in a frequency interval containing, say, a few lines. Instead, it is in principle necessary to integrate the transport equation at a large enough number of frequencies within every one of these intervals. This correct approach clearly demands an impossible amount of computational

effort which has to be avoided. There are two limiting situations where this can be readily done. The one situation arises for a transparent medium where the optical depth $\mu_\nu L$ (L being the size of the radiating region) is uniformly small compared to unity. In that case I_ν is very much smaller than B_ν and one can neglect the absorption altogether. In that case we have $\dot{Q} = -\dot{Q}_{em}$ which we know from Eq. (1.2-7).

In the opposite extreme of an opaque region for which $\mu_\nu L \gg 1$ one can simplify Eq. (1.2-6) directly. The heating rate can in that case be expressed in the form*

$$\dot{Q} = -\vec{\nabla} \cdot \vec{F} \quad (1.2-8)$$

The flux vector is given by Eq. (2.5-8), (2) which we rewrite in the form

$$\vec{F} = -\frac{4}{3} \lambda_R \sigma \vec{\nabla} T^4 \quad (1.2-9)$$

Tables and graphs of the Rosseland mean free path λ_R or the related opacity can be found in (3)** , p. 12, pp. 446 to 449 and pp. 622 to 625.

The above method of treating radiative transfer was originally developed by Eddington nearly half a century ago. In its application it was however, limited to astrophysical problems where it was not coupled to hydrodynamics. An early discussion of the use of this so-called diffusion approximation to radiation hydrodynamics has been given by Magee and Hirschfelder (1953). The first calculations carried out with this method to appear in the open literature were presented by Marshak (1958).

* The operator $\vec{\nabla}$ is defined in Eulerian space. In plane or spherical geometry it is well known how to express it in Lagrangian form.

** DASA 1917-3.

1.3 Average absorption coefficients

In the temperature range where molecular transitions occur and where optical depths are neither uniformly small nor uniformly large one has to resort to approximation schemes. It is clearly necessary to apply some kind of frequency averaging which will do a fair amount of violence to the "correct approach" of solving the transfer equation for a few million values of the frequency. The basic mathematical problem is that one wants to average the product $\mu_{\nu}' I_{\nu}$ which enters in Eq. (1.2-6) as well as in the transport equation*

$$\frac{dI_{\nu}}{ds} = \mu_{\nu}' (B_{\nu} - I_{\nu}) \quad (1.3-1)$$

by equating the average of the product and the product of the averages, i.e. one wants to replace $\overline{\mu_{\nu}' I_{\nu}}$ by $\overline{\mu_{\nu}'} \overline{I_{\nu}}$ and that is of course not correct. The quality of this approximation depends on the amount of fluctuation among the values of μ_{ν}' and I_{ν} that are being averaged and in a line spectrum this fluctuation may be quite severe. A number of averaging schemes have been proposed and are used in various computing programs.

One scheme divides the spectrum into groups (10 to 100) whose widths are chosen fairly narrow at the low energy end and wider as the energy goes up. Within each interval a Rosseland type average is obtained. Such group averages have been used, for example, in the SPUTTER program of AWFL as reported in RTD-TDR-63-3128 Vol. II and in a code developed by J. Zinn of LASL.

* Strictly speaking, the left hand side of this equation should contain the additional term $\frac{1}{c} \frac{\partial I_{\nu}}{\partial t}$ but because of the large value of the light velocity this time dependence is usually left out. We note further that light rays are straight lines in Eulerian space and in this section we temporarily abandon the Lagrangian system.

A second method of averaging uses the average transmission function (Eq. (2.6-12b), (2))

$$\overline{\text{Tr}(\mu'_\nu s)} = \frac{1}{\Delta\nu_1} \int_{\Delta\nu_1} e^{-\mu'_\nu s} d\nu \quad (1.3-2)$$

and the slab absorption coefficient related to it by Eq. (2.6-19), (2)

$$\overline{\mu_\nu(s)} = -\frac{1}{s} \ln \overline{\text{Tr}(\mu'_\nu s)} \quad (1.3-3)$$

These averages are defined for slabs of thickness s in which the temperature and density of the air are uniform. The intervals $\Delta\nu_1$ are much narrower than the groups of the first mentioned method. The spacing between intervals is 10 to 20 times as large as the interval size. The calculated averages depend smoothly on the frequency so that it seems reasonable to interpolate. The slab average is made to order for use in finite difference equations where the fluid is divided into zones. It has been used in a number of LMSC codes which will be discussed later in this chapter.

A variation of the group average procedure consists of subdividing the frequencies within a group into subgroups which are ordered according to the magnitude of the absorption coefficient rather than by frequency. The spread between the absorption coefficients within each subgroup is obviously less than between those in the entire group and subgroup averages

will therefore be more meaningful. To use subgroup averages we must also introduce individual intensities for each subgroup. Even the use of only two subgroups would improve the accuracy considerably. A short-cut for the calculation of two subgroup absorption coefficients consists of fitting the average transmission function in the form (Eq. (2.6-46), (2)).

$$\overline{\text{Tr}(\mu_{\nu}'s)} = \frac{1}{2} (e^{-\mu_1' s} + e^{-\mu_2' s}) \quad (1.3-4)$$

Tables of μ_1' and μ_2' are given by Churchill et al. (1963). We don't know of any code which has utilized this type of average.

1.4 Solution of the equation of transfer

Having obtained an average absorption coefficient which permits us to replace the average product $\overline{\mu_{\nu} I_{\nu}}$ by the product of averages $\overline{\mu_{\nu}} \overline{I_{\nu}}$ the transfer equation becomes*

$$\frac{d\overline{I_{\nu}}}{ds} = \overline{\mu_{\nu}} (\overline{B_{\nu}} - \overline{I_{\nu}}) \quad (1.4-1)$$

The formal integration of this equation along a ray is straightforward and leads to

$$\overline{I_{\nu}}(s) = e^{-\tau_{\nu}} \overline{I_{\nu}}(s_0) + \int_0^{\tau_{\nu}} \overline{B_{\nu}}(s') e^{(\tau_{\nu}' - \tau_{\nu})} d\tau_{\nu}' \quad (1.4-2)$$

* The absorption coefficient is still meant to include the correction factor for induced emission (Eq. (2.2-11a), (2) and the prime is left out for convenience of writing only.

$$\tau_{\nu} = \tau_{\nu}(s) = \int_{s_0}^s \bar{\mu}_{\nu}(s_1) ds_1 \quad ; \quad \tau_{\nu}' = \tau_{\nu}(s') \quad (1.4-3)$$

The difficulty arises because one has to determine the value of this integral for all the rays through a given point to evaluate the rate of absorption of radiative energy at that point. This is required for carrying out the angular integration in Eq. (1.2-6).

There are basically two approaches to this problem. One is the brute force approach to follow this program directly and to evaluate $I_{\nu}(s)$ along a large number of rays. This approach has been used in the SPUTTER program with one tangential ray through the center of each zone. Fig. 1-1 shows how these rays are combined to obtain the various values of \bar{I}_{ν} at the center of zone 4. Of the 7 rays which are drawn 3 are redundant because of symmetry and one obtains 3 different values of \bar{I}_{ν} going out, 3 going in and 1 grazing the zone.

In the other approach one defines certain moments, i.e. angular integrals of \bar{I}_{ν} which now depend only on the radius and not on the direction. To solve for these moments one integrates a system of coupled linear differential equations which are only approximately correct but which give exactly the right answer when one considers the limit where the diffusion approximation applies. Such schemes have been used widely in astrophysics and are discussed in great detail by Chandrasekhar (1960) and Mustel (1958). Some of the more sophisticated schemes use a large number of moments but quite good results can be obtained by restricting that number to two and using only the outgoing and ingoing flux which

are defined as the integrals

$$F_{\nu}(\pm) = \int_{\substack{\cos \theta > 0 \\ (\cos \theta < 0)}} \bar{I}_{\nu} \cos \theta \, d\Omega \quad (1.4-4)$$

where θ is the angle between the ray and the radial direction.

We consider first the case of plane geometry where the medium is stratified in plane parallel layers. This geometry has been studied extensively by astrophysicists and applied to the radiative equilibrium in the outer regions of stars where it is indeed unnecessary to worry about the curvature. By treating the radial coordinate R as if it were a cartesian coordinate the angle θ of a ray remains constant along the ray path. The optical path length between two surfaces is therefore simply the optical path length along the normal divided by $|\cos \theta|$. We shall express this in terms of the optical depth conventionally defined by astrophysicists as the optical path length measured radially inward from the surface of a star (or in our case a fireball), i.e. the integral

$$\tilde{\tau}_{\nu}(R) = \int_R^{R_s} \bar{\mu}_{\nu}(R') \, dR' \quad (1.4-5)$$

To evaluate $I_{\nu}(s)$ as given by Eq. (1.4-2) for an outgoing ray we place s_0 far enough inside that the factor $e^{-\tau_{\nu}}$ is essentially zero; for an ingoing ray we start at the surface where $\bar{I}_{\nu}(s_0) = 0$. The first term of

Eq. (1.4-2) can therefore be left out in both cases. For the exponent under the integral one can write

$$\tau_{\nu'} - \tau_{\nu} = - \left| \frac{\tilde{\tau}_{\nu'} - \tilde{\tau}_{\nu}}{\cos \theta} \right| \quad (1.4-6)$$

and for outgoing and ingoing rays one obtains

$$\bar{I}_{\nu} = \frac{1}{|\cos \theta|} \int_0^r \bar{B}_{\nu}(R') \bar{\mu}_{\nu}(R') e^{-\left| \frac{\tilde{\tau}_{\nu'} - \tilde{\tau}_{\nu}}{\cos \theta} \right|} dR' ; \cos \theta > 0 \quad (1.4-7a)$$

$$\bar{I}_{\nu} = \frac{1}{|\cos \theta|} \int_r^{r_s} \bar{B}_{\nu}(R') \bar{\mu}_{\nu}(R') e^{-\left| \frac{\tilde{\tau}_{\nu'} - \tilde{\tau}_{\nu}}{\cos \theta} \right|} dR' ; \cos \theta < 0 \quad (1.4-7b)$$

Entering these expressions into Eq. (1.4-4) one obtains the outgoing and the ingoing flux

$$F_{\nu+} = 2\pi \int_0^r \bar{B}_{\nu}(R') \bar{\mu}_{\nu}(R') E_2(|\tilde{\tau}_{\nu'} - \tilde{\tau}_{\nu}|) dR' \quad (1.4-8a)$$

$$F_{\nu-} = 2\pi \int_r^{r_s} \bar{B}_{\nu}(R') \bar{\mu}_{\nu}(R') E_2(|\tilde{\tau}_{\nu'} - \tilde{\tau}_{\nu}|) dR' \quad (1.4-8b)$$

where

$$E_2(\tau) = \int_1^{\infty} e^{-u\tau} u^{-2} du \quad (1.4-9)$$

A useful approximation is obtained if one replaces $|\cos \theta|$ in Eq. (1.4-7) by an average $c = \overline{\cos \theta}$. Substituting the approximate form of $I_{\nu \pm}$ into Eq. (1.4-4) gives expressions similar to those in Eqs. (1.4-8) but the exponential integral is now replaced by a simple exponential function, i.e. we have the approximation

$$E_2(\tau) \approx \frac{1}{2c} e^{-\tau/c} \quad (1.4-10)$$

The average intensities calculated from the approximate fluxes

$$\bar{I}_{\nu \pm} = F_{\nu \pm} / \pi \quad (1.4-11)$$

satisfy the differential equations

$$c \frac{d\bar{I}_{\nu \pm}}{dR} = \pm \bar{\mu}_{\nu} (\bar{B}_{\nu} - \bar{I}_{\nu \pm}) \quad (1.4-12)$$

These average intensities are therefore identical with the intensities in the directions for which $|\cos \theta| = c$. The idea of the two stream model with intensities in a characteristic direction goes back to Schwarzschild and Schuster who suggested to use $c = \frac{1}{2}$. A much better choice is $c = \frac{2}{3}$ which gives the correct net flux

$$F_{\nu+} - F_{\nu-} = - \frac{4\pi}{3\bar{\mu}_{\nu}} \frac{d\bar{B}_{\nu}}{dR} \quad (1.4-13)$$

in the high opacity limit.

In spherical geometry one has no simple rigorous expressions for I_{ν} like those given in Eqs. (1.4-7) from which to derive two stream equations. It seems, nevertheless, reasonable that one should be able to use equations which are essentially of the same character but with minor modifications to maintain conservation of energy. It is easy to see that this is achieved by the pair of equations

$$\frac{2}{3} \frac{d}{dR} \left(R^2 \bar{I}_{\nu\pm} \right) = \pm R^2 \bar{\mu}_{\nu} \left(\bar{B}_{\nu} - \bar{I}_{\nu\pm} \right) \quad (1.4-14)$$

With the definition given in Eq. (1.4-11) one obtains the outgoing and incoming flux simply by multiplying the corresponding intensities $\bar{I}_{\nu\pm}$ by a factor π . From the total integrated net flux

$$\mathcal{F} = \int (F_{\nu+} - F_{\nu-}) d\nu \quad (1.4-15)$$

one can finally obtain the heating rate

$$\dot{Q} = - \frac{1}{R^2} \frac{d}{dR} \left(R^2 \mathcal{F} \right) \quad (1.4-16)$$

for use in the energy equation.

1.5 Finite difference equations

It is obviously impossible to find exact analytical solutions to the equations of RH and one must be satisfied with approximate numerical solutions. To obtain these one replaces infinitesimal increments of dependent as well as independent variables by finite differences. Mathematically RH

can be characterized as an initial value problem and the methods and problems arising in treating this by means of finite difference equations have been thoroughly discussed by Richtmyer (1957). We shall review some general considerations and then turn to questions which are specifically relevant to our problem.

In a finite difference scheme continuous variables are replaced by discrete ones but there are numerous possibilities for doing this. Thus one can regard the discrete values of a variable as representing either the values of the corresponding continuous variable at a set of discrete meshpoint or the average values between meshpoints. There are other variations but they are not needed in the following discussion. One can treat some variables in the first and others in the second manner. To indicate the actual choice one can use integral subscripts for variables defined at the meshpoints and half integral ones for those defined in the intervals. It is convenient and natural to let R_i and U_i represent the radius and the velocity of the particle at the meshpoint i and this leads almost automatically to defining $V_{i+1/2}$, $P_{i+1/2}$, $E_{i+1/2}$, and $T_{i+1/2}$ as the averages of specific volume, pressure, internal energy density and temperature in the interval between the meshpoints i and $i+1$.

Another element of choice enters in the methods used for advancing variables in time. Almost all variables are defined at meshpoints in time which are indicated by integral superscripts. It may, however, be useful to define the velocity between meshpoints which can be indicated by half integral superscripts. With this definition and abbreviating the right hand side of Eq. (1.2-3) by a (for acceleration) that equation and Eq. (1.2-2)

lead to the integration procedure

$$U^{n+1/2} = U^{n-1/2} + a^n \delta t \quad (1.5-1)$$

$$R^{n+1} = R^n + U^{n+1/2} \delta t \quad (1.5-2)$$

Having obtained R^{n+1} one can then obtain V^{n+1} by differencing which follows from Eq. (1.2-1). So far we have not bothered to look at alternate schemes because the procedures outlined above are very straightforward and there seems to be no good reason for doing anything more elaborate. In the purely hydrodynamic case, i.e. if $\dot{Q} = 0$ the energy equation (1.2-4) can also be integrated very simply. Centering the difference equation at $(n+1/2)$ leads to

$$E^{n+1} - E^n + \frac{1}{2} \left(p^{n+1} + p^n + 2q^{n+1/2} \right) \left(V^{n+1} - V^n \right) = 0 \quad (1.5-3)$$

If E is expressed as a function of V and p this equation can be solved for p^{n+1} , the one variable which is still unknown. Anticipating the problems which arise when one has radiative heating it is really more useful to express both E and p as functions of V and T and to solve Eq. (1.5-3) for T^{n+1} . Either way one has to solve for only one unknown at a time which causes no real difficulty even though it may have to be done by iteration.

This situation changes drastically when the radiative heating rate \dot{Q} becomes important. The heating term to be added on the right hand side of Eq. (1.5-3) should be centered at the level $t^{n+1/2}$ like the remaining

part of the equation but the temperature distribution from which it must be calculated is only known up to the time t^n . There are two major avenues of attack. One is to forget about centering \dot{Q} and use its value as calculated at t^n . If this is done one can still solve explicitly for T^{n+1} and this is as the explicit method of integration.

In the other attack one uses the properly centered heating rate $\frac{1}{2}(\dot{Q}^{n+1} + \dot{Q}^n)$. This means that the equation which describes the heating in any one zone depends on the values of T^{n+1} in all zones so that one has to solve a large number of equations (one per zone) simultaneously. This implicit method involves a considerable amount of algebraic labor. If centering was only required for accuracy it would not be worthwhile to go to all this trouble because one could increase the accuracy more easily by reducing δt . What is really involved is the question of mathematical stability which we shall briefly discuss.

It is physically clear that a fluid responds to any pressure or temperature disturbance by a motion or heat flow which counteracts the disturbance. In an integration by means of difference equations which uses too large time intervals it may happen that the disturbance is overcompensated so that an excess turns in one step into a deficit, in the next step again into an excess etc. If the magnitude of this alternating disturbance increases each time any small disturbance will eventually cause the solution to blow up. In principle one can cure such an instability by taking δt small enough but this could seriously increase the running time of a problem.

There are two cases where the stability condition has been obtained analytically. The first arises when the dominant mode of energy transfer is of a hydrodynamic nature. The maximum δt in this case is found as

follows. One calculates for each zone the traversal time $\Delta t_{i+1/2} = \frac{(R_{i+1} - R_i)}{V_{s(i+1/2)}}$ of a signal traveling with the local sound speed. Going through all intervals one then finds the smallest, say Δt_{\min} . The time increment is then limited by the so-called Courant-condition

$$\delta t < k \Delta t_{\min} \quad (1.5-4)$$

where k is a numerical factor near unity which depends on the integration scheme. In the scheme where one uses the three equations at the beginning of this section one has $k = 1$.

When radiative heating dominates, the stability analysis has been carried out for the case where one can use the diffusion approximation. In the explicit scheme the limit for δt is proportional to $\bar{\mu}_R \delta R^2$ which decreases together with the Rosseland mean absorption coefficient of the air. If the air is fairly transparent δt is limited to very small values and this makes an explicit calculation very costly in computer time. The implicit method does not have this trouble and is in fact unconditionally stable. On the other hand it is of course also time consuming to solve a large number of coupled equations simultaneously. One can attempt to approach the implicit solution by iteration. On the first go-around one can advance T by the explicit method. With the advanced temperature distribution one can then work out \dot{Q}^{n+1} , form the average $\dot{Q}^{n+1/2} = \frac{1}{2}(\dot{Q}^n + \dot{Q}^{n+1})$ and reevaluate T^{n+1} . This procedure can be repeated several times and if it converges it will lead to a stable solution. The time step δt is now limited by the condition that the solution should converge. In contrast to the stability condition of the explicit method this limit of δt

is inversely proportional to $\bar{\mu}_R$ and independent of the zone size. The actual convergence criterion is almost equivalent with imposing a limit on the fractional energy change per time step within every zone. That form of the condition is easy to use and experience has shown that a fraction like one percent ensures the convergence. In a purely implicit procedure there is no such limitation on the magnitude of the time step. For the sake of accuracy one should also impose a limit on the fractional energy change per time step but it does not need to be as small. This limit can be allowed to vary from zone to zone to require greater accuracy in those zones where the changes make a significant contribution to the overall picture.

It is obvious that the allowed time interval changes throughout the calculation. For reasons of economy one should always run fairly close to the maximum without, however increasing δt too abruptly. To change δt generally requires some interpolation (or extrapolation) and all programs nowadays have provisions for carrying the necessary changes out automatically. Although the preceding arguments were based on the diffusion approximation they apply equally in the more general case. It is true that one can not readily obtain analytic stability or convergence criteria but experience with numerical calculations indicates the same pattern.

In addition to the various decisions described above one also has to make a choice on zone sizes. There are two parts to this decision relating to the total number of zones and to their relative sizes at different radii. Part one involves a compromise between conflicting requirements for accuracy and economy because it takes a large amount of computer time to use very many zones. This is amplified if the choice of δR also limits the time step as in hydrodynamic calculations where $\delta t \sim \delta R$ and even more in the explicit

calculation of radiative transfer where $\delta t \sim \delta R^2$.

Part two involves a judgment as to where the really significant changes are taking place and it is of course at those regions where one should use the finest zoning. In the course of a calculation the location of significant changes moves so that one has to make provisions in the program to detect this and to react to it by rezoning. Furthermore the overall radius of the fireball changes during an average calculation by as much as 3 orders of magnitude so that rezoning is also necessary to keep the number of zones at a more or less constant level.

The pseudo viscous pressure q introduced in Eq. (1.2-5) is a device for calculating the entropy rise behind the shock. Without the damping mechanism provided by q the changes induced behind the shock overshoot and produce lasting oscillations which physically do not belong there. A large value of ℓ will kill these improper oscillations most effectively but at the cost of making the transition region very wide which is also incorrect. Experience has shown that $\ell = 2\Delta R$ will stop the fake oscillations reasonably fast without spreading the shock transition over more than about 4 zones.

One can also express q in terms of $\frac{\partial v}{\partial t}$ rather than $\frac{\partial u}{\partial r}$ and Richtmyer suggests to use the formula

$$q = \frac{(\rho_0 \ell)^2}{v} \left(\frac{\partial v}{\partial t} \right)^2, \quad \frac{\partial v}{\partial t} < 0 \quad (1.5-5)$$

with

$$\ell = a \left(\frac{r}{R} \right)^2 \Delta r \quad (1.5-6)$$

so that the transition region covers the same number of zones near the center and further away from it. The numerical factor a should again be approximately 2.

In differencing either Eq. (1.2-5) or (1.5-5) one is led to expressions at half integral times. To obtain the acceleration in Eq. (1.5-1) it should be known at t^n but to achieve that, one would have to use an implicit routine. In this case that is not worthwhile since the use of q is an artifice anyway and it is customary to have q lag half a time step behind. In the energy equation (1.5-3) q is automatically in step.

The total energy which is obtained by summing the kinetic and internal energy within the fireball and the energy carried away by radiation should always stay at a constant level. The internal energy should in principle contain a part due to radiation but as mentioned in section 1.1 this does not amount to much. A trivial point, but one which must nevertheless be kept in mind is, that one should only count the excess over the energy in the ambient unheated air; otherwise the nominal energy would grow with the volume of the fireball.

It is important to keep track of any violations of energy conservation which may creep in through the use of finite difference schemes. Any program should therefore contain a routine for checking energy conservation.

The point at which R.H. goes beyond standard methods comes with the calculation of radiative transfer. The various methods require the evaluation of certain space integrals before one can calculate the energy deposition in a specified zone. Because of the very strong temperature dependence of the integrands these integrals depend critically on the radial dependence of the temperature. The common method of approximating

this dependence by assuming constant values of the temperature within the zones may lead to serious errors. An attempt to correct these has been made by Hillendahl (1964).

We shall present the analysis for the plane case which is formally easier. The transition to spherical geometry can be made later and requires only minor changes which are rather obvious. The starting point is Eq. (1.4-12) but before one has carried out any frequency averaging. Thus the line character is still preserved and μ_ν and $I_{\nu\pm}$ are rapidly changing functions of frequency. Integrating Eq. (1.4-12) across the zones which are separated by the interface at R_1 one finds for the outgoing and ingoing stream (represented by the upper and lower sign

$$I_{\nu\pm,1} = I_{\nu\pm,1\mp 1} e^{-\frac{3}{2}\Delta_{\nu,1\mp 1/2}} \pm \frac{3}{2} \int_{\tilde{\tau}_{\nu,1}}^{\tilde{\tau}_{\nu,1\mp 1}} B'_\nu e^{-\frac{3}{2}\Delta'_{\nu,1}} d\tilde{\tau}'_\nu \quad (1.5-7)$$

where B'_ν and $\tilde{\tau}'_\nu$ are taken at the same point R' , and

$$\Delta'_{\nu,1} = |\tilde{\tau}_{\nu,1} - \tilde{\tau}'_\nu| \quad ; \quad \Delta_{\nu,1+1/2} = |\tilde{\tau}_{\nu,1} - \tilde{\tau}_{\nu,1+1}| \quad (1.5-8)$$

To carry out the integral we use the first two terms of the power expansion

$$B'_\nu = B_{\nu,1} + \left(\frac{dB_\nu}{d\tilde{\tau}_\nu} \right)_{\tilde{\tau}_{\nu,1}} (\tilde{\tau}'_\nu - \tilde{\tau}_{\nu,1}) + \dots \quad (1.5-9)$$

and obtain

$$I_{\nu \pm, 1} = I_{\nu \pm, 1 \mp 1} e^{-\frac{3}{2} \Delta_{\nu, 1 \mp 1/2}} + B_{\nu, 1} \left(1 - e^{-\frac{3}{2} \Delta_{\nu, 1 \mp 1/2}} \right) \pm \frac{2}{3} \left(\frac{dB_{\nu}}{d\tilde{\tau}_{\nu}} \right) \left[1 - \left(1 + \frac{3}{2} \Delta_{\nu, 1 \mp 1/2} \right) e^{-\frac{3}{2} \Delta_{\nu, 1 \mp 1/2}} \right] \quad (1.5-10)$$

Integrating over frequency we obtain formally

$$I_{\pm, 1} = I_{\pm, 1 \mp 1} Z_{\pm, 1} + \left(B_1 1 - A_{\pm, 1} \right) \pm \frac{2}{3} \left(\frac{dB}{d\tilde{\tau}} \right)_1 W_{\pm, 1} \quad (1.5-11)$$

where

$$I_{\pm, 1} = \int I_{\nu \pm, 1} d\nu \quad (1.5-12)$$

$$Z_{\pm, 1} = \int \frac{I_{\nu \pm, 1}}{I_{\pm, 1}} e^{-\frac{3}{2} \Delta_{\nu, 1 \mp 1/2}} d\nu \quad (1.5-13)$$

$$A_{\pm, 1} = \int \frac{B_{\nu, 1}}{B_1} e^{-\frac{3}{2} \Delta_{\nu, 1 \mp 1/2}} d\nu \quad (1.5-14)$$

$$W_{\pm, 1} = \int \frac{\left(\frac{dB_{\nu}}{d\tilde{\tau}_{\nu}} \right)}{\left(\frac{dB}{d\tilde{\tau}} \right)_1} \left[1 - \left(1 + \frac{3}{2} \Delta_{\nu, 1 \mp 1/2} \right) e^{-\frac{3}{2} \Delta_{\nu, 1 \mp 1/2}} \right] d\nu \quad (1.5-15)$$

and where B_1 is the integrated intensity

$$B = \int B_{\nu} d\nu = \frac{\sigma}{\pi} T^4 \quad (1.5-16)$$

at the point R_1 . No limits of integration have so far been specified and one is free to divide the spectrum into any set of frequency intervals. As a first approximation Hillendahl used the entire spectrum without subdividing it.

Before Eq. (1.5-11) can become operational one has to define the average optical depth $\tilde{\tau}$ which enters in the derivative $\frac{dB}{d\tilde{\tau}}$ and one has to face the difficulty of an unknown ratio I_ν/I entering into the definition of Z .

The procedure devised by Hillendahl for obtaining an average for $\tilde{\tau}$ is specifically intended for use with finite zone sizes. The prescription is designed to keep the emissivity of a zone of constant density and temperature unchanged if one replaces the frequency dependent optical depth $\Delta\tilde{\tau}_\nu = \mu_\nu \Delta R$ by its average $\Delta\tilde{\tau}$. Thus, i.e., by making this substitution in the exponent of Eq. (1.5-14) one is led to

$$A = \int \frac{B_\nu}{B} e^{-\frac{3}{2}\mu_\nu \Delta R} d\nu = e^{-\frac{3}{2}\Delta\tilde{\tau}} \quad (1.5-17)$$

We note that the factor $\frac{B_{\nu,1}}{B_1}$ in Eq. (1.5-14) is taken at the edge of the zone. Since this ratio varies only very slowly with T we will take it at the center of the zone instead, so that there is only one emissivity A per zone and not different ones for the ingoing and outgoing ray. In the above integral for A one can clearly replace the rapidly varying exponential by a smooth one in which one uses the slab absorption coefficient $\bar{\mu}_\nu$ as defined in Eqs. (1.3-2) and (1.3-3). In

the new expression

$$A = \int \frac{B_\nu}{B} e^{-\frac{3}{2} \bar{\mu}_\nu \Delta R} d\nu \quad (1.5-18)$$

the zone with ΔR enters not only as a factor in the exponent but also as one of the variables in $\bar{\mu}_\nu = \bar{\mu}_\nu(\rho, T, \Delta R)$. Various methods for calculating $\bar{\mu}_\nu$, which apply when the dominant absorption is molecular, atomic or free-free, have been described in (2). The results are tabulated in and have been used in the above integral to obtain $A(\rho, T, \Delta R)$. It is convenient to express this in terms of a mean absorption coefficient $\bar{\mu}_H(\rho, T, \Delta R) = -\frac{2}{3} \ln A/\Delta R$ and to write:

$$A = e^{-\frac{3}{2} (\bar{\mu}_H \Delta R)} \quad (1.5-19)$$

Depending on ΔR as well as on ρ and T , $\bar{\mu}_H$ differs from the Rosseland mean ($\bar{\mu}_R$) and the Planck mean ($\bar{\mu}_P$) which depend only on ρ and T .

For the function W , which should in principle be calculated from Eq. (1.5-15) we use an approximation and set

$$W = 1 - \left(1 + \frac{3}{2} \bar{\mu}_H \Delta R\right) e^{-\frac{3}{2} \bar{\mu}_H \Delta R} \quad (1.5-20)$$

which looks reasonable and leads to the correct energy deposition when $\bar{\mu}_H \Delta R$ is large enough that one can use the diffusion approximation. As in the case of A we are using only one W per zone.

The coefficients $Z_{\pm, i}$ as defined by Eq. (1.5-13) depend on the unknown spectral distribution $I_{\nu \pm, i} / I_{\pm, i}$ at the point i . Since the difference equations (1.5-11) apply only to the integrated intensities $I_{\pm, i}$ their solution does not give us any direct information about the spectral distribution and we must rely on educated guesses for the latter. The basic clue which we follow is that the radiation at some point i comes by and large from a zone (the radiating zone) which lies an optical depth unity behind that point in the direction where the stream comes from. The distribution has therefore the distribution of a blackbody source at the temperature T_R of the radiating zone but modified by selective absorption in the intermediate zones.

When we apply this model we distinguish 3 typical situations for the ingoing and 3 for the outgoing stream. This comes from the peculiar temperature dependence of mean absorption coefficients. For all these means, whether we talk of $\bar{\mu}_R$, $\bar{\mu}_P$ or $\bar{\mu}_H$, one can distinguish a central temperature range where $\bar{\mu}$ is large and the low and high T ranges where it drops to very low values.

The temperature profile of a fireball is typically a monotonically decreasing curve. While the central temperature is still large this profile looks like the sketch in Fig. 1-2 with a central section where $\bar{\mu}$ is small so that radiative transfer maintains a nearly constant temperature. Beyond that plateau comes a more opaque region with a relatively large temperature gradient and at the point where the temperature has dropped to where the air is again transparent the profile becomes again more level. Superimposed on this one finds usually

some structure due to shocks or other disturbances but this does not alter the main conclusion that there are 3 distinct regions.

In the opaque intermediate region the spectral distribution I_ν/I can be identified with that of a blackbody at the local temperature so that one is led to $Z_+ = Z_- = A$. In the interior region the radiation comes mainly from its boundary where it is in contact with the opaque region. Since the temperature profile is quite level one does not commit a significant error by identifying I_ν/I again with the local B_ν/B which varies much less with T than either B_ν or B itself. As in the previous case we therefore use the approximation $Z_+ = Z_- = A$.

Only in the outer section do we have to make a more careful choice of I_ν/I and only for the outgoing stream. The ingoing stream carries essentially no energy and it doesn't matter much what one does. The simplest choice is again to set $Z_- = A$.

The point where it really counts that our model should adequately represent the true physical nature of radiative transport comes when we consider the outgoing stream as it emerges from the opaque region. The absorption to which this stream is subjected is largely due to molecules. In calculating which parts of the spectrum are and which are not transmitted one is greatly helped by the character of the energy dependence of $\bar{\mu}_\nu$. Fig. 1-3, which is a typical example taken from SACHA type calculations shows that $\bar{\mu}_\nu$ is a very rapidly rising function of frequency. From this graph we find by inspection that a zone of about 10 m thickness would transmit practically no photons above 5 eV and practically all photons below 3.8 eV. Approximately one can assume that there is a critical photon energy $h\nu_c$ in the

vicinity of 4.4 eV at which the transmitted flux is sharply cut off. For a stream which starts out as a blackbody spectrum $\frac{B_\nu}{B} = b_\nu(T_R)$ one finds that the transmitted fraction of the energy is a known integral

$$L(T_R, h\nu_c) = \int_0^{\nu_c} b_\nu(T_R) d\nu \quad (1.5-21)$$

The procedure for determining Z_+ for any zone $i - 1/2$ outside the opaque region starts out with finding the radiating zone which belongs to it and whose temperature has been designated as T_R . We assume that the model spectrum I_ν starts out there as a blackbody spectrum $B_\nu(T_R)$. Any of the zones through which it passes will not transmit any radiation above its cut-off energy $h\nu_c$ and the model spectrum which finally enters into zone $i - 1/2$ remains $I_\nu = B_\nu(T_R)$ up to the lowest cut-off energy $h\nu_{\min}$ encountered by the stream but is reduced to $I_\nu = 0$ above $h\nu_{\min}$. If zone $i - 1/2$ has a lower cut-off $h\nu_{c, i-1/2}$ we set therefore

$$Z_{+,i} = \frac{L(T_R, h\nu_{c, i-1/2})}{L(T_R, h\nu_{\min})} \quad (1.5-22)$$

If the cut-off energy is equal to or larger than $h\nu_{\min}$ the model spectrum would lead to $Z_{+,i} = 1$ which can't be right and indicates that the sharp cut-off approximation is too crude to fit this case. An upper limit for Z can be obtained by setting it equal to the local A since the bulk of the true spectral distribution lies at somewhat higher energies than the local blackbody spectrum. Thus the true I_ν will suffer somewhat more absorption than B_ν which leads to the inequality

$Z < A$.

The modifications which are necessitated by going to spherical symmetry can be written down without difficulty. One only has to note that Eq. (1.4-14) differs from Eq. (1.4-12) by the factor R^2 which multiplies both I and B . Clearly this factor must enter when one modifies the corresponding set of Eqs. (1.5-11). As we write down the modified set we incorporate the result that the coefficients A and W depend only on the zone and not on the direction of the stream, and obtain:

$$R_1^2 I_{\pm,1} = R_{1\mp 1}^2 Z_{\pm,1} I_{\pm,1\mp 1} + R_1^2 B_1 \left(1 - A_{1\mp 1/2}\right) \pm \frac{2}{3} R_1^2 \left(\frac{dB}{d\tau}\right)_1 W_{1\mp 1/2} \quad (1.5-23)$$

The A and W are as before given by Eqs. (1.5-19) and (1.5-20) and $Z_{\pm,1}$ is nearly always equal to $A_{1\mp 1/2}$ except in a few zones just outside the opaque region where one should use Eq. (1.5-22).

In the two stream model the fluxes differ from the intensities by a factor π as shown in Eq. (1.4-11). The relation carries over when one performs the frequency radiation so that

$$F_{\pm,1} = \pi I_{\pm,1} \quad (1.5-24)$$

Having determined the intensities by solving the set of Eqs. (1.5-23) one is therefore ready to evaluate $-\nabla \cdot \vec{F}$ which according to Eq. (1.2-8) gives us the radiative heating rate. Thus one obtains:

$$\dot{Q}_{1+1/2} = \frac{3}{R_{1+1}^3 - R_1^3} \left[R_1^2 (F_{+,1} - F_{-,1}) - R_{1+1}^2 (F_{+,1+1} - F_{-,1+1}) \right] \quad (1.5-25)$$

which is the final equation of the two stream method. Before leaving it let us take a somewhat closer look how this equation handles a zone in the opaque region. In any region where one replaces Z_+ and Z_- by A one finds that Eq. (1.5-23) reduces to:

$$I_{\pm,1} = B_1 \pm \frac{2}{3} \left(\frac{dB}{d\tau} \right)_1 W_{1 \mp 1/2} \quad (1.5-26)$$

from which one obtains in turn

$$F_{+,1} - F_{-,1} = \frac{2\pi}{3} \left(\frac{dB}{d\tau} \right)_1 \left(W_{1-1/2} + W_{1+1/2} \right) \quad (1.5-27)$$

In an opaque region this simplifies still further because the factor $e^{-\frac{3}{2} \bar{u}_H \Delta R}$ in Eq. (1.5-20) becomes negligible compared to unity. One can therefore set $W = 1$ and obtain:

$$F_{+,1} - F_{-,1} = \frac{4\pi}{3} \left(\frac{dB}{d\tau} \right)_1 \quad (1.5-28)$$

and since $B = \frac{\sigma}{\pi} T^4$ this is clearly equivalent to Eq. (1.2-9) i.e., to the basic equation of the diffusion approximation. This is of course no surprise because we picked $\overline{\cos \theta} = \frac{2}{3}$ precisely in order to achieve this equivalence.

In an opaque region, the diffusion approximations contains all the physics needed for the calculation of radiative energy transfer and it is superior to other methods as far as speed and possibly accuracy of calculation are concerned. Hillendahl's formulation of the two stream

method automatically leads to this procedure. More elaborate methods such as the multiple ray technique do not, but it is of course possible to switch to a diffusion theory calculation when one considers an opaque region. This is indeed done in the SPUTTER program.

In the form outlined in this section the two stream method is not applicable at high altitudes where the ambient air has a density less than about $\rho/\rho_0 = 10^{-4}$. At such densities the air becomes transparent in the spectral region where B_ν has its maximum and the fireball has no opaque region. There is still a significant amount of radiation at frequencies above and below this window but one has to devise new methods for dealing with this problem. At these altitudes the mathematical difficulties are further aggravated by the non-spherical energy deposition which takes place when the mean free path of x-rays get large compared to the atmospheric scale height. Eventually, say at about $\rho/\rho_0 \approx 3 \times 10^{-6}$ the air becomes transparent in all parts of the spectrum and thermal radiation is no longer a significant factor.

References

- Chandrasekhar, S., Radiative Transfer, Dover, 1960.
- Hillendahl, R.W., LMSC Report 3-27-64-1, DASA 1522, 1964.
- Magee, J.L. and J.O. Hirschfelder, Chapter 3 of Los Alamos Report LA 2000, 1953.
- Marshak, R.E., Phys. Fl. 1, 24, 1958.
- Mustel, E.R., in Theoretical Astrophysics, by V.A. Ambartsumian, ed., Pergamon Press, 1958.
- Richtmyer, R.D., Difference Methods for Initial-Value Problems, Interscience, 1957.
- Von Neumann, J. and R.D. Richtmyer, J. of Appl. Phys. 21, 232, 1950.
- Churchill, D.R., S.A. Hagstrom and R.K. Landshoff, The Spectral Absorption Coefficient of Heated Air, JQSRT 4, 291, 1964.

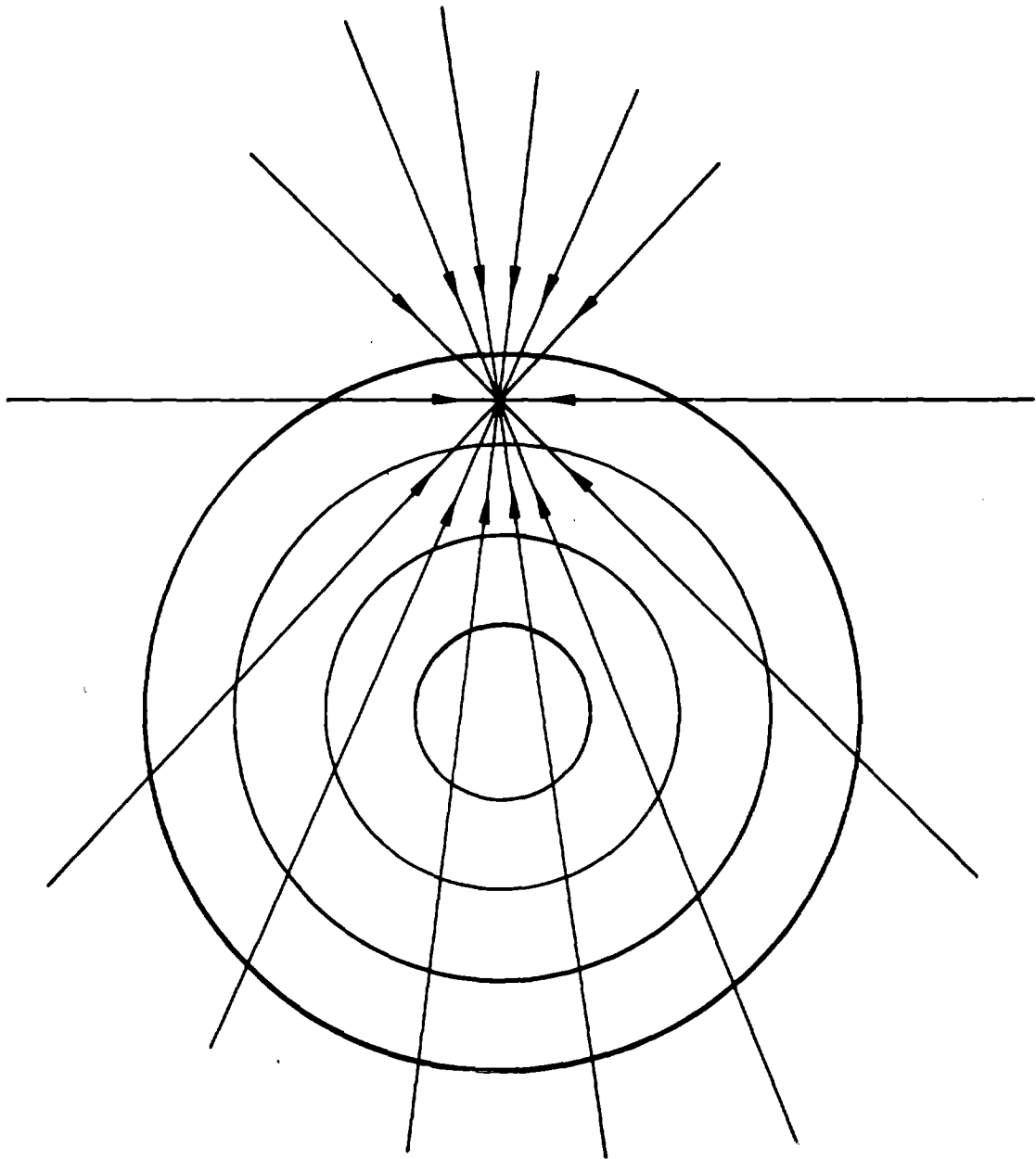


FIG. 1-1 RAYS CONVERGING UPON ZONE 4 WHICH ARE USED TO COMPUTE I_v AS FUNCTION OF ANGLE

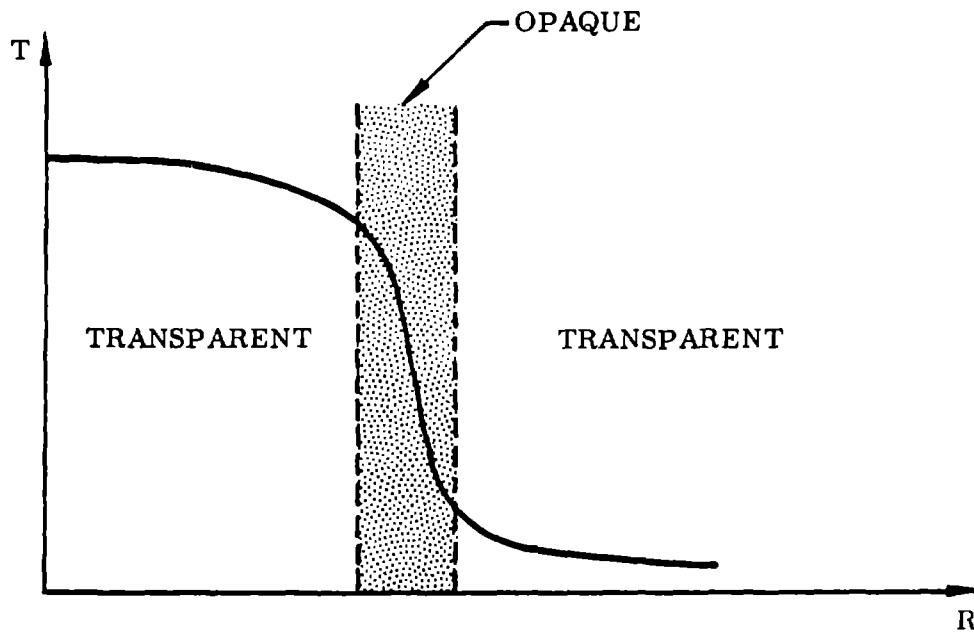


FIG. 1-2 SKETCH OF TEMPERATURE PROFILE IN A FIREBALL INDICATING OPTICAL PROPERTY OF THE AIR

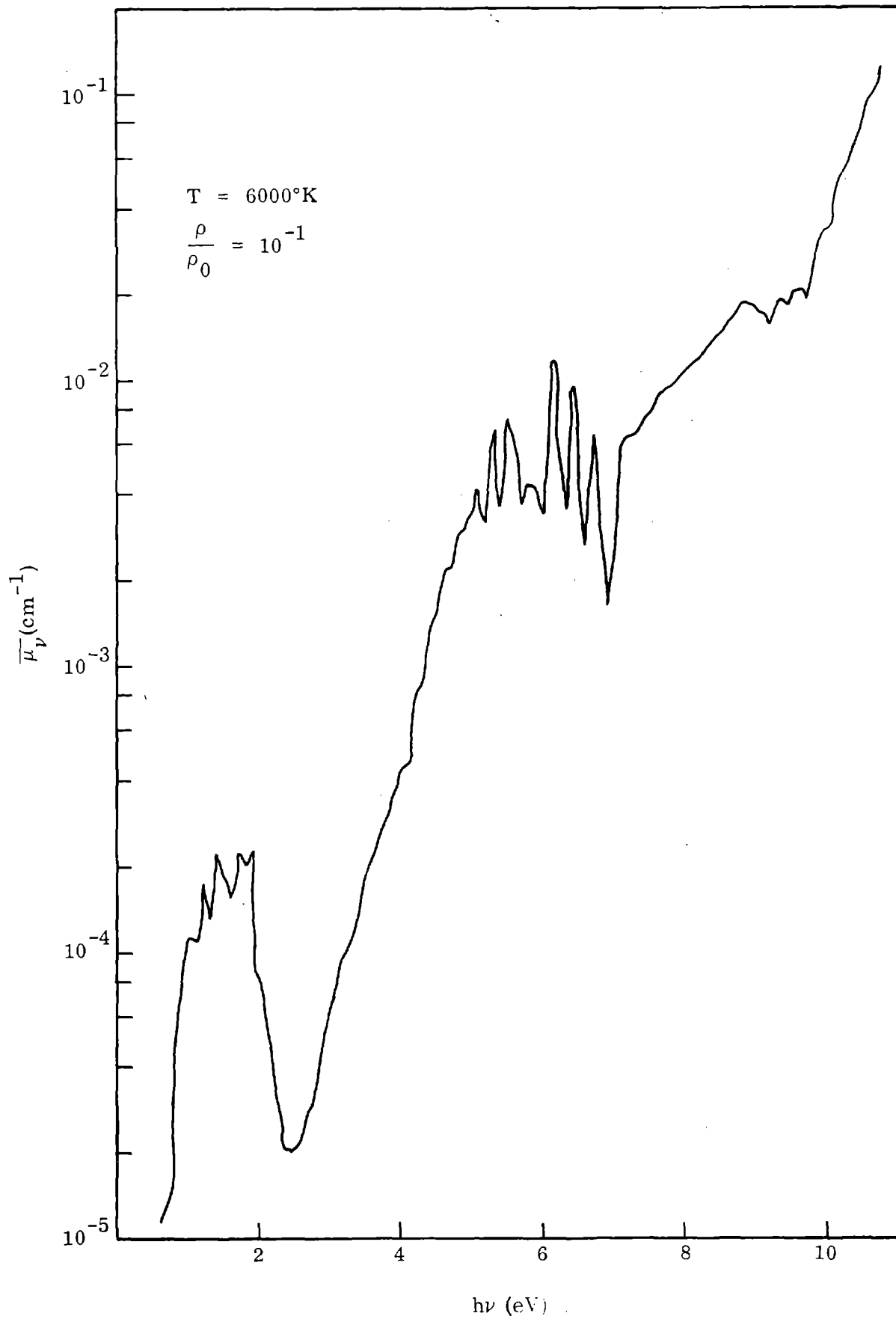


FIG. 1-3 TYPICAL ENERGY DEPENDENCE OF ABSORPTION COEFFICIENT

Chapter 2. THE PHYSICS OF FIREBALLS

2.1 Introduction

A nuclear explosion in the atmosphere creates a fireball whose development depends in large measure on the physics of hot air. All of the previously discussed properties of hot air and all of the mechanisms for energy transport developed in previous chapters are a part of nuclear fireball physics. However, these energy transforming and transporting relations and the detailed knowledge of the properties of air find considerably wider application. They have or can contribute to the study of stellar dynamics, the nature of stellar atmospheres, the radiation from various astrophysical sources, and they can aid in the study of hypervelocity flight, upper atmosphere physics, aurora, and other atomic and molecular physics problems which involve high temperatures.

It is certainly the case that the information presented in these previous chapters makes the conditions created in a nuclear explosion more understandable. Some knowledge of air heating mechanisms, of air excitation, of radiation transport, and of hydrodynamics, of absorption properties, and of the thermodynamics of air is necessary before a full description of a nuclear explosion can become more than heuristic.

Much of the present knowledge about fireballs has been gleaned from test observations, but by far the greatest detail has come from numerical computer calculations, as have the quantitative estimates of fireball interior dynamics which appear in this chapter. Calculations of widely varying detail and sophistication now abound, and it is not the intention in this chapter to review such results or analyze computing methods. Most current calculations rely for their measure of success on the extent to which the physical concepts and properties covered in the

preceding chapters have been taken into account in a mathematical model. The principal objective of this chapter is to outline the physical features of nuclear fireballs and their thermal radiations, stressing where possible those factors which are most general and which provide the best understanding on which to base predictions and extrapolations. The approach adopted is to begin by considering a small yield explosion (1 kiloton) at sea level and to describe the sequence of events which occur unencumbered with interactions from the earth's surface or inhomogeneous environments. This development will then be extended to higher yields and altitudes. There will be no attempt at completeness and no great concern for quantitative rigor, but it is intended to display as much as possible the current understanding of the physics of nuclear fireballs.

2.2 One kiloton at sea level

A one kiloton explosion in a sea level atmosphere provides an appropriate example for an initial examination of the sequence of events that constitute a fireball history. The now familiar usage of kilotonage and megatonage refers to the total energy release in a nuclear explosion with the usual metric prefixes for a thousand or a million and with the understanding that a ton of high explosive - TNT - releases 10^9 calories of effective energy, i.e., one gram of TNT is taken as equivalent to one kilocalorie or 4.185×10^{10} ergs.

For any nuclear explosion the sequence of events is remarkably complex. In following its development for this one kiloton sea level explosion, the reader may appreciate that the present understanding,

although not complete, has become quite detailed and much of it has grown directly from the material reviewed in this series of volumes.

The nuclear energy is released in an extremely short time - a small fraction of a microsecond - and always in a small mass and volume. It is the properties of this small mass, constituting the weapon itself and its carrier that determine the early source of energy for the fireball, and some of these properties may influence the character of the later thermal radiation. Everything starts in this nuclear source and all of the initial radiations - gamma rays, neutrons, and x-rays - are generated by it. However, the air or other immediately surrounding material absorbs almost everything emitted within a few hundred meters and the nature of the observable fireball is largely determined by the properties of this surrounding air. For our example of one kiloton in a sea level atmosphere, the air within a few feet of the weapon stops nearly all of the x-rays, and the prompt gamma rays and the neutrons have removal mean free paths of about 400 and 240 meters, respectively. These rapid absorptions make knowledge of specific details of the nuclear device largely unnecessary in describing the fireball phenomena. Consequently, we shall be able to proceed without reference to classified aspects of nuclear weapons and yet without significantly truncating our description of the fireball and its thermal radiations.

The fraction of the energy which may be radiated out of the weapon as x-rays before it begins to blow apart under hydrodynamic action depends largely on its yield-to-mass ratio and to some extent on other construction details. This fraction may range from almost nothing at all (or a very small percent) to a significantly more than 80% of the total

energy generated (Glasstone, 1962; Brode, 1964 b).

Before the air has had a chance to re-radiate any of the energy deposited by the x-rays, the bulk of this energy is concentrated in a relatively small sphere and at a temperature which is typically of the order of several million degrees K. There is, however, a small fraction of x-rays, from the high frequency end of the spectral distribution function, which penetrates to a distance of perhaps a few meters, and heats this shell to temperatures in the $10,000^{\circ}\text{K}$ range. Energywise this heating is insignificant but it makes a contribution to the fireball phenomenology which is of some interest. By consulting the table of mean free paths on p. 447 of (3)* we discover that this shell is opaque. As long as it exists such an opaque shell hides the much hotter sphere on its inside and all that can be observed is the radiation from the shell itself, which is comparatively dim.

This phase is always very short-lived and terminates when the radiation from the center floods into the shell and heats it up. During the next phase the fireball can be characterized rather well as an extremely high temperature sphere of air surrounding the nuclear source and showing a fairly sharp temperature drop at its edge. The interior of this high temperature sphere may be at a fairly uniform temperature, and the whole may contain quite a large fraction of the nuclear explosion energy in the form of heat. Some small fraction always remains in the dense bomb vapors, but most of the early phases of the fireball development are quite independent of the details of the weapon design. The subsequent explosion and radiation behavior can be derived almost entirely from the properties of this hot air. Such a model will be less true in high altitude or space

* DASA-1917-3.

environments where the immediate external surroundings fail to contain as thoroughly the explosion energy because they lack sufficient opacity or optical thickness.

Throughout the explosion development, radiant energy is emitted by the fireball. That fraction which is transmitted by the cold exterior atmosphere is called thermal radiation. The rate of energy emission, or radiated power, has shape as shown in Fig. 2-1. If the opaque fringe layer has been penetrated early enough and if the instruments used for measuring the thermal power have sufficient time resolutions, the signal will include the early peak which is shown as a dotted line. Otherwise, one sees the two-peak curve which is drawn as a full line. The explanation of this curve is an important objective of any theory.

Although it is a rather simple exercise, it is instructive to note the rather small size of air volumes required to contain the large amounts of energy at the high temperatures created by the absorption of the initial flux of x-rays. The following table indicates the radii of spheres for a few examples of energy content and temperatures. These temperatures, of course, are too high for the air to remain that hot for very long, but in the immediate first fractions of a microsecond these radii are representative of the sizes and temperatures of the earliest (x-ray) fireballs.

Size of Spheres of Sea Level Air Necessary
to Contain 1 KT, 1 MT or 100 MT of Energy at
Various Uniform Temperatures

Temperature Millions of °K	1 KT	1 MT	100 MT
7 1/2	3/4 m	7.5 m	35 m
6	1	10	46
5	1 1/4	12	57
4	1.6	16	74
3	2.1	21	100

In a very few microseconds, these fireballs would have grown much larger and much less hot by the continued diffusion of radiation into the external cold air.

For most considerations these earliest phases of x-ray deposition and re-radiation remain both obscure and of little probable importance. When the flux of source radiations has been sufficiently intense as to completely strip the electrons from the air ions, then that volume of plasma can offer only Compton scattering as further resistance to the x-ray flux or as opacity to its own re-radiation. The most appropriate physical model for the continued expansion of this low emissivity, high energy density region is neither by hydrodynamics (which requires relatively long times to accelerate masses of gas) nor by radiation diffusion which presumes many interactions over any appreciable temperature gradient. The growth of such a heated volume is a radiative process which can be characterized roughly by its emissivity, temperature, and volume together with the heat capacity of the external cold air. The single further physical characteristic necessary to include in a growth rate prediction is the fact that the surrounding air is essentially opaque to the radiations from this hot air. Detailed knowledge of the opacity between this blackness at cold temperatures and its transparent nature at sufficiently high temperature is at this point unnecessary. Thus, the rate of energy lost, expressed as a grey-body loss rate, is the rate at which energy is deposited in the cold air at the surface of the high temperature sphere, viz.,

$$\frac{dW}{dt} = 4 \pi R^2 \sigma T^4 e \quad , \quad (2.2-1)$$

in which e is the emissivity, T the temperature of the hot isothermal sphere, R its radius, and dW/dt the rate of energy change. When an appropriate specific heat is introduced, a differential prescription for the volume growth and temperature drop results.

Following this approximation, one can express the rate of growth, dR/dt , in the same terms as

$$\frac{dR}{dt} = \frac{e\sigma T^4}{E\rho} \quad , \quad (2.2-2)$$

in which E represents the internal energy per unit mass, and ρ the density of the air just behind the front, while T is the inner temperature. The usefulness of this approximation in estimating the rate of growth of a partially transparent fireball is largely dependent on the accuracy with which average or "effective" interior temperatures, specific energies, and emissivities can be chosen. During the most rapid expansion, the interior is likely to be considerably non-isothermal, i.e., the interior may be more than twice as hot as the region just behind the front. The dependence on the fourth power of the temperature makes this rate quite sensitive to such differences. The most uncertain quantity is likely to be the effective emissivity, since it represents some average over the emitting region, and may also disguise some geometric dependence - not all the radiation being emitted radially. Appropriate choices of effective emissivity and temperature may make this simple formula appropriate for predicting the growth rate during the subsequent radiation diffusion phase.

The temperature profiles illustrated in Fig. 2-2 are typical of this early radiative growth for a one kiloton sea level burst. The curves represent the air temperatures as a function of radius for six selected instants in time. The dashed curve indicates the shock temperatures. It is the lowest temperature within the fireball at each of these times. After about 15 microseconds, the radiation diffusion growth becomes so slow that a shock wave begins to form, to compress the newly engulfed air and heat it to a temperature substantially below that of the radiatively heated inner sphere. With either the early radiative expansion or the subsequent adiabatic expansion behind the forming shock front, the inner temperatures drop with time in an approximately exponential fashion. During this early growth, the power radiated or the thermal radiation to points outside the fireball is not a significant fraction of the energy it contains. The time is short, the size is small, its opacities are high, and the fireball exterior so well shields the hotter core that the radiation out is less than half a per cent of the available energy.

Of course, the radiative properties are influenced by the air density as well as by the temperature, and the gradual formation of the shock causes an appreciable increase in the air density at the fireball surface (as much as tenfold increase at sea level). In the process, the outer surface of the fireball passes from a rather diffuse radiation-driven front to a sharp, dense shock front. Fig. 2-3 shows some typical early density profiles, in which the shock is seen to grow and the fireball interior is seen to expand to much less than the external ambient density.

Reference to the opacities for air as given in Volume 3 will

confirm that the shock front at these early densities and temperatures is quite opaque. For instance, at the 250 μ sec time of Figs. 2-2 and 2-3, the emission mean free path for a shock temperature of 30,000^oK and a density of 8 times normal is about 0.01 cm. The fireball will expand to much lower temperatures and much larger size before anything behind the shock front will become visible. It is during this period that the thermal radiation rate decreases toward a minimum and the fireball appears to grow dimmer. (Fig. 2-1, before one millisecond.)

If the fireball growth rate defined in Eq. (2.2-2) is computed for the earliest time illustrated in the temperature profiles of Fig. 2-2, assuming for the moment an emissivity of unity, the rate is about 4.4×10^8 cm/sec. This rate is too high by an order of magnitude in comparison with results of the numerical calculation example. The calculation showed that the expansion at this 1.2 microsecond time was still being determined by radiation diffusion. The calculation, however, also treated the earliest times by diffusion, and not (as suggested above) by transport within a transparent heated region with a radius less than one mean free path for the emitted radiation. The appropriate mean free path for diffusion is the so-called Rosseland average, hereafter abbreviated as Rmfp. The Rmfp is defined as

$$\lambda_R \equiv \frac{\int_0^\infty \lambda_\nu \frac{dB_\nu}{dT} d\nu}{\int_0^\infty \frac{dB_\nu}{dT} d\nu} \quad (2.2-3)$$

in which λ_ν is the spectral mean free path, $B_\nu(T)$ the Planck function, and $\int_0^\infty d\nu$ denoting integration over all frequencies. The Rmfp used in

the calculation approaches the Compton limit at high temperatures, however, and allows the rate of growth to be equally fast. In fact, without special consideration for relativistic effects, the diffusion growth can exceed even the speed of light.

At the earliest time illustrated in Figs. 2-2 and 2-3, the fireball has grown to more than one mean free path in radius which reduces the effectiveness of the inner temperature in driving the continued expansion. A more heuristic interpretation of the growth rate formula allows the emissivity to be interpreted as a resistance parameter which reduces the growth rate to less than the blackbody rate for that central temperature. An alternative interpretation treats this efficiency factor as one which compensates for the use of the shielded innermost temperature when the effective temperature is at some radial position further out and is lower in value, i.e., $e \approx (T_o/T_i)^4$ where T_o is the effective outer temperature and T_i is the screened central temperature. A crude measure of this correction and of an appropriate value for this viscosity constant might be the ratio of the Rmfp to the radius of the front, i.e., the reciprocal of the number of mean free paths between the radiating interior and the front. For the diffusion approximation, such a correction might better be expressed in terms of the local temperature gradient as well.

The inner temperature of our example calculation at 1.2 micro-seconds is around 10^6 °K (Fig. 2-2) and the density is still normal (1.29×10^{-3} gm/cm³) (see Fig. 2-3). The Rmfp is a bit less than one meter, while the radius is about 3.2 meters. Taking ϵ to be $1/3.2$ brings the growth rate down to about 1.3×10^8 , which is still high compared to that for the numerical calculation. The mean free path decreases rapidly as the temperature falls below 10^6 °K, however, and since the front at 1.2 μ sec is at around half the interior temperature, a more appropriate mean free path might be between 0.92 (the value at 10^6 °K) and 0.12 (the value at 5×10^5 °K). Taking the average of their reciprocals, i.e., averaging the opacities, gives about 0.2, so that the correction factor, ϵ , becomes $0.2/3.2$, and the corrected rate becomes $\sim 3 \times 10^7$ which agrees well with the growth rate at that time from the detailed diffusion calculation.

The most appropriate specific energy and density values for use in the growth rate approximation are those just behind the front of the wave, since it is to those conditions that the cold air is to be heated, i.e., it is that heat capacity that will absorb the subsequent radiation energy flux. Fig. 2-4 displays the specific energy profiles for this one kiloton example for the same time as those of Figs. 2-2 and 2-3.

It is interesting to test the simple growth rate formula (Eq. 2.2-2) against the fireball growth speed that results from the numerical calculations. The calculation should show a rate faster than hydrodynamic shock growth until the radiation growth has fallen below the speed of hydrodynamic motions, and this simple form should show a comparable rate until that time, then a much slower rate as the shock wave takes over.

Fig. 2-5 compares these rates for the same time period as covered by the profiles of Figs. 2-2, 2-3, and 2-4 and beyond. In these comparisons, several approximations are represented by dashed curves, while the numerical calculation rate is shown as a solid curve. The rate calculated as blackbody at the inner temperature, shown as circled points, is clearly too high at all times. Even when the lower temperatures of the outer edge of the hot region are used to determine a blackbody rate (the triangles Δ of Fig. 2-5), the rate is at all times too high.

When the radiative resistance parameter is represented as the ratio of the R_{mfp} to the hot region radius, using the R_{mfp} evaluated at the hot interior temperature, the modified rate is still high at the early times when diffusion is still dominant (the square points of Fig. 2-5). It drops precipitously as the interior cools and becomes opaque at just the times when a shock begins to form (at about 10 microseconds in this example). Although this approximation is not correct in value, the sharpness of the decrease as hydrodynamics takes over can make it a useful indicator of the transition onset, and so a reasonable prediction tool.

The more accurate estimate of the early diffusion growth rate, involving the averaged opacity between interior and front, is also more subject to error due to the difficulty in judging appropriate front conditions. These estimates are indicated in Fig. 2-5 by diamonds. These values are closest to the numerical calculations rate of growth at the earliest times when diffusion is the dominant mechanism. The earliest profile front temperatures are difficult to define because the front is not sharp. The rate of growth estimated at these approximate front temperatures with

a corresponding resistance parameter leads to the estimates indicated by the triangles \blacktriangleright in Fig. 2-5. Again, the shock formation time is denoted by a sharp drop in the rate estimated in this manner. Both of the blackbody rate curves (upper curves of Fig. 2-5) show a fairly sharp drop at shock formation time. Such a simple but uncertain formula may be preferable to the use of the radiation resistance notion in determining shock formation radius and time. Since in this range of temperature and densities, the Rmfp decreases with decreasing temperature as about the fourth power of the temperature, using the Rmfp as a correction factor then means that the adjustment parameter is as sensitive to temperature changes at the blackbody rate itself. Such critical opacity dependences may provide some sharp distinctions in estimates but at the same time present some hazards in choosing effective temperatures too casually.

After shock formation, the rate of growth of the fireball should follow the shock growth itself until the shock cools to transparency. The shock speed for a strong shock is approximately given by

$$\dot{R}_s \sim \sqrt{\frac{(\gamma_s + 1)P_s}{2\rho_o}} \quad (2.2-4)$$

where $\gamma_s = (P_s/\rho_s E_s) + 1$, ρ_o is the ambient air density and P_s , ρ_s , and E_s are shock front values of pressure, density and internal specific energy. This approximation is shown in Fig. 2-5 by the symbol \blacktriangleleft . For the earliest times, the expansion is faster than this shock rate, but at later times it corresponds well.

Using the particle velocities (u_s) at the front and the density at the front (through the mass conservation relation) provides the relation

$$\dot{R}_s = \frac{u_s \rho_s}{\rho_s - \rho_0} \quad (2.2-5)$$

The rate derived from corresponding values of u_s and ρ_s for the numerical calculation is indicated in Fig. 2-5 by triangles pointing down (∇). After nuclear shock catch-up this curve coincides with the solid curve for the directly computed rate.

In the temperature region of interest, a shock can be pictured as a sharp gasdynamic jump imbedded in a region of radiation-induced temperature variation (Fig. 2-6). The internal structure of this type of wave has been investigated extensively by Zeldovich (1957), Raizer (1957), and Heaslett and Baldwin (1963), to name a few, all of whom employed the equations of steady continuum gas dynamics with gray radiative transport.

The important feature of this picture is the temperature precursor which runs ahead of the sharp front. This precursor is created by the radiation from the high temperature region behind the sharp front. One can estimate the temperature of the precursor by equating the power radiated by this front with the rate of heating in the precursor. In the resulting relation

$$\rho u e_p = \sigma T_s^4 \quad (2.2-6)$$

ρ , u and e_p stand for the ambient air density, the shock velocity and the internal energy of the air in the precursor. From the latter quantity and the equation of state, one can then obtain the temperature of the precursor. Using the Hugoniot relations (Section 5.1 of (4)) and a simple analytic fit

to the equation of state, one obtains at sea level the relation

$$T_p = 3.45 \times 10^{-7} T_s^{2.17} \quad (2.2-7)$$

For a shock temperature of 10^5 °K we calculate a precursor temperature of 23,000 °K and note that a millimeter layer of air at that temperature is opaque. Up to the time when the shock temperature drops to 10^5 °K all the thermal radiation comes therefore from the precursor. To make a quantitative evaluation of the power radiated during this phase requires a more detailed analysis of the radiative transfer problem. Qualitatively one can see that the power must decrease with time and this is the decrease following the early peak in Fig. (2-1).

As the shock temperature drops below 10^5 °K, the precursor cools to where it gradually becomes transparent so that the radiation from the shock front begins to shine through. When this happens the power-time curve goes through the minimum which is shown in Fig. 2-1 as the shock precursor minimum (SPM). While the shock front gets more and more exposed, the power rise because of the exposure is eventually compensated by the temperature drop of the shock itself and at that time the power level reaches the maximum which is shown on Fig. 2-1 as the shock exposure maximum (SEM).

During the phase following this maximum the rate of thermal radiation loss from the fireball can be characterized as that from a blackbody sphere at the shock front temperature and of radius equal to that of the shock radius. Although such a rate describes the fireball emission, the power observed at any distance will contain only that fraction which the cold air

outside the fireball is capable of transmitting. To a good approximation, that fraction can be calculated by assuming a simple cut-off in the transmitted spectrum. Values of this fraction $f(T_s, \nu_c)$ where ν_c is the frequency corresponding to a cut-off at 1860\AA (representing the edge of the O_2 absorption) are shown as functions of the temperature (T_s) in Fig. 2-7). The fraction is evaluated from a tabulation of the Planck radiation function and its partial integral by Gilmore (1956). The fraction is defined as

$$f(T_s, \nu_c) = \frac{15}{\pi^4} \int_0^{x_c} \frac{x^3 dx}{e^x - 1} \quad (2.2-8)$$

where $x_c = h\nu_c/kT_s$ and h and k are Planck's and Boltzmann's constants, respectively ($h \approx 6.625 \times 10^{-27}$ erg sec, $k \approx 1.380 \times 10^{-16}$ erg/ $^\circ$ K).

During this phase which lasts until the shock temperature has dropped to so low a value as to make the shock front transparent, the following simple expression characterizes the thermal radiation rate for an air burst nuclear explosion:

$$P \approx 4\pi R_s^2 \sigma T_s^4 f(T_s, \nu_c) \quad , \quad (2.2-9)$$

in which R_s represents the shock radius, T_s the temperature, σ the Stefan-Boltzmann constant (5.672×10^{-5} erg/cm²/deg⁴/sec) and $f(T_s, \nu_c)$ the fraction passed by the cold air.

Unit optical depth for most frequencies grows longer as the shock front cools, so that emission from hotter air behind the front begins to shine through. The shock front itself becomes fainter and appears to pull ahead of the luminous fireball, a phenomenon which is referred to as the

"breakaway" (Gladstone, 1962, Section 2.110). Because the shock has been carrying the shock-heated air outwards with its expansion, a rather steep gradient in temperature is maintained just behind the front, so that a slight increase in unit optical depth exposes higher temperatures but at no appreciable decrease in radius of effective radiating surface. At this time the power curve goes through the principal minimum (PMIN) in Fig. 2-1.

Fig. 2-8 indicates the geometry of fireball temperatures (in cross-section) at a time somewhat beyond the time of minimum thermal power. While the thermal radiation increases, and while progressively deeper parts of the fireball are exposed, the hydrodynamic expansion dominates so that the visible or apparent fireball size continues to grow. Eventually, the luminous fireball stops expanding and the power output reaches the final maximum (FMAX).

Throughout this radiative and then hydrodynamic expansion of the fireball, right up to the time of minimum light intensity, something less than half of one percent of the total yield has been radiated out of the fireball. Both integrals of the measured power-time data from tests and of the simple expression given above for radiation from the fireball (as determined by shock front conditions) lead to an answer close to 0.44%. In the latter integral, the properties of the shock front are sufficiently well defined by almost any calculation - even those not accounting for radiation transport in the early phases, but necessarily taking account of the real gas properties of air. (e.g., Brode, 1956a,b).

Since the air just behind the shock is much hotter and much less dense than the air at the front itself (see Figs. 2-2, 2-3, and 2-4), the rate of thermal radiation increases rapidly when that air is exposed, until the hottest temperatures at the back of the steep gradient

behind the shock front become visible and are radiating directly to the exterior. Thereafter, as the size of the radiating sphere shrinks and the interior cools, the rate decreases. This is the period in which the fireball history comes closest to the cooling wave notion expressed in a simple form by Zel'dovich, Kompaneets and Raizer (1958) and applied into a fireball theory by Bethe (1964). The notion is that a recognizable and fixed form cooling wave erodes the hot fireball interior, beginning at the exterior and working inwards. After the shock front has become transparent, such a cooling wave process is very likely operating, but it is not at first working into a fixed or uniform temperature or density, and it is not shrinking the fireball. The outward hydrodynamic expansion is still too strong. When the outer regions have all become sufficiently cool and transparent so that the inner radiation-heated region is exposed, then the conditions suggested for a cooling wave are approximated. Even then the temperatures are not constant and the surface area is shrinking rapidly, so that the cooling rate decreases. When this interior sphere has cooled to below about $10,000^{\circ}\text{K}$, the whole of the fireball has become relatively transparent, and the subsequent radiation losses are characterized more by a grey body approximation, i.e., characteristic of a volume of air of low emissivity - one of less than unit optical thickness. It may also still be expanding adiabatically, and contributing energy to the shock growth.

Temperature profiles spanning this period from principal minimum through final maximum and on to a transparent fireball are illustrated in Fig. 2-9. For a yield of one kiloton, the cooling wave is less obvious as a wave than as a rather sudden depletion of the hottest interior region. At larger

yields, where more optical thickness is represented at every stage, the progress of a cooling wave from outside toward the center is more easily imagined (Brode, 1964a, Fig. 5, b Fig. 15).

In this rather complex power radiated history of two or three maxima, as illustrated in Fig. 2-1, the final pulse represents a total energy of 30 or 40% of the total yield of the nuclear device. When all the energy is accounted for, including that in the infrared which originates in shock heated air outside the visible fireball and is radiated only very slowly, the fraction may be even larger.

There are several features of this one kiloton explosion that have not yet been mentioned and that are of lesser influence on the thermal radiation and fireball behavior at sea level, but which become relatively more important at other yields or altitudes. One such feature is a second shock wave which originates within the bomb vapors, traverses the early sphere of hot air behind the radiation front, and overtakes the strong shock that forms the fireball surface at later times. This debris or bomb shock is seldom in evidence in sea level explosions, and has lost most of its energy long before it overtakes the main shock, so that it contributes little to the fireball surface or thermal radiation histories. Because the hot interior of the fireball is for most of the fireball expansion a region of long mean free path, it is a region of nearly uniform temperature. When the case shock compresses and heats this air further, some of that heat is promptly re-radiated ahead, forcing this interior shock to behave isothermally rather than adiabatically. This isothermal shock can lose energy very rapidly by this means, and may persist only through the

continuation of its outward momentum.

A history of the radii of this shock and other fronts in this kiloton example is shown in Fig. 2-10. When this debris shock travels outward to the edge of the fireball, it encounters a sharp discontinuity in density. At that point, a reflected shock originates and is returned inward to implode upon the origin. Here again, is a phenomenon which has no consequence for this example, but may be prominent in high altitude events. The vaporized bomb expands along behind this debris shock, but at sea level is not visible until very late - after the second maximum in the thermal power. This bomb debris is not realistically treated in any of the usual calculations, since they invariably assume radial symmetry and allow no mixing or turbulent flow. When it emerges in the transparent fireball at late times, the vaporous debris has become highly turbulent and has evidently mixed with considerable fireball air.

Although Fig. 2-10 indicates a transition from radiation expansion to strong shock expansion, the radiation diffusion does not stop. As the shock brings down the density in the interior air, the opacity of that air decreases also, and the radiation is allowed to diffuse into some of the now shock-heated air. The dotted curve below the shock front curve of Fig. 2-10 indicates the position of the radiation front. Most of its outward excursion is due to the flow of air in the expansion behind the shock itself. At times later than shown in Fig. 2-10, the radiation front and the visible fireball drop behind. The short dashed curve near the end of the shock front curve of Fig. 2-10 represents a position close to the fireball front - being the locus of points at 5000°K - with higher temperatures inside of that radius, and colder temperatures outside.

The continued flow of radiation is made more obvious in a plot of the temperature histories of several shells of gas representing the air that was shocked to a particular temperature, cooled in the subsequent adiabatic expansion, but then reheated by the radiation wave following. Such a set of curves are shown in Fig. 2-11, where at particles shocked to 10^5 , 70,000 and 40,000^oK the adiabatic cooling is arrested by the arrival of the radiation diffusion wave which causes that shell of air to rise in temperature again. The air starting at the 20,000^oK shock point is never over-run by the radiation wave, i.e., the radiation wave stops before it gets that far, having run out of energy and not being aided by further expansion which would help to reduce the opacity of the cooler air in front of it.

A great many nuclear weapon applications, tests, and effects interests involve the thermal and fireball effects of nuclear explosions on or close to the surface of the earth. Many interesting and novel interactions occur which are not evident in air bursts well away from the surface. However, there is no intention of providing a review of these factors in this current effort. It should suffice to point out that all of the essential features which are described and followed here are also an important part of surface bursts, while the latter are further complicated by the early injection into the fireball of massive amounts of earth material, and by the geometric distortions of the fireball that occur as a consequence of shock and thermal reflections from the earth's surface. The change in radiator shape from spherical to at best hemispherical or worse a partially obscured hemisphere means that the thermal flux to other points on the earth's surface will be less than that from an air burst. Total flux at

points in the air above the burst may at the same time be increased.

As the earliest pictures of nuclear explosions (Glasstone, 1962) clearly show a further consequence of the ground involvement is the "dust skirt" which precedes the fireball shock and largely obscures the base of the fireball. Although not visible in any of the pictures, there must also be vast amounts of earth shovelled into the hot fireball interior at an early time (Brode and Bjork, 1960), and this material cannot fail to have profound effects on both the temperature and thermodynamic state of the fireball gases and on the opacities or optical properties of that region. Test observations indirectly attest to the influence of such surface effects.

Observations and measurements at very late times in the fireball history show that the radiation rate trails off with a very long tail (as in Fig. 2-1) and comes from shapes other than simple spheres. The fireball at late times is like a bubble in the atmosphere - having very low densities in its interior - and so it rises, and in rising breaks up at the bottom to transform itself into the familiar atomic cloud ring or torroid which rolls its way up through the atmosphere. The torroidal circulation that is induced is quite strong and serves to severely limit mixing of the hot fireball gases with the exterior cold air, thus prolonging the existence of air and debris at temperatures of thousands of degrees Kelvin, while the cloud rises in the atmosphere. When much earth material and/or water vapor is present, the late fireball remains opaque, and the rate of late radiation is more determined by the rate of turbulent mixing which brings hot gases to the cloud surface rather than by the radiation transport

properties alone. For an air burst well above the surface, however, the late fireball becomes quite transparent, so that only a faintly luminous ring assures us that the rise and circulations are much the same as for lower bursts.

2.3 Other yields and altitudes

The example of a one kiloton detonation at sea level contains all the basic physical phenomena which enter into consideration at other yields and at altitudes up to about 70 km. The overall appearance is, nevertheless, appreciably different since the individual events which are responsible for the various maximum and minima in Fig. 2-1 occur at different times.

In carrying out a discussion of these changes, it is useful to note that the relation between shock radius and time can be approximately represented by a hydrodynamic scaling law. To formulate this we introduce the scaled variables

$$R^* = \left(\frac{\bar{\rho}}{Y} \right)^{1/3} R \quad (2.3-1)$$

$$t^* = \left(\frac{\bar{\rho}}{Y} \right)^{1/3} t \quad (2.3-2)$$

where Y is the yield of the explosion and $\bar{\rho} = \rho/\rho_0$ the ambient air density relative to that at sea level. In our 1 kiloton sea level example the scaling factors are of course unity.

The scaling law is not valid until after the debris shock has caught up with the somewhat slower shock which is driven by only a fraction of the total yield. The scaling law can be deduced from the strong-shock solution for a point source (Taylor, 1950; and Sedov, 1959). This limits the validity of the scaling laws at late times when the shock becomes weak. The law obtained in this manner takes the form

$$R_s^* = k(t^*)^{2/5} \quad (2.3-3)$$

where the subscript s denotes that the value is taken at the shock front.

From the radius $R_s = 20 \text{ m}$ read off Fig. 2-10 for $t = 1 \text{ msec}$, one determines the proportionality factor to be

$$k = 20 \text{ m (msec)}^{-2/5} (KT)^{-1/5} \quad (2.3-4)$$

In the above scaling law the scaling factors cancel out of the expression for the shock velocity

$$\frac{dR_s}{dt} = \frac{dR_s^*}{dt^*} = \frac{2}{5} k(t^*)^{-3/5} \quad (2.3-5)$$

which makes this velocity a function of t^* only. Applying the Hugoniot relations one can now show that the temperature T_s behind the shock is

also very nearly a function of t^* only. This is not an exact result because it depends on certain assumptions about the equation of state which are only approximately true. If one checks the prediction that T_s is a function of the scaled time only against computed results, one finds that it fits the changes with yield at a given altitude very well. The changes with altitude at a given yield are not given with quite the same accuracy, but are still sufficiently close for most purposes.

It should be noted that the above scaling procedure differs somewhat from the so-called Sachs scaling where one introduces the variables

$$\tilde{R} = (p/Y)^{1/3} R \quad (2.3-6)$$

$$\tilde{t} = (p/Y)^{1/3} (p/\rho)^{1/2} t \quad (2.3-7)$$

If one expresses the ambient pressure and density p and ρ , the yield Y and the variables R and t all in the same system of units, the scaled variables are dimensionless. It is more convenient, however, to replace p and ρ by the ratios $\bar{p} = p/p_0$ and $\bar{\rho} = \rho/\rho_0$ relative to the sea level values, and to express Y as before in KT. With this choice, the strong shock relation between \tilde{R} and \tilde{t} is the same as between R^* and t^* , i.e. Eq. (2.3-3) with the same value of the constant k .

The two methods of scaling differ in regard to what are considered similar situations. For the starred variables similarity implies that for example the hydrodynamic velocity and the temperature are unchanged; for the variables with the tilde the Mach number and the temperature ratio T/T_0 are unchanged. Either choice is acceptable, but ours has the advantage of using only one parameter to characterize the altitude.

From the time of shock formation until breakaway the thermal radiation comes partly from the shock precursor and partly from the shock front, and it is evident that the shock temperature is a major factor in determining the timing of the maxima and minima during this period. At a given altitude where one has a one-to-one relation between shock and precursor temperature (see Eq. 2.2-7 for the sea level case) it is fairly accurate to state that the shock formation maximum, the shock precursor minimum and the shock exposure maximum occur at fixed values of the shock temperature and therefore at fixed values of the scaled time. As one considers different altitudes the relation between T_p and T_s changes and one finds different values of the scaled times associated with these features of the power curve.

After breakaway the radiation comes from points to the inside of the shock front whose locations depend on the optical properties of the air and in turn on the temperature and density distribution. This is a radiative transfer problem and hydrodynamic scaling, where times vary as the cube root of Y , is replaced by radiative scaling, where times vary approximately as the square root of Y (Glasstone, 1962, section 7.92).

Altitude scaling is a more difficult problem than yield scaling. We have already mentioned the effect of the changing relation between T_s and T_p . To this we must add that the relative importance of hydrodynamics and radiation transfer shifts with increasing altitude in favor of the latter. Thus shocks form more slowly and radiation is emitted more rapidly as one goes to higher altitudes. As a result the features before breakaway are increasingly delayed and the maxima and minima tend to become weaker. The final radiative pulse on the other hand advances in time and becomes more prominent. At about 50 km the early features have become washed out and what was the final pulse is now the only pulse.

References

Bethe, H.A., Theory of the Fireball,
LASL, LA-3064, Feb. 1964

Brode, H.L., Point Source Explosion in Air,
RAND, RM-1824-AEC, Dec. 1956 (a)

Brode, H.L., The Blast Wave in Air Resulting from a High Temperature, High
Pressure Sphere of Air, RAND, RM-1825-AEC, Dec. 1956 (b)

Brode, H.L., A Review of Nuclear Explosion Phenomena Pertinent to Protective
Construction, RAND, R-425-PR, May 1964 (b)

Brode, H.L., Fireball Phenomenology,
RAND, P-3026, Oct. 1964 (b)

Brode, H.L. and R.L. Bjork, Cratering from a Megaton Surface Burst,
RAND, RM-2600, June 1960

Gilmore, F.R., A Table of the Planck Radiation Function and its Integral,
RAND, RM-1743, July 1956

Glasstone, S., The Effects of Nuclear Weapons,
Superintendent of Documents, 1962

Heaslet, M.A. and B.S. Baldwin, Predictions of the Structure of
Radiation-Resisted Shock Waves, Phys. of Fluids, 6, 781, 1963

Raizer, Iu. P., On the Structure of the Front of Strong Shock Waves in Gases,
J.E.T.P. 5, 1242, 1957

Sedov, L.I., Similarity and Dimensional Methods in Mechanics,
Academic Press, 1957

Taylor, G.I., The Formation of a Blast Wave by a Very Intense Explosion,
Proc. Roy. Soc. (London), A201, 159, 1950

Zeldovich, Ia. B.J., Shock Waves of Large Amplitude in Air,
J.E.T.P., 5, 919, 1957

Zeldovich, Ia. B.J., A.S. Kompaneets and Iu. P. Raizer, Cooling of Air by
Radiation, J.E.T.P., 7, 882, 1001, 1958

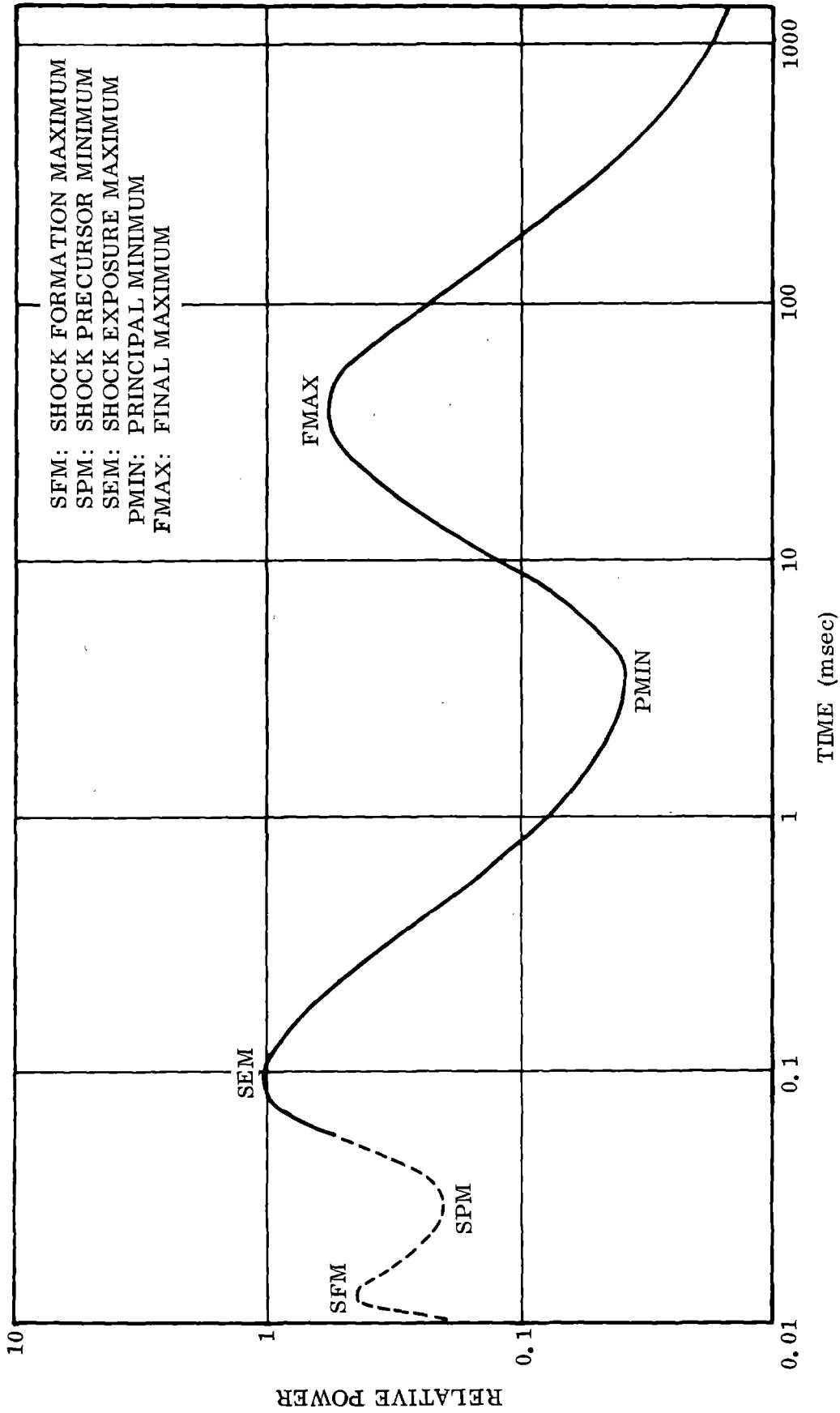


FIG. 2-1 THERMAL POWER RADIATED FROM ONE KILOTON AT SEA LEVEL

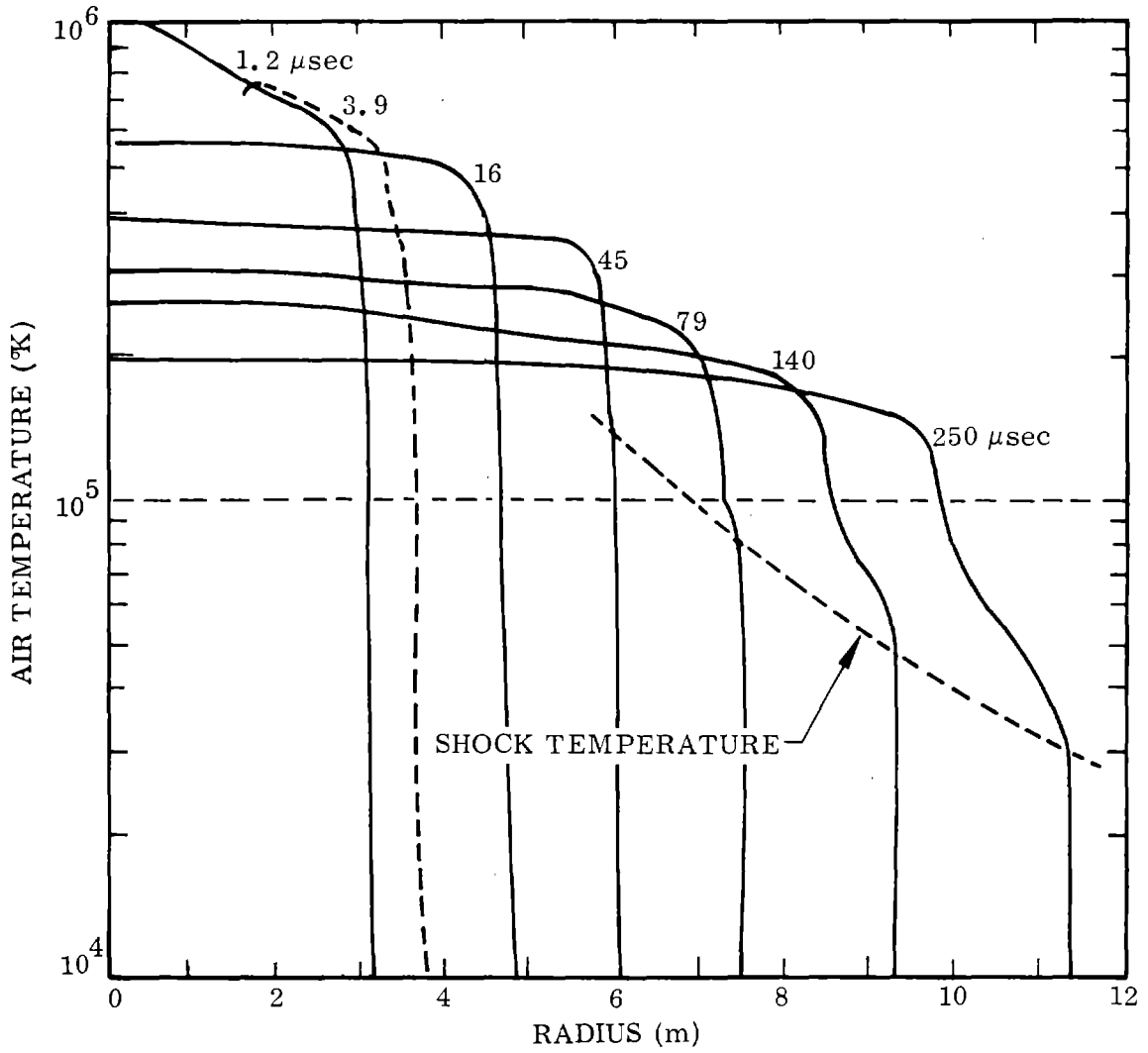


FIG. 2-2 EARLY TEMPERATURE PROFILES - 1 KT, SEA LEVEL

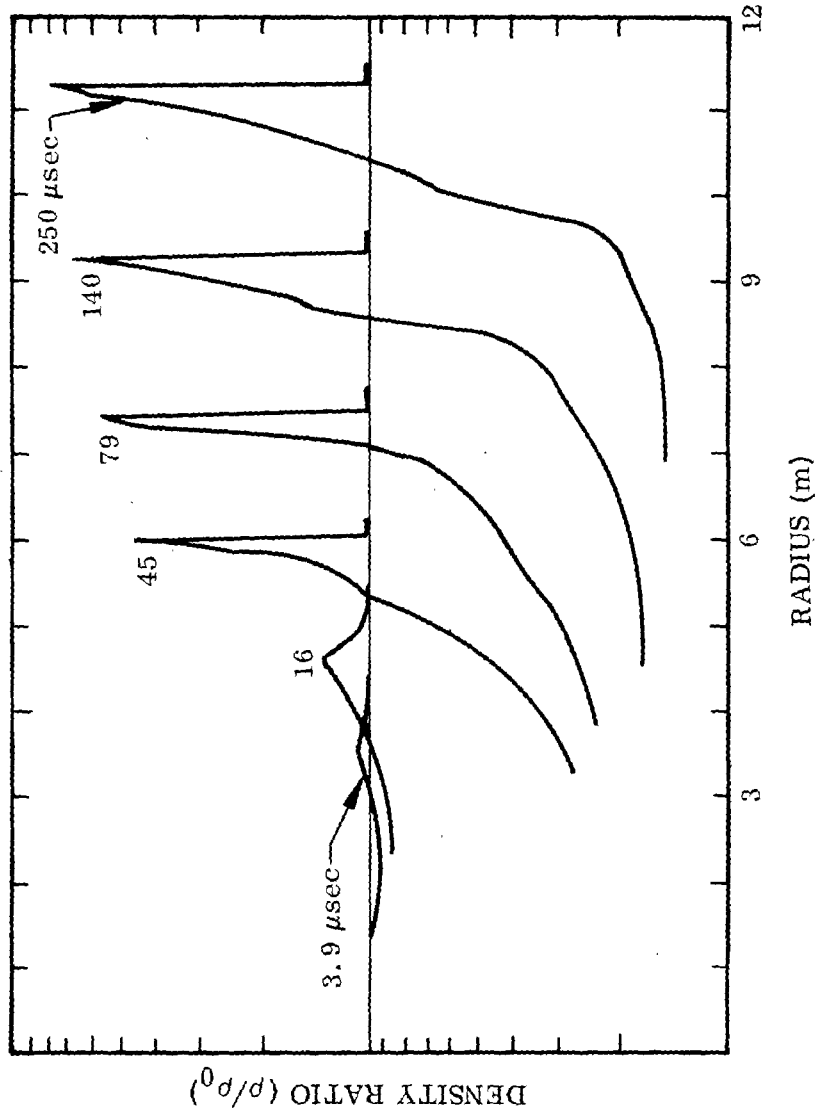


FIG. 2-3 EARLY DENSITY PROFILES - 1 KT, SEA LEVEL

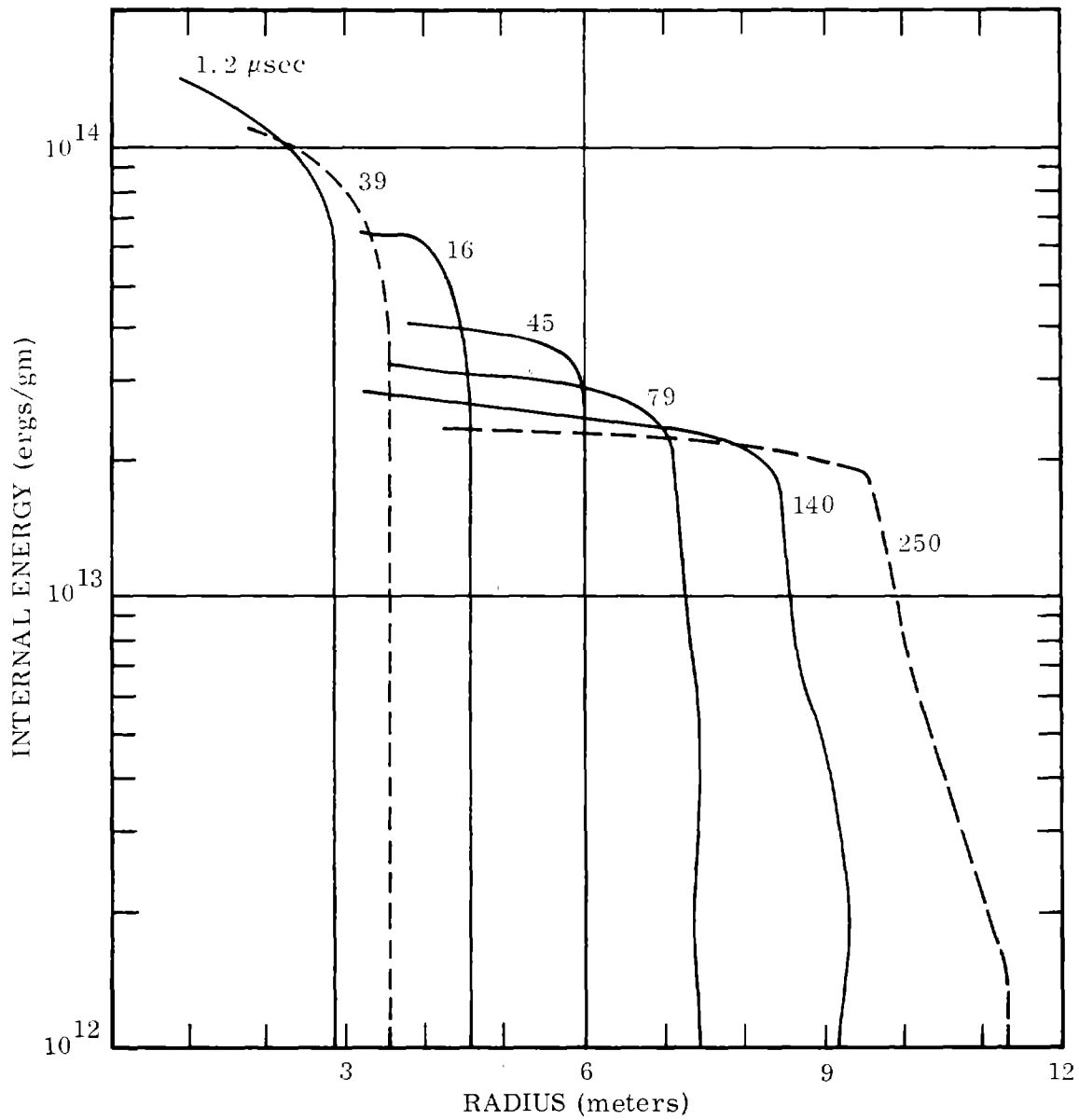


FIG. 2-4 EARLY ENERGY DENSITY PROFILES - 1 KT, SEA LEVEL

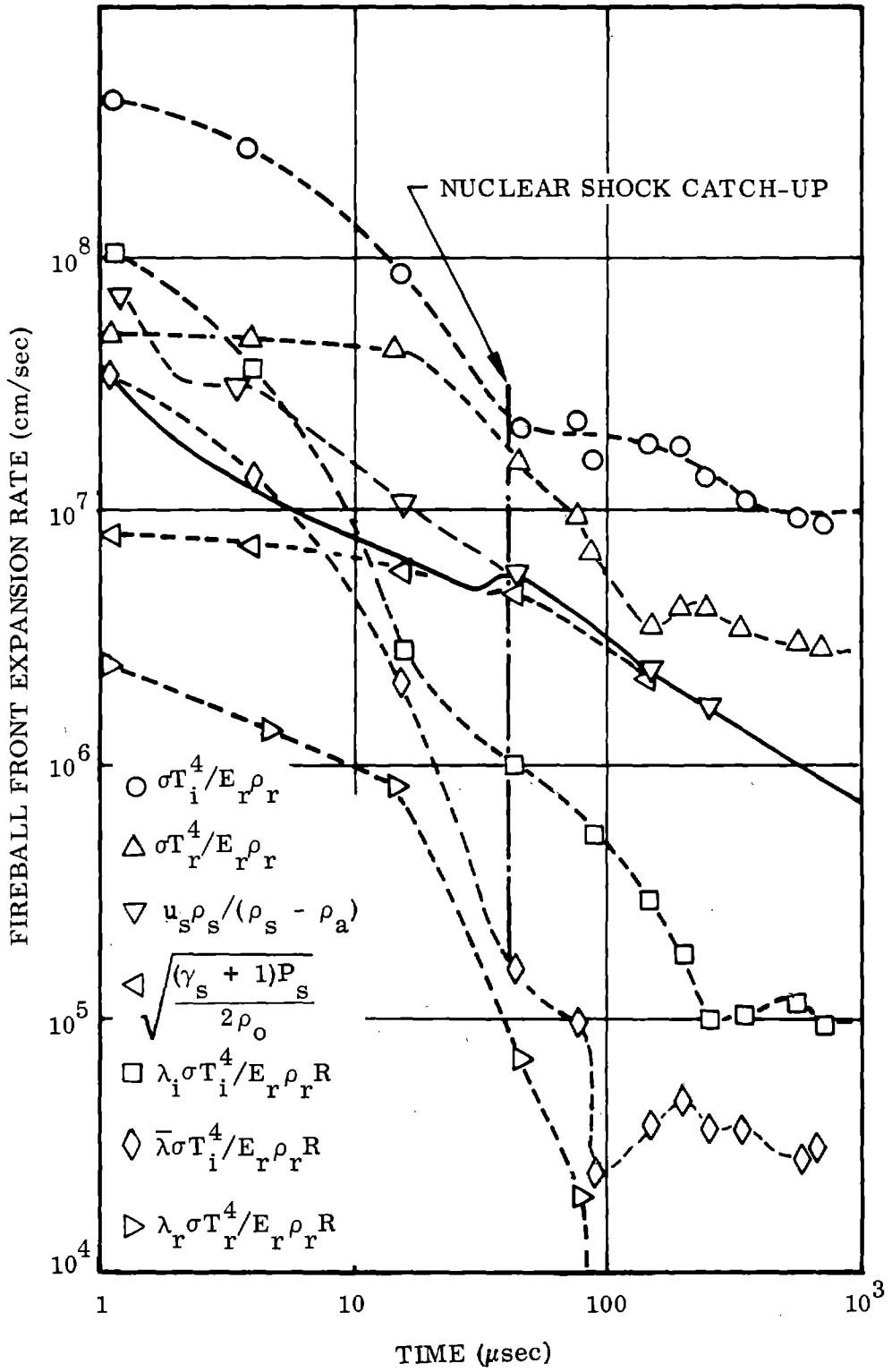


FIG. 2-5 COMPARISON OF VARIOUS APPROXIMATE RATES WITH EARLY FIREBALL GROWTH RATE

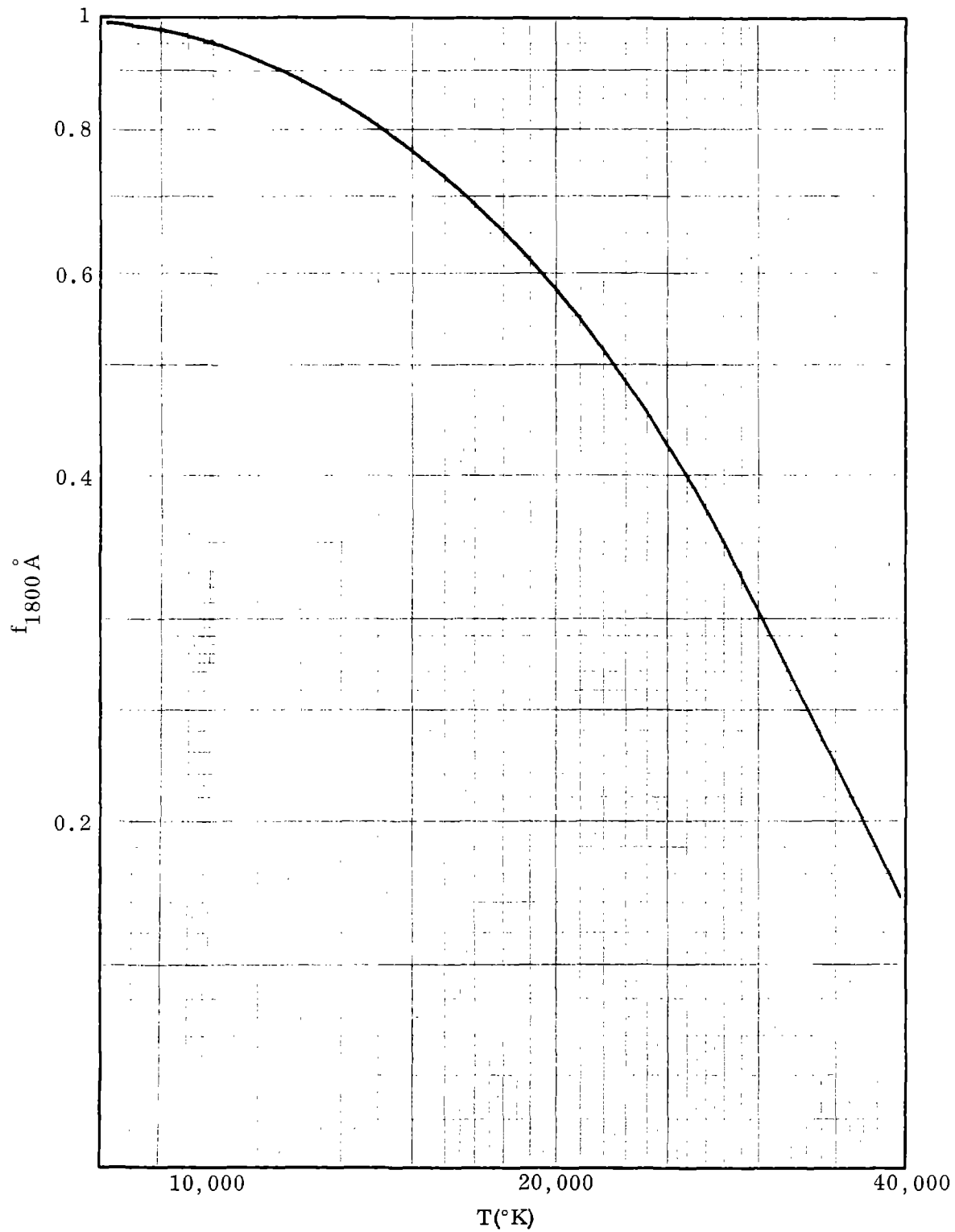


FIG. 2-6 FRACTION OF BLACKBODY RATE AT WAVELENGTHS LONGER THAN CUTOFF AT 1860Å

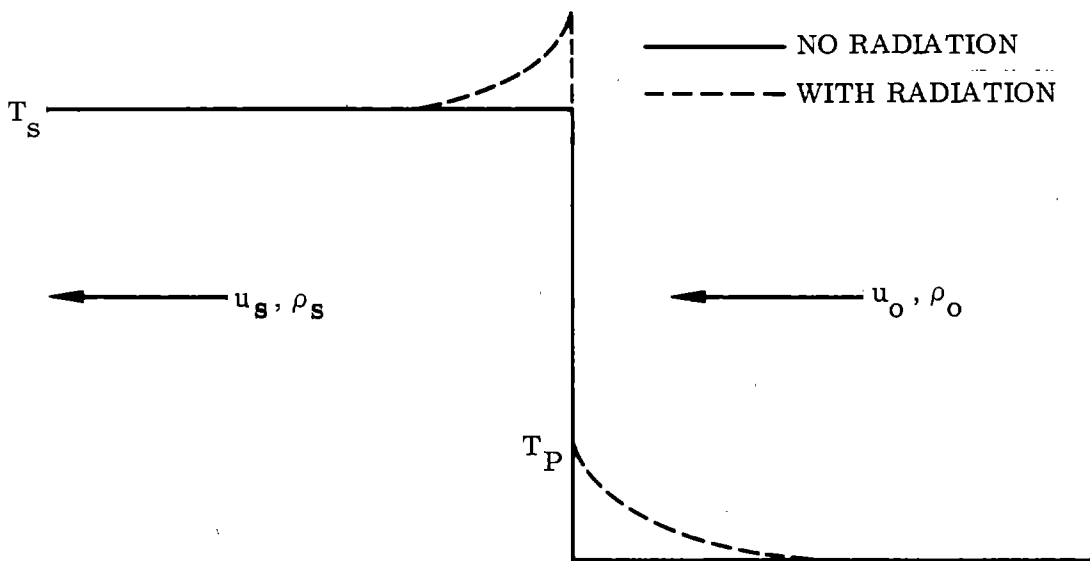


FIG. 2-7 SHOCK TEMPERATURE PROFILES WITH AND WITHOUT RADIATIVE TRANSPORT

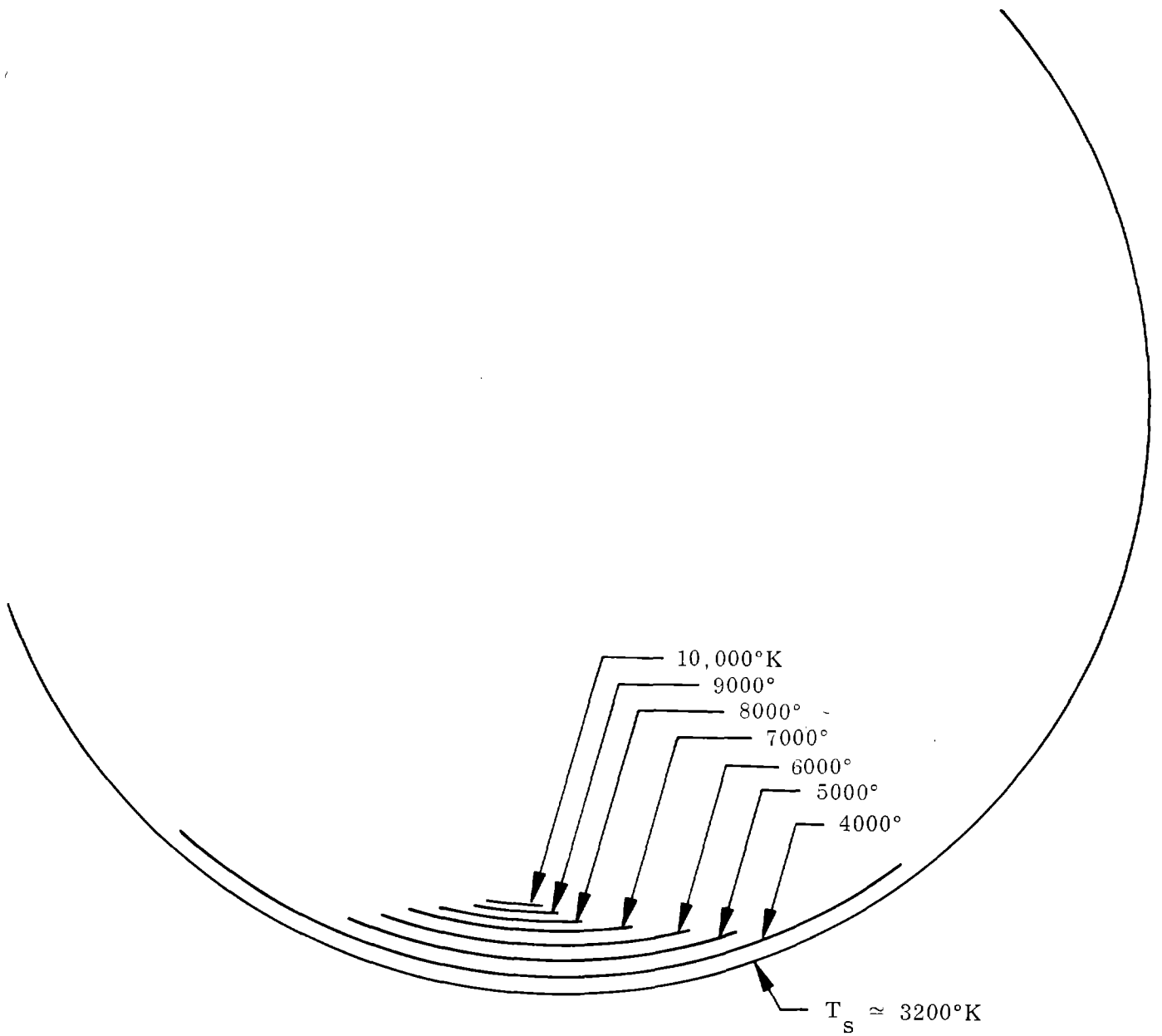


FIG. 2-8 FIREBALL THERMAL GRADIENTS AT TIMES NEAR MINIMUM LIGHT INTENSITY

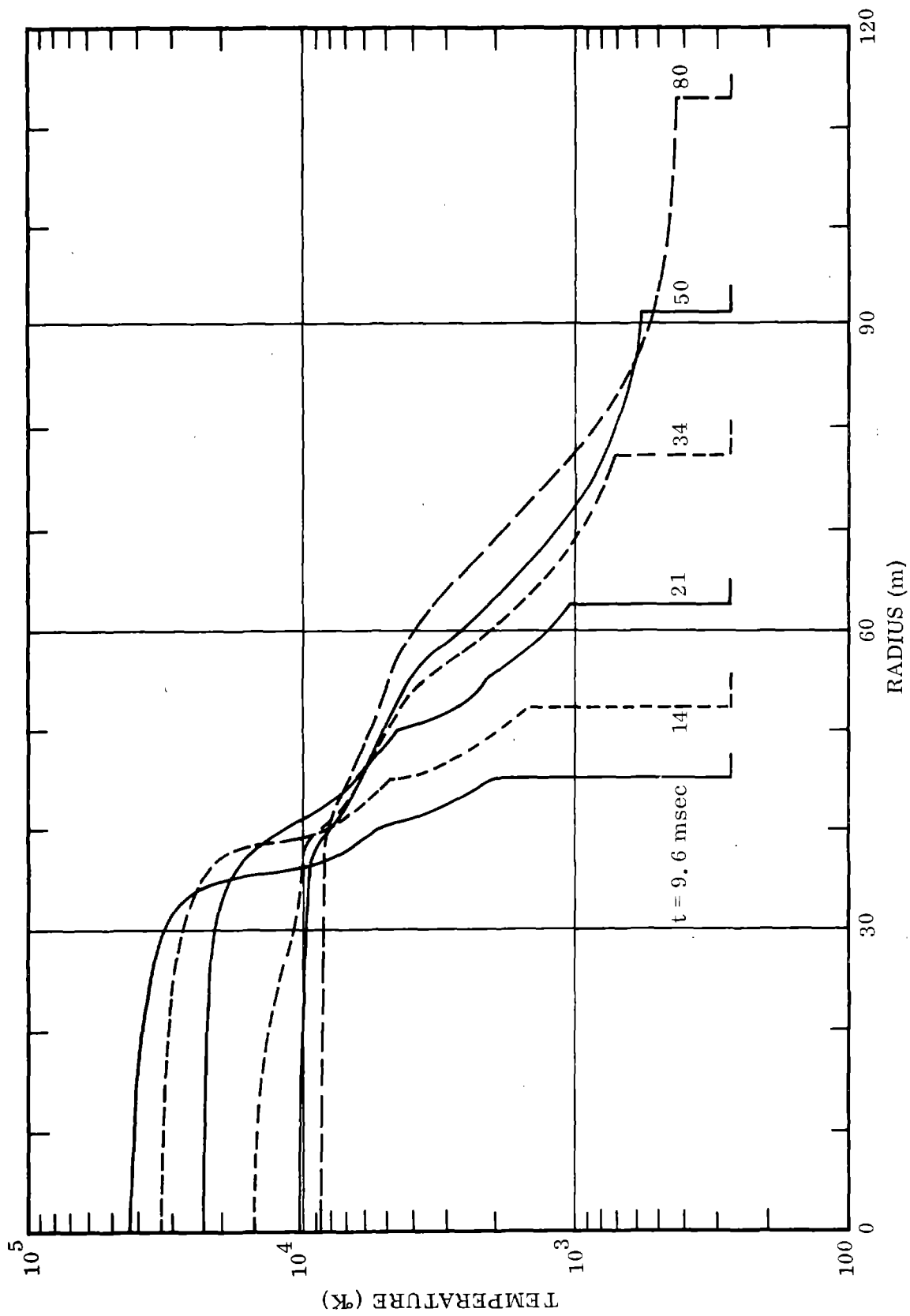


FIG. 2-9 LATE FIREBALL TEMPERATURE PROFILES - 1 KT, SEA LEVEL

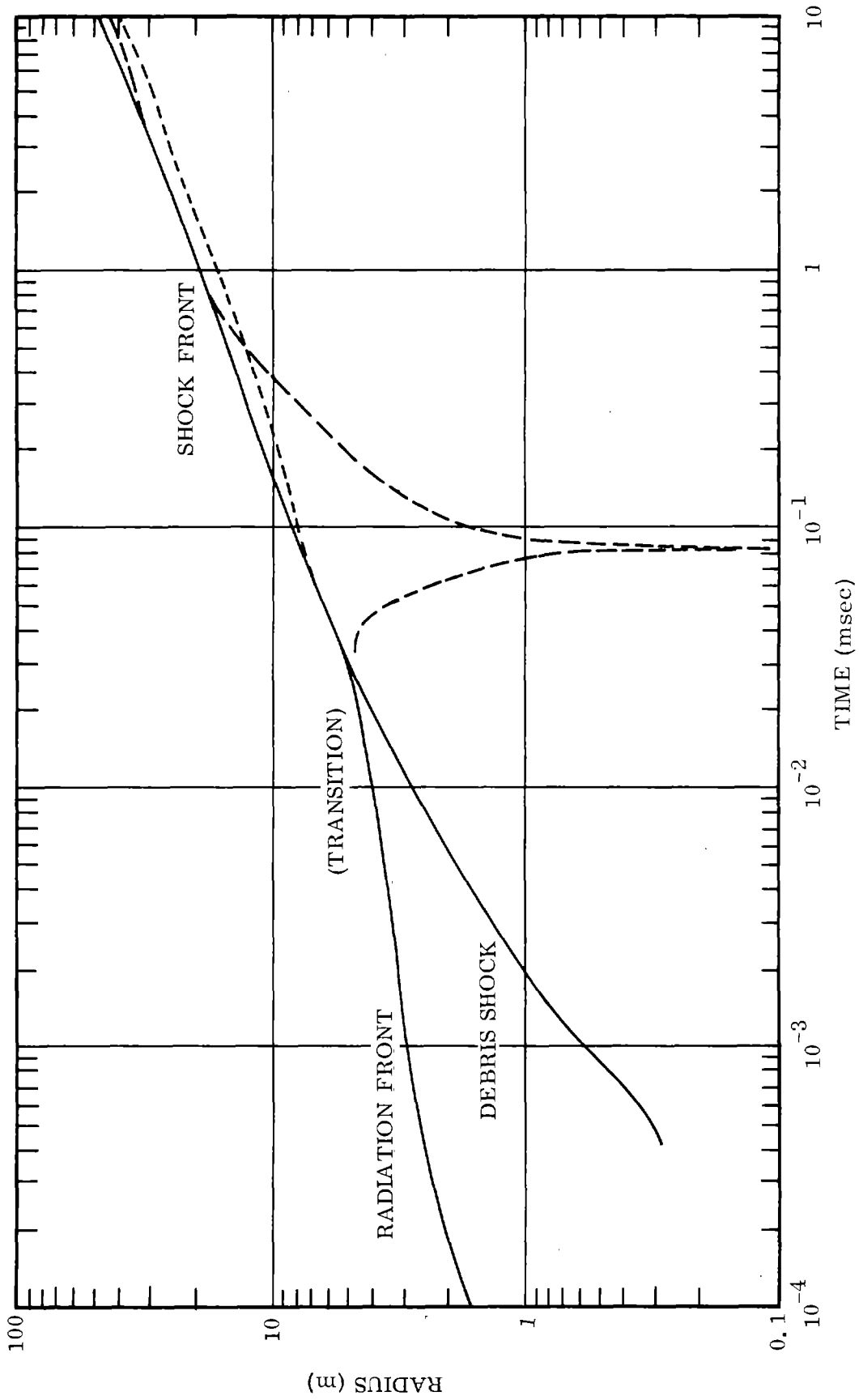


FIG. 2-10 EARLY RADIUS-TIME FOR A ONE KILOTON - SEA LEVEL FIREBALL

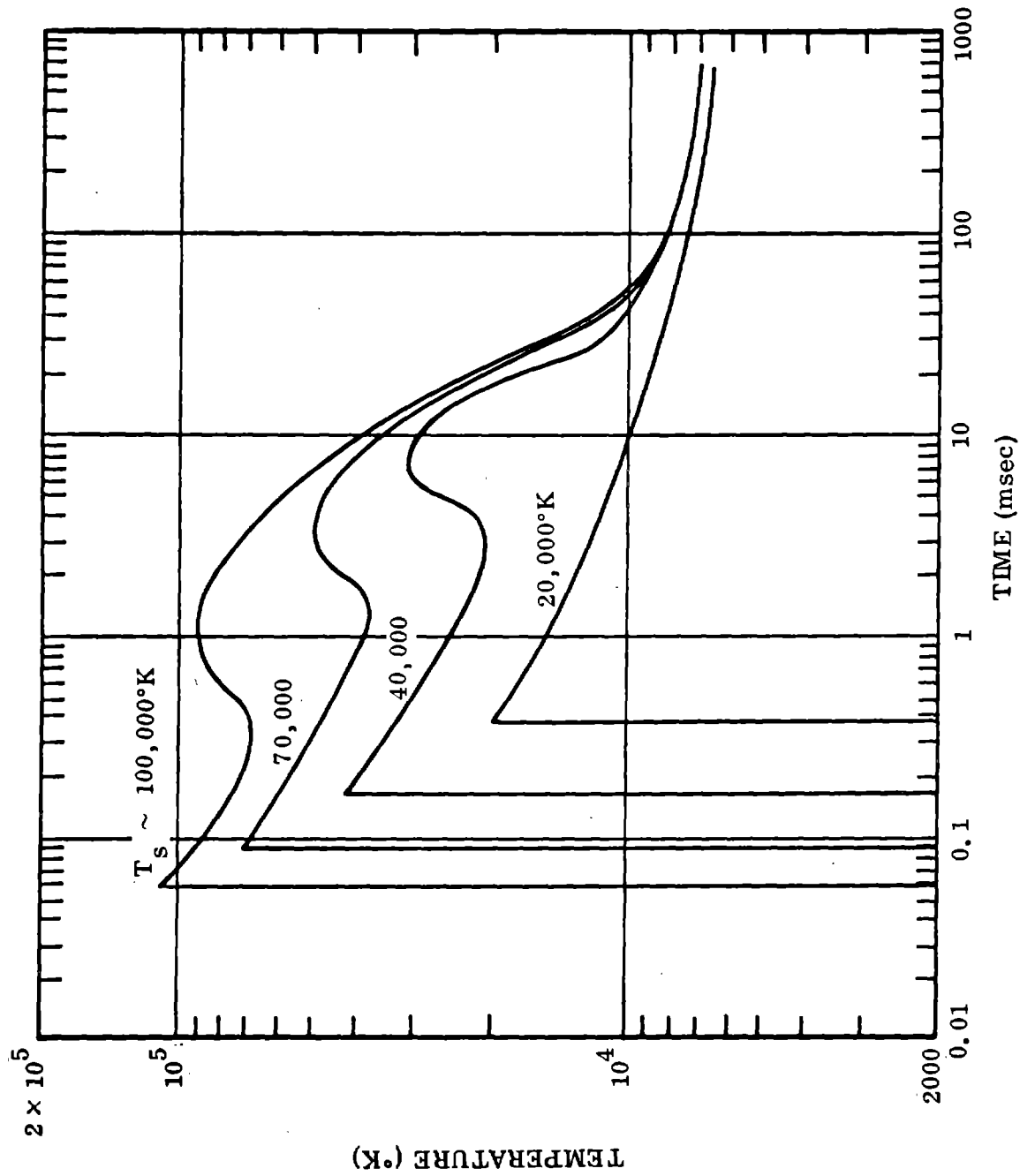


FIG. 2-11 AIR MASS TEMPERATURE HISTORIES - SHOWING ADIABATIC EXPANSION COOLING AND THE HEATING BY THE FURTHER GROWTH OF THE RADIATION DIFFUSION WAVE

Chapter 3 . SUMMARY

As the reader of this report will have gathered any attempt at following the evolution of a fireball by numerical means utilizes a whole spectrum of facts and assumptions ranging all the way from being undisputable to being highly suspect. This is likely to leave him with a somewhat uncomfortable feeling about the reliability of such a calculation. In this summary we will put the finger on some of the underlying assumptions, point out what we know about their validity and evaluate how strongly our lack of basic information or of the willingness to spend computing dollars will influence the final product.

3.1 Equation of state

Nearly all calculations make the basic assumption that the air remains throughout in a state of LTE.* Once this is accepted it follows that the relation between the various state variables can be found by the methods of statistical mechanics. The application of these methods is very straightforward and the results as presented in (1) and (3)** are probably correct to within a few percent. In some instances analytic fits which were made to feed these results into a computer have been poor but this problem can certainly be overcome and should not contribute significantly to errors in hydrodynamics or other phases of the main calculation. Some problems may arise in the central region where one has debris rather than air and even more so in the transition region where one may have a debris air mixture. Fortunately many important results are rather insensitive to these details.

* Local Thermodynamic Equilibrium (LTE).

** (1) stands for DASA-1917-1, etc.

3.2 Absorption coefficients

This subject has been discussed in detail in (2) and related facts are brought up in Chapter 1 of this volume. There are several ways of describing the absorption which differ in the amount of detail which is presented. The most detailed description consists of a listing of lines with intensities and line shape parameters on top of a continuum. All these factors are subject to errors as we shall briefly discuss.

In the low temperature case where the lines are due to molecular systems the information comes largely from experimental spectroscopic studies. The limitations of our knowledge about frequencies and intensities is discussed in (2) Chapter 7. The information on line shapes is almost non-existent. To this one should add that one can hardly afford to include any but the strongest band systems. Even the rather minimal choice of eight band systems in the most recent version of the SACHA program brings the number of transitions to over 190,000.

In the high temperature case the absorption comes from inverse Bremsstrahlung and from transitions in atoms and atomic ions. There is a strong continuum due to the first and due to photoionization. There is a fairly well developed theory and some experimental information backing it up. On top of the continuum is a large number of lines. A few levels have been observed experimentally but the majority, especially for the highly ionized atoms, have not been observed and must be obtained theoretically. It is certainly necessary to find the transition probabilities by quantum mechanical methods. These are so complex that one is forced to make radical approximations to get any answers and the results are not very reliable.

The calculation of the line contribution is the most elaborate part of the program and again one can hardly afford to include any but the strongest lines. This involves a somewhat arbitrary cut-off procedure whose practical effect can only be evaluated when one specifies how the absorption coefficient is to be used.

The detailed description of absorption with fine spectral resolution greatly exceeds the requirements of radiative transfer calculations. As shown in (2) Chapter 2, it is unfortunately difficult to define averages which permit satisfactory calculations. Thus Planck and Rosseland means which average μ_ν and μ_ν^{-1} respectively apply only in limiting situations; the one for very transparent, the other for very opaque media. Nevertheless such means are useful and have been calculated. In the specific case of line effects, mentioned in the preceding paragraph, the contribution is not very large until one reaches temperatures like 2×10^5 °K and high densities.

Because of the many uncertainties entering the calculation of absorption coefficients one has no systematic way of estimating their accuracy. The responsible authors of opacity calculations are generally confident that their results lie within a factor of three of the true values.

In the intermediate temperature range where the opacity reaches a maximum, the accuracy is probably somewhat better. Because of the large opacity the averaging procedures, which are appropriate for radiative transfer calculations, put the most weight on those parts of the spectrum where μ_ν is small and very little weight on the lines. The Rosseland mean does and the Planck mean does not fall into this class. Because of

the emphasis on the continuum, where one has more reliable information, the Rosseland mean is expected to be more accurate.

The extent to which opacity errors falsify fireball calculations depends on the temperature range. Inspecting the temperature profiles of Fig. 2-2 which are typical for the early stage of a fireball one finds large temperatures near the center which makes the air in that region very transparent. Further out the temperature drops so that the opacity rises, goes through a maximum and then drops again. In the transparent central region radiative heat transfer is rapid and keeps that region at a fairly uniform temperature, as one sees in Fig. 2-2. Just how uniform this profile is has very little effect on the rate of expansion and therefore opacity errors by a factor twice or even more are not serious in that region.

The opaque zone around the central region acts as a radiative barrier and the development of the fireball does depend quite critically on the opacity there. During the very early phase where hydrodynamic motion is still negligible compared to the radiative expansion the section of the opacity-temperature relation near the maximum determines the rate of that expansion. It also determines when and where the hydrodynamic shock begins to form.

When shock temperatures are still high, the opaque shell forms in a temperature toe ahead of the shock. This is the precursor which has been sketched in Fig. 2-7 and which causes the early structure in Fig. 2-1. At this stage the opacity is still of interest, since it determines the character of the escaping radiation and other observable phenomena, but the rate at which the fireball expands is given by the shock speed which does not depend on the opacity in the toe.

The next phase starts when the shock temperature has dropped low enough that the shocked air becomes opaque. This is aided by the high density directly behind the shock which can be seen for example, in the density profiles of Fig. 2-3. Up to that time radiative transfer plays a major role in feeding energy to the expanding shock front. Now that source fades out and hydrodynamics takes over as the dominant mechanism for energy transfer. The details of the change depend quite critically on the opacity relation.

Upon further cooling the shock front becomes transparent again and the opaque shell recedes toward the center. This starts the long time interval during which the power vs. time curve of Fig. 2-1 goes through its minimum, rises back to the final maximum, and starts to drop again. The calculation of this phase also depends quite critically on the opacity. A test calculation made with an opacity twice the accepted value stretched the total duration of this phase by almost a factor of two with a corresponding reduction of the maximum power level to about half of what it was in the earlier calculation. Thus, errors in the opacity relation could lead to fairly severe discrepancies between fireball models at the time of the second maximum.

3.3 Radiation hydrodynamics codes

The purely hydrodynamic part of any code is probably as accurate as the equation of state that is being used except for the smearing out of the shock front introduced by the artificial viscosity method. The accuracy of radiative transfer calculations is less certain, unless one is justified in using the diffusion approximation. In that case the limiting factor is

probably the accuracy of the opacity. Difficulties do arise, however, at the front of an opaque shell. Consider, for example, two zones labeled *a* and *b* whose temperatures place them on the rising branch of the opacity curve as indicated in Fig. 3-1. As the heating wave progresses these points move up on the curve. The radiation escaping to the outside comes at first from zone *a* and passes without attenuation through zone *b*. As zone *a* climbs higher the radiation rises as T^4 but when zone *b* becomes sufficiently opaque to take over the role of zone *a* the power output drops. This cycle is repeated when zone *c* and others after it climb into the position originally held by zone *a*. The result of this is a sequence of maxima and minima in the power versus time curve which has no physical reality. This spurious effect can be counteracted by using finer zone sizes but at the expense of increasing the running time which increases as the square of the number of subdivisions per zone. Actually this is not necessary, since test calculations show that the cruder zone divisions lead to the same average power and to the same rate of expansion as a very fine division. A related problem arises when the artificial viscosity routine introduces improper heating ahead of the shock front. Letting the point *a* in Fig. 3-1 represent the shocked zone and *b* and *c* the zones just ahead of the shock, this heating would make points *b* and *c* lie at too high temperatures. The calculated attenuation of the radiation from the shock is therefore larger than what it should really be and leads us to predict too low a brightness of the fireball. The reduced output has, however, practically no effect on the calculated motion of the fireball air because at that stage the amount of energy lost by radiation is still too small to influence the hydrodynamics.

Other errors may be introduced by the use of approximate integration routines such as the multiple ray or the two stream techniques which have been discussed in Chapter 1. Given a set of experimental data one can, within limits, adjust the opacity temperature relation so that either model will reproduce these data. It is therefore not really possible to disentangle errors which may arise from the use of these models on the one hand, and from incorrect absorption coefficients on the other hand.

3.4 Deviations from LTE

As we have repeatedly stated, nearly all calculations assume the air to be always in LTE. There are, however, some equilibration processes which are decidedly slow on the time scale of nuclear fireballs. At somewhat elevated altitudes one finds for example, that the processes responsible for populating the vibrationally excited levels of O_2 and N_2 fall into this class. These processes are discussed under the heading "vibrational relaxation" in (4) section 6.1. In the case of O_2 , populating the vibrational levels reduces the photon energy required for reaching the Schumann-Runge continuum below the 8.5 eV which it takes from the ground state. As long as these levels are not populated the actual absorption is therefore less than it would be in equilibrium. Similar considerations apply to the Birge-Hopfield transitions in N_2 . In most codes these delays are just ignored. Hillendahl (see Appendix A) has attempted to account for them by means of a fairly crude model assumption.

Other deviations from LTE are caused by the slowness of chemical reactions at temperatures, say, below 6000°K (see (4) sections 6.9 and 7.5.) Among the molecules which can form in this temperature range is

NO_2 which has a large absorption coefficient. The delay in forming this molecule when air is suddenly heated by a shock and the subsequent delay in removing it again when the air cools down can change the absorption significantly from the value at equilibrium conditions. If the temperature drop is rapid enough the NO_2 concentration may stay for a long time at the high concentration corresponding to 3000°K even though the temperature has dropped below 2000°K . In this situation one speaks of NO_2 as being frozen in.

Non-equilibrium processes also occur at the debris air interface. It has been pointed out in (4) section 5.2 that this is very poorly understood. It is, in particular, quite uncertain what temperature the shocked air would reach and what X-ray spectrum would be emitted by that air.

The questions raised in this chapter clearly do not exhaust the subject of possible errors in the present state of the art. It is, in fact, quite likely that effects with more practical significance have been overlooked. Still, this enumeration should provide the reader with some guidance what he should watch.

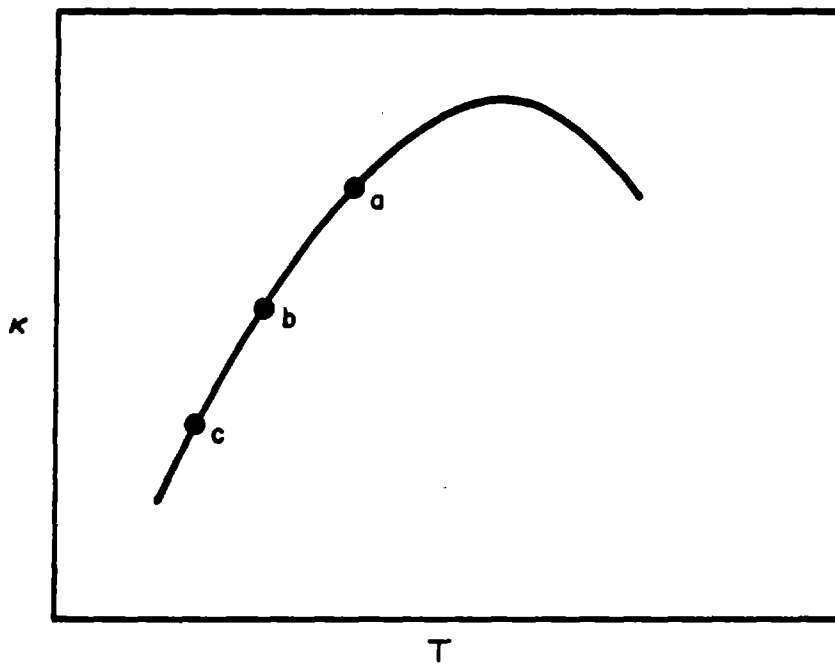


FIG. 3-1 LOCATION OF 3 ADJACENT ZONES ON OPACITY CURVE

Appendix A. A Radiation-Hydrodynamics Code

A.1 Introduction

In this appendix, a sample radiation-hydrodynamics code is presented which employs, with varying degrees of sophistication, much of the physics and basic data presented elsewhere in this volume.

In keeping with Chapter 2, this code describes the radiative and hydrodynamic properties of a sphere of hot air. Details of the weapon itself are not of interest in the present context, and rather crude generalizations have been used to represent the gross properties of the hardware.

The code is presented as a means of demonstrating some of the techniques of radiation-hydrodynamics, as described in Chapter 1, the application of basic physical data, as described in Volume 2, and as an illustration of the results discussed in Chapter 2. The code is not intended as a demonstration of the programming art and has not been polished-up for presentation here. A great deal of the program could be deleted were the program to be used only for present purposes. Much of the basic philosophy of this code has been presented in Chapter 1 and by Hillendahl (1964), and will not be repeated in detail.

The basic equations of the problem are the conservation equations of radiation-hydrodynamics for a one-dimensional spherical system which can be written in Lagrangian form as

$$\frac{\partial U}{\partial t} = - 4\pi R^2 \frac{\partial (P + Q)}{\partial m} \quad \text{Conservation of momentum} \quad (\text{A.1})$$

$$U = \frac{\partial R}{\partial t} \quad \text{Definition of velocity} \quad (\text{A.2})$$

$$V = 4\pi R^2 \frac{\partial R}{\partial m} \quad \text{Conservation of mass} \quad (\text{A.3})$$

$$Q = c \frac{(\rho_0 \Delta R)^2}{V} \left[\frac{\partial V}{\partial t} \right]^2 \quad \text{on compression} \quad \left. \vphantom{Q} \right\} \text{Definition of Artificial Viscosity} \quad (\text{A.4})$$

$$Q = 0 \quad \text{otherwise}$$

$$\frac{\partial E}{\partial t} + (P + Q) \frac{\partial V}{\partial t} + 4\pi \frac{\partial (R^2 \mathcal{J})}{\partial m} = 0 \quad \text{Conservation of energy} \quad (\text{A.5})$$

$$E = E(V, T) \quad (\text{A.6})$$

$$P = P(V, T) \quad (\text{A.7})$$

$$\mathcal{J} \text{ is an integral functional of } V \text{ and } T \quad (\text{A.8})$$

where

U = local fluid velocity

t = time

R = radius

P = pressure

Q = artificial viscosity

m = mass

c = an arbitrary constant near unity

ρ_0 = initial density

V = specific volume (reciprocal density)

\mathcal{J} = radiative net flux at R

E = internal energy

Quite generally, the mathematical formulation of the problem may be characterized as an initial value problem whose solution consists of a time-wise and mass-wise integration of a well defined set of hyperbolic partial differential and partial integro-differential equations.

The solution of these equations is carried out by numerical techniques in which values of the dependent variables are determined in terms of the two independent variables (the time and lagrangian zone mass) by means of finite difference equations which are used to represent Eqs. (A.1) - (A.8).

For purposes of numerical computation, the fireball configuration is represented by a series of concentric, contiguous, spherical mass shells. The mass of the k^{th} zone is designated by m_k (gm/cm^3). Since the mass zones retain their identity throughout the time-wise development of the configuration, the zone index k and the time t (seconds) are convenient choices for the independent variables.

Integration of the set of 8 equations (Eqs. (A.1) - (A.8)) then determines the values of the 8 dependent variables as functions of k and t . $U(k,t)$ (cm sec^{-1}) and $R(k,t)$ (cm) are used to specify the instantaneous values of the interface velocity and radius of the outer surface of the k^{th} mass shell. $\mathcal{J}(k,t)$ ($\text{ergs cm}^{-2} \text{sec}^{-1}$) is used to specify the instantaneous value of the net radiative flux at the outer boundary of the k^{th} mass zone. $P(k,t)$ (dynes cm^{-2}), $Q(k,t)$ (dynes cm^{-2}), $V(k,t)$ ($\text{cm}^3 \text{gm}^{-1}$), $T(k,t)$ ($^{\circ}\text{K}$), $E(k,t)$ (ergs gm^{-1}) are used to represent the instantaneous values of

the pressure, artificial viscous pressure, specific volume (reciprocal density), temperature and internal energy of the mass zone m_k .

In a purely hydrodynamic problem without radiative transfer, it is the standard practice to reckon the thermodynamic properties of a zone (i.e.: pressure, internal energy, density, temperature) as constant average values over each zone. These values are also considered to be the central values of these variables at the geometrical zone centers. Particle velocities are reckoned at the zone interfaces; the interface density and pressure gradient are formulated in terms of the values at the zone centers. The zoning mesh must be chosen fine enough so that the variation in properties from zone to zone is small enough to insure that these average values are meaningful.

In a problem which also includes radiative transfer, the above restrictions must also be met. Zone sizes in a problem including radiation will generally be smaller than the zone sizes required by hydrodynamics alone. The addition of radiative transfer to the problem will, in general, add further restrictions.

If the temperature is taken as constant across each zone, temperature discontinuities will occur at the zone interfaces. Radiative variables like T^4 will have even greater discontinuities. More detailed examination indicates that the temperature and its spatial derivatives should be continuous at the zone interfaces. Thus, consistent with the expansion used in Eq. (2.5-9), the source function B is taken as linear between zone centers. Then the discontinuous spatial derivatives of the source function which occur at the zone centers do not appear in the formulation. In a more general formulation, a higher order polynomial could be used to

fit the source function through the zone centers, but numerical experience has indicated such a procedure resulted in only minor improvement in the computations.

The central zone temperature T is used as the average over the zone for purposes of computing average zone pressures, internal energies, and is used also in the Z , A , and W computations (Eqs. (2.5-13) through (2.5-15)). This is done primarily for purposes of convenience, but can be at least partially justified. In regions of small temperature gradient, no problem occurs since the central and average zone temperatures are nearly identical. In regions of large temperature gradients, the "average value" of the temperature is poorly defined in terms of the rapidly varying radiative variables, and it is preferable to keep the problem well poised hydrodynamically.

The specific volume V is taken as having a linear variation across each zone. The values of V at the zone centers and zone interfaces are then uniquely defined and afford no further difficulty.

The Z , A , and W functions are then computed using the average zone temperature T and specific volume V . Use of the average specific volume is justified since these functions show a relatively weak density dependence. Neglecting the variations in temperature across the zone causes only relatively small errors in the high temperature inner fireball regions since these functions show only a weak dependence upon temperature. In the low temperature regions, the Z , A , and W functions vary about as the ninth power of the temperature. Even with extremely fine zoning, large temperature gradients occur across each zone, and the Z , A , and W functions would be ill defined in terms

of any average temperature no matter how the average be defined. But the emission from these low temperature regions is small compared to the emission from the high temperature regions further inside, and these layers act primarily as a selective absorber for radiation from larger optical depths. Hence the Z^{\dagger} function must be known with some accuracy, but small errors in the A function, originating because of the use of the average zone temperature, can be tolerated.

The Z^{\dagger} function, however, has peculiar properties in the low temperature region which allow its values to be obtained with sufficient accuracy. As discussed in Chapter 8, the spectral absorption coefficient varies extremely rapidly with wavelength so that the spectrum is effectively divided at some wavelength into absorbed and transmitted fractions. This transition wavelength, however, depends only weakly on the zone temperature, and hence the average zone temperature will again suffice.

It should always be born in mind that these numerical approximations all improve as the zone size is decreased and can, in principle be made accurate to any desired precision. In practice, however, the fineness of the zone mesh is limited by the cost of computation. Skill is thus required to accomplish a large computational program within a limited budget. One tries to test each situation for sensitivity to zone sizes and achieve a compromise between economy of computation and accurate representation of the physics.

For purposes of carrying out the integration procedure by numerical methods, the basic equations (Eqs. (A.1) - (A.8)) are replaced by a set of centered finite difference equations as follows. The notation and

centering can best be seen by reference to Fig. A-1.

$$\frac{U_k^{n+1/2} - U_k^{n-1/2}}{t^{n+1/2} - t^{n-1/2}} = \frac{-8\pi (R_k^n)^2 (P_{k+1/2}^n + Q_{k+1/2}^{n-1/2} - P_{k-1/2}^n - Q_{k-1/2}^{n-1/2})}{m_k + m_{k+1}} \quad (\text{A.9})$$

$$R_k^{n+1} = R_k^n + U_k^{n+1/2} (t^{n+1} - t^n) \quad (\text{A.10})$$

$$V_{k-1/2}^{n+1} = \frac{4\pi}{3m_k} \left\{ (R_k^{n+1})^3 - (R_{k-1}^{n+1})^3 \right\} \quad (\text{A.11})$$

$$\left\{ \begin{aligned} Q_{k-1/2}^{n+1} &= \left(\frac{c}{V_{k-1/2}^{n+1} + V_{k-1/2}^n} \right) \left(\frac{m_k}{4\pi R_k^{n+1}} \right)^2 \left(\frac{V_{k-1/2}^{n+1} - V_{k-1/2}^n}{t^{n+1} - t^n} \right)^2 \\ Q_{k-1/2}^{n+1} &= 0 \quad \text{if } V_{k-1/2}^{n+1} > V_{k-1/2}^n \end{aligned} \right. \quad (\text{A.12})$$

$$\frac{E_{k-1/2}^{n+1} - E_{k-1/2}^n}{t^{n+1} - t^n} + \left(\frac{P_{k-1/2}^{n+1} + P_{k-1/2}^n}{2} + Q_{k-1/2}^{n+1/2} \right) \left(\frac{V_{k-1/2}^{n+1} - V_{k-1/2}^n}{t^{n+1} - t^n} \right) \quad (\text{A.13})$$

$$+ \frac{2\pi}{m_k} \left\{ (R_k^{n+1})^2 \mathcal{F}_k^{n+1} - (R_{k-1}^{n+1})^2 \mathcal{F}_{k-1}^{n+1} + (R_k^n)^2 \mathcal{F}_k^n - (R_{k-1}^n)^2 \mathcal{F}_{k-1}^n \right\} = 0$$

$$E_{k-1/2}^{n+1} = E\left(v_{k-1/2}^{n+1}, T_{k-1/2}^{n+1}\right) \quad (\text{A.14})$$

$$P_{k-1/2}^{n+1} = P\left(v_{k-1/2}^{n+1}, T_{k-1/2}^{n+1}\right) \quad (\text{A.15})$$

$$\mathcal{G}_k^{n+1} = \mathcal{G}_k\left(v_i^{n+1}, T_i^{n+1}\right) \quad i = 1, \dots, \dots, L \quad (\text{A.16})$$

Eq. (A.9) expresses the conservation of momentum and is centered over the grid point (n, k) .

Eq. (A.10) simply expresses the definition of velocity and is centered over the grid point $(n+1/2, k)$.

The conservation of mass, expressed by Eq. (A.11), is centered over the grid point $(n+1/2, k-1/2)$, i.e. over $Q_{k-1/2}^{n+1/2}$.

The difference expression (Eq. (A.12)) for the artificial viscosity is centered on the grid location $(n+1/2, k-1/2)$ except for the R_k^{n+1} factor. The artificial viscosity is thus correctly centered for use in the energy Eq. (A.13), but lags a half time step behind in the equation of motion (Eq. (A.9)).

The energy equation (Eq. (A.13)) is centered over the grid location $(n+1/2, k-1/2)$ and constitutes an implicit expression to determine the local temperature $T_{k-1/2}^{n+1}$.

Eqs. (A.14) and (A.15) are equations of condition rather than finite difference equations, and express the equations of state for the fluid at the location $(n+1, k-1/2)$ in terms of $v_{k-1/2}^{n+1}$ and $T_{k-1/2}^{n+1}$.

Eq. (A.16), which is written above only in symbolic form, expresses that the local net flux \mathcal{J}_k^{n+1} is an instantaneous integral functional of the temperatures and densities of all of the L zones in the configuration. The set of Eqs. (A.9) - (A.16) thus constitutes a set of 8L equations in 8L unknowns.

The following set of 11 auxiliary equations are used to evaluate Eq. (A.16):

$$ZO_{k-1/2}^{n+1} = ZO\left(v_{k-1/2}^{n+1}, T_{k-1/2}^{n+1}, TR_{k-1/2}^{n+1}, t^{n+1}\right) \quad (\text{A.17})$$

$$ZI_{k-1/2}^{n+1} = ZI\left(v_{k-1/2}^{n+1}, T_{k-1/2}^{n+1}, t^{n+1}\right) \quad (\text{A.18})$$

$$\lambda H_{k-1/2}^{n+1} = \lambda H\left(v_{k-1/2}^{n+1}, T_{k-1/2}^{n+1}, t^{n+1}\right) \quad (\text{A.19})$$

$$\Delta\tau_{k-1/2}^{n+1} = \left(R_k^{n+1} - R_k^{n-1}\right) / \lambda H_{k-1/2}^{n+1} \quad (\text{A.20})$$

$$A_{k-1/2}^{n+1} = \exp\left(-\Delta\tau_{k-1/2}^{n+1}\right) \quad (\text{A.21})$$

$$BC_{k-1/2}^{n+1} = \sigma \left(T_{k-1/2}^{n+1}\right)^4 \quad (\text{A.22})$$

$$S_{k-1/2}^{n+1/2} = \frac{BC_{k-1/2}^{n+1} - BC_{k+1/2}^{n+1}}{\Delta\tau_{k-1/2}^{n+1} + \Delta\tau_{k+1/2}^{n+1}} \quad (\text{A.23})$$

$$W_{k-1/2}^{n+1} = 1 - A_{k-1/2}^{n+1} - A_{k-1/2}^{n+1} \Delta\tau_{k-1/2}^{n+1} \quad (\text{A.24})$$

$$BB_k^{n+1} = \frac{\sigma \left[\left(R_{k+1}^{n+1} - R_k^{n+1} \right) \left(T_{k-1/2}^{n+1} \right)^4 + \left(R_k^{n+1} - R_{k-1}^{n+1} \right) \left(T_{k+1/2}^{n+1} \right)^4 \right]}{\left(R_{k+1}^{n+1} - R_{k-1}^{n+1} \right)} \quad (\text{A.25})$$

$$FO_k^{n+1} = FO_{k-1}^{n+1} \left(\frac{R_{k-1}^{n+1}}{R_k^{n+1}} \right)^2 Z\varphi_k^{n+1} + FI_k^{n+1} \left[1 - \left(\frac{R_{k-1}^{n+1}}{R_k^{n+1}} \right)^2 \right] ZI_k^{n+1} \quad (\text{A.26})$$

$$+ B_k^{n+1} (1 - A_k^{n+1}) + 2S_k^{n+1} W_k^{n+1}$$

$$FI_k^{n+1} = FI_{k+1}^{n+1} ZI_{k+1}^{n+1} + BB_k^{n+1} (1 - A_{k+1}^{n+1}) - 2S_k^{n+1} W_{k+1}^{n+1} \quad (\text{A.27})$$

$$\mathcal{J}_k^{n+1} = FO_k^{n+1} - FI_k^{n+1} \quad (\text{A.28})$$

where $\sigma = 5.67 \times 10^{-5}$ is the Stephan-Boltzmann constant, and TR is the temperature used to specify the spectral character of the radiation incident upon the zone from regions of smaller radius.

The analytic expressions for Eqs. (A.18) and (A.19) are not given explicitly in the written text, but are available in the FIREBALL code listing which follows.

In carrying out the numerical integration scheme, it is assumed that the initial values of R , T , V , E , P , U , Q , and \mathcal{J} are known at the initial time t^n for all values of k . The difference equations (Eqs. (A.9) - (A.28)) are then used to determine values for these variables at $t^{n+1} = t^n + \Delta t$ for all values of k . The procedure is repeated as n is increased until the desired period of time has been covered by the integration.

The initial values of Q and U are chosen at t^n rather than $t^{n-1/2}$ in the above procedure, but little error is introduced since the initial values may be adjusted accordingly and the time step Δt may be chosen as very small on the initial cycle.

The actual input model consists of a set of R , U , T , and V values for each zone of the configuration. Initial values of Q , E , P , Q , and \mathcal{J} are then found by use of Eqs. (A.12), (A.14), (A.15), and (A.16) before starting the first time cycle.

The set of Eqs. (A.9) through (A.12) depend only on the localized properties of the fluid and they can be advanced explicitly in space and time, subject to the limitations on the time increments according to the Courant criterion (see Chapter 2).

The set of Eqs. (A.13) through (A.28) must be solved simultaneously for all of the L zones in the configuration because of the linkage between distant zones caused by the radiative flux. Since the advanced values

$V_{k-1/2}^{n+1}$ of the specific volumes are known by advancing Eq. (A.11) explicitly, a set of trial temperatures $T_{i-1/2}^{n+1}$, $i = 1, \dots, L$ are estimated, substituted into the Eqs. (A.13) - (A.28), and a Newton-Raphson iteration scheme is then used to adjust the estimated values of temperature until Eq. (A.13) is satisfied to a predetermined accuracy.

The iteration is carried out by numerical methods. The equation of state derivatives, at fixed V , are carried out by raising and lowering the temperature 2% from its trial value, e.g.:

$$\frac{\Delta E}{\Delta T} = \frac{E(V, 1.02T) - E(V, 0.98T)}{1.02T - 0.98T} \quad (\text{A.29})$$

The derivatives of the radiative quantities are computed by a ripple zone technique in which the temperature of a single zone is raised 2%, the set of Eqs. (A.17) - (A.28) is evaluated and the desired derivatives formed, and the displaced temperature is then returned to its undisplaced value. This procedure is repeated for each zone in the configuration until all the desired derivatives are available. In practice, radiative derivatives for zones more than 2 zones distant are small, so that only a 5 zone set of derivatives is carried. Neglect of the more distant derivatives does not constitute a neglect of radiative transfer between distant zones; their neglect only influences rate of convergence of the iteration procedure.

For a system of L zones, the iteration procedure then results in L linear algebraic equations in L unknown temperature increments, each equation consisting of a set of terms involving 5 of the unknowns. This array is then solved by direct elimination and back substitution. The temperature increments are then used to adjust the trial values of

temperature until all temperature increments for all zones are simultaneously less than 10% of their respective zone temperatures.

The FIREBALL code is written in a programming language called FORTRAN; the particular vintage is known as FORTRAN II, Version 2. The various types of FORTRAN currently in use differ from each other only in minor details. This particular version was selected primarily because it has been in use for a number of years, and has achieved a measure of stability and reliability not to be found in the more recent efforts of the computer industry.

The FORTRAN language little resembles the machine language coding of a decade ago, and its resemblance to ordinary algebra is so close that the average physicist or engineer can learn to read FORTRAN with a very minimum of effort. This allows one to communicate the solution of a complicated theoretical calculation to his fellow scientists in complete detail and complete scientific honesty.

Section A.2 is devoted to a brief discussion of how to read FORTRAN and is designed for the scientist who is not familiar with this type of language. The remainder of Appendix A is devoted to the scientific aspects of the FIREBALL code and is intended to be independent of the language details. Readers not interested in great detail may thus skip over Section A.2, while those interested in such detail will find this section helpful in reading the code itself which is listed in full. The four digit numbers which appear in parenthesis throughout this appendix, e.g. (0136), refer to serial numbers (line numbers) in the code listing.

A.2 Reading FORTRAN

Variables and Constants

Algebraic variables are represented by symbols as in ordinary algebra and may take on values from about $\pm 1.7 \times 10^{-38}$ to $\pm 1.7 \times 10^{+38}$, and zero. Arithmetic is accurate to 8 significant figures.

Variable names must consist of 1 to 6 characters, the first of which must be a letter of the alphabet other than I, J, K, L, M, or N.

Examples: YIELD, X, A47, FI, DIVFAR

Integer Variables

Integers are used in subscripts, counting, indices, and sometimes in exponents. They are represented by symbols of 1 to 6 characters and must begin with I, J, K, L, M, or N.

Examples: N, J63, MCOUNT

Subscripts

Variables may have up to three subscripts, but no superscripts. The subscripts may be positive integers, but not zero.

Examples: X(K+1), Z(J,N), BB(I,J,K)

Arithmetic Operations

The symbols for standard arithmetic operations are little different from those used in ordinary algebra:

X + Y means add X and Y
X - Y means subtract Y from X
X * Y means multiply X by Y
X / Y means divide X by Y

Normal algebraic sign conventions are used. A double asterisk is used for exponentiation, i.e.:

R ** 2 means R^2
R ** BETA means R^B
Q ** 0.5 means $Q^{1/2}$

Operations are carried out in the preferential order of first exponentiation, then multiplication and division, and finally addition and subtraction.

Equal Sign

The equal sign has a meaning slightly different from algebraic usage, e.g.:

$$XYIELD = XYIELD + (A ** 2) - B$$

means carry out the algebraic operations to the right of the equal sign and store the result of this computation as the new value of XYIELD. Note that the previous value of XYIELD is first used, then destroyed and replaced.

Parenthesis

Parenthesis may be used to group information, indicate subscripts, or indicate the argument of a function.

Examples:

$(A+B)*C$ means add A and B , then multiply by C

$X(K+1)$ means $K+1$ is a subscript of the variable X

$SINF(X)$ means X is the argument of the sine function

Usually parenthesis will be used for grouping; subscripts can be recognized because they are integers, i.e., I, J, K , etc.; functions can usually be recognized by the letter F and the lack of an arithmetic operation symbol.

Library Functions

Certain library functions may be called in by name in order to save programming labor.

Examples:

$$\text{EXPF}(X) = e^X$$

$$\text{SQRTF}(Y) = \sqrt{Y}$$

$$\text{LOGF}(Z) = \log_e Z$$

Program Flow

Statements are processed by the computer in order of occurrence unless other directions are provided. Formula numbers, which occur in the first 5 spaces to the left, are not required unless control is to be

switched to that particular formula. The most common control commands are:

GO TO 436	sends control to statement 436
IF(X(K) - 3.0) 450, 500, 750	tells the computer to test the sign of the expression in parenthesis (X-3) and to transfer control to statement 450 if negative, 500 if zero, 750 if positive.

The IF statement provides the only means by which the computer makes judgments.

Subroutines

Complete subprograms, designed to accomplish a particular set of computations many times, can be used. For example:

CALL STATE

appearing in a program will send the computer to subroutine STATE, the set of computations indicated in that subroutine will be carried out, and control will return to the main program at the statement following CALL STATE.

Repetitive Operations

To save labor in programming, the DO statement may be used:

DO 100 K=1, 95

instructs the computer to carry out all instructions following this statement until statement 100 is reached. Do this first with K equal to 1 ; repeat this process, increasing K by unity each time, making the final pass with K equal to 95.

This statement can be used to compute repetitive formulae, or it can be used to select values from an array of numbers. For example:

	TESTV = 1.6 E+02	means set TESTV = 1.6×10^2
	DO 50 K=1, 100	
	IF(X(K) - TESTV) 50, 50, 10	
10	XCRIT = X(K)	sets XCRIT equal to X(K)
	N = K	retain the value of K as the symbol N
	GO TO 70	exit from the DO statement
50	CONTINUE	a dummy statement
	XCRIT = 0.0	set XCRIT to zero
70	YSTART = XCRIT + DELTAY	the next step in the computation

selects the first X value that is greater than 160 out of a list of 100 values of X, starting at X(1) , X(100) . If no such value is found, then XCRIT is set equal to zero.

The above material has been brief and oversimplified, but should enable those unfamiliar with FORTRAN to decipher formulae from a program listing and to follow the scheme of computation. Additional help can usually be obtained from programmers if additional questions of interpretation should arise. Books on FORTRAN are available, but none are recommended.

A.3 The computational scheme

The general computational scheme is cyclic in nature, each completed cycle representing an advance in the time variable.

The method of computation is illustrated in the schematic flow chart, Fig. A-2. Each block in this illustration represents a principal feature of the computation; numbers in the upper left corner of each block refer to a line number to the far-right of each page in the code listing.

The computation begins by reading in an initial configuration from data cards. The configuration consists essentially of the initial density, temperature, velocity, and dimensions of each of the 100 zones in the model. The data cards may represent an initial configuration, or the data might represent the results of a previous computer run on a model that is being done in short segments.

If the entry is a restart rather than an initial start, a dummy subroutine `rejust (0693)` is provided to make minor changes in program control parameters without the need for recompiling the major subroutines.

After reading in the initial configuration, the data is tested for obvious errors (`0367`), the equation of state subroutine (`0387`), the radiative properties subroutine (`0389`), and finally the flux subroutine (`0410`) are used to complete the details of the initial configuration. The computation cycle proper is then initiated (`0402-0405`). The initial time, which has been modified (`0404`), is now restored to its proper value (`0123`).

A sequence is then used to determine the number of zones, out of the possible 100, that are to be used at the present stage of the computation. (`0124-0138`). The number of zones in use is continuously adjusted during the computation to avoid unnecessary computation. When the data is loaded,

zone 100 must have the ambient temperature and density at burst altitude. The code then probes inward to a point where the temperature is twice the ambient value or the particle velocity reaches 1 m per second. The number of zones in use is then arrived at by adding a 6 zone safety factor to the result of the above selection.

The next sequence (0139-0162) selects the times at which the data print-out routine (0833) is called, selects the magnetic tapes to be used for the data, and sets up the necessary parameters to integrate the total energy lost by radiation between two data printouts, and to find the radiant power by differentiation of the energy vs time. The data print-out routine will be described in detail in Section A.4. The data printout routines are one-way streets so far as the main stream of the computation is concerned. Data is siphoned off, but no feed back into the computation proper occurs.

The sequence (0164-0177) provides an emergency data saving mechanism for use in case the computation becomes numerically unstable. In order to provide an economical computation, the time step used must be just below the critical value prescribed by the various criteria which will be described in the hydrodynamic routine (0360). These criteria are not fool-proof, and should the computation become numerically unstable (or should the computer operator err), the already completed computation might be lost unless there were a mechanism for restarting. Once the calculation has become unstable, the data presently in the computer may be invalid. The present sequence writes the fireball configuration on a magnetic tape at the completion of each 50 code cycles. Each time another 50 cycles are completed, the tape is rewound and the next configuration

written. Finally, at the end of the run, the last configuration remains on the tape, is read into the computer (0305), and data cards are punched (0312). Should this data card punching process fail, the tape itself is saved and the cards can then be punched directly. At the time of termination due to any type of error, data cards are then available not more than 50 cycles back. On occasion, an instability may occur just after a configuration has been written in the tape, in which case the computation is lost. But this has a probability of occurrence of about 1 chance in 50.

The next two sequences (0179-0257) select the rezoning subroutine (0179) and the zone splitting subroutine (0225). These sequences will be discussed below in Section A.5 dealing with these subroutines. In principle, one tries to remove fine zoning where it is not needed, and to create fine zoning when the physics of the problem so demands. Use of fine zoning throughout is not feasible because of the increased computational costs and also because the computer can only accommodate a total of 100 zones at one time. If the finest zoning in the problem were used throughout, the entire fireball could not be accommodated. So far as is known, other codes (Brode and Whittaker, private communications, 1965) currently in use are rezoned manually by visual inspection. The present sequences are an attempt to carry out this process automatically during the computation.

The sequence (0259-0264) provides for the printing of detailed diagnostics at the initial cycle, the next cycle following, and at one selected by data card input. The diagnostic routine (1125) is called for this purpose.

A termination sequence is provided (0266-0342) which is used whenever the computation is terminated, except in those cases where the normal course of the computation is interrupted by a machine difficulty or an operator error. The termination sequence provides for a final data printout (0274), the printing of program diagnostics (0273), the punching of current data cards (0275-0282) for possible restart purposes, completes, copies, combines, and unloads various tapes (0283-0326), and punches data cards containing the configurations from 1 to 50 cycles prior to the termination (0303-0319), before completing the run (0343).

The series (0123) through (0345) has dealt primarily with control mechanisms, rather than the actual computation, which is resumed at (0346). In the course of the computation it is necessary to carry most of the program variables for all mass zones, but only for the current point in time. A few of the variables must be carried for all space zones, but for two consecutive points in time. For example, the present value of the specific volume for zone K is represented by the symbol $V(K)$, while the specific volume from one time-step in arrears, the retarded value, is represented by $VR(K)$. As the program cycles, the present value becomes the new retarded value, and a new "present" value is computed.

The shifting process, in which the retarded values are set equal to the present values, takes place in the next sequence of commands (0346-0356). Also in this sequence, the present values of the variables are independently saved under the symbol $W(K,I)$ for possible use in the event that the entire cycle requires restarting. The restarting procedure is discussed at the end of this section.

Following retardation of the variables, a hydrodynamics routine (0360) is called, which will be described in detail in Section A.6. This routine advances the velocities, radii, specific volumes, and artificial viscosities.

One of the more important steps in the program is accomplished by a single dummy statement (0364). The first step in solution of the energy equation (Eq. (A.13)), is the estimation of a new trial temperature for each zone. Skillful selection of the trial values will make the iteration process converge faster and thus speed up the computation. However, in an iteration process the equation being solved is never satisfied identically, and any prejudice used in estimating the new temperatures may tend to impose non-random errors in the final results. For this reason, the old values of temperature are used as the first estimates for the new values. The iteration scheme itself then, in a sense, becomes a basic part of the system of equations. As will be discussed later, the iteration scheme used employs the same set of equations as are used to represent the energy equation itself. This procedure should tend to minimize any bias.

The iteration cycle proper (0365) begins by testing the set of temperatures for negative or zero values. Such values are likely to occur in the event of a numerical instability, in which case the computation is immediately terminated through the sequence previously described.

In the next sequence (0371-0387) the equation of state subroutine (1217) is called on three successive occasions. This subroutine is discussed in Section A.7. At this point in the computation, the advanced values of the specific volume are known for each zone. A trial set of temperatures has been selected. The derivatives of the internal energy and pressure,

with respect to temperature, at constant specific volume, are formed by first increasing the temperatures 2% above the trial values, passing through the equation of state to obtain energies and pressures, then repeating the process after lowering the temperatures 2% below the trial values. The required derivatives are then formed numerically from the above data (0384-0385).

The temperatures are then returned to the original trial values and a final pass through the equation of state is made to obtain trial values of the internal energy and pressure (0387).

Two subroutines are then called to provide the necessary radiative flux divergences for use in the energy equation. Subroutine SWABZ (0490) uses the values of V , T , and the dimensions of the zones to compute values of the SWAB and Z functions and is discussed in Section A.8. These values are used in subroutine FLUXS (1183) to compute fluxes and flux divergences as described in Section A.9.

A temperature test occurs next in the computation, but is bypassed on the initial trial of the energy equation.

The energy equation itself is then evaluated (0415-0424). A residue, comprising the imbalance of the energy equation due to the use of trial temperatures, is computed for each zone (0422).

The temperature iteration of the energy equation then commences (0425). Two types of iteration schemes can be selected. If the configuration is entirely optically thin (i.e. the total optical depth from the outer edge to the center is less than a given value) a non-radiative iteration (0429) can be used. Radiative transport is still included in the energy balance, but explicit radiative derivatives do not appear in the iteration scheme. If this alternative is selected, the temperature increments for each zone are

computed immediately (0431).

When radiation is included in the iteration (0439), the radiative and hydrodynamic derivatives are carried only in the inner zones, while only hydrodynamic derivatives are carried in the outer zones.

In the radiative iteration procedure, subroutine COEFF (1395) is called to form the required coefficients for the solution (0447) for the temperature increments. This subroutine is described in Section A.10.

Once the full set of proposed temperature increments is known, they are tested (0457) to see if they are within arbitrary bounds which have been developed by experience. Should these bounds be exceeded, there is a high probability that the time increment used by the computer was too large. Program diagnostics are then printed, the variables are restored to their values at the beginning of the cycle, and the cycle is repeated using a smaller time increment. This recycling is allowed 3 times, after which the computation proceeds even though the test bounds were violated. If the test criteria were correct, a numerical instability results, and the computation is terminated from one of the several points in the program where the instability can be positively detected. An instability does not always occur, however, since the tests are not infallible.

Usually a recycling occurs when a time increment just slightly too large has been used and a single recycle cures the difficulty. Use of this stability check "after the fact" enables the various time step selection criteria to be pushed close to their limits. Use of large safety factors in these criteria, as is the common practice, would be prohibitive as the total computation time would be seriously increased. If the proposed temperature increments satisfy the stability tests, they are accepted and

the trial temperatures are modified accordingly (0485).

These new temperatures become a new set of trial temperatures and the iteration cycle is begun again (0367). The iteration convergence test (0409) is made well into the second and subsequent passes through the iteration sequence. Should the test be satisfied, then the best values of internal energy, pressure, and fluxes, etc., are available as the cycle is completed. If the test is failed, the iteration cycle then progresses with all the necessary data. The code as written performs some unnecessary computations in that the state derivatives are computed but not used if the convergence test is satisfied. This technique was a compromise between several alternatives and was adopted because it required less computer storage at a period when the program was storage limited.

The actual convergence test used (0408) consisted of the requirement that the temperature increments for all zones be simultaneously less than 10% of their respective zone temperatures. This method proved to be more efficient than several other methods tried which were based directly on the degree of imbalance of the energy equation.

The number of passes through the iteration sequence is limited to 3 on any one code cycle (0416). It is a characteristic of the Newton method that convergence takes place very rapidly or not at all, and that on odd number of attempts is usually better than an even number. Should an abnormally large temperature increment occur after 3 iterations, a convergence check at the beginning of subroutine HYDRO detects this and forces a smaller time step on the following cycle. This test differs from the main program stability check in that it is applied only after 3 full iterations and uses stricter criteria.

A.4 Data printout routines

The data printout sequence is contained in subroutine CGSPO (0833). This routine samples the data from the computation proper, generates additional parameters of interest from this information, and produces two magnetic tapes: the main listing and the user tape.

The general problem of determining observables from a list of temperature and density values is a difficult one. Many of the "observable" parameters generated by the printout routine are extremely crude and must be used with extreme caution. These "observables" have been printed below the main tables of data and include the shock radius, fireball radius, effective temperature, color temperature, and the spectral distributions. For example, the code defines the fireball radius (FBR) as the radius at which the optical depth is 0.44 as measured from outside the fireball. This simple definition is easy to code and is useful radius to have printed out. But for comparison with an experimental radius measured photographically, a complete brightness profile is required for comparison with the corresponding densitometer traces from the experiment.

The routine begins by testing for temperature inversions (0864) and causes program diagnostics to be printed if such inversions are found. Placement of this test in the printout routine causes the diagnostics to coincide in time with the data printout so that any unusual features seen in the listings may be studied in detail.

In the sequence (0868-0874) a number of variables to be printed out are set up. This sequence works in conjunction with the sequence (0139-0162) in the main program. The variable CN(LZ) is the average time step between two successive printouts. The variable SAVE1 is the value of the last time step before the printout. The total power being radiated

in watts (POWER), the color temperature (TCOL), and the effective temperature (TEFF) all depend upon the value of the total flux (TFLUX) which is the power being radiated in ergs. TFLUX is computed in the main program (0155). The instantaneous total flux at the end of each cycle is called FLOX and is summed continuously (0139) throughout the computation and called FLEX. The average power TFLUX over the time interval between printouts is obtained by numerical differentiation of FLEX (0155). This method gives more representative results for the power output since the instantaneous power tends to fluctuate due to the finite zoning of the model. The instantaneous total power corresponding to the time of a given printout can easily be obtained since the radius and outward flux at the last zone are available from the printout.

The code definition of the effective temperature (TEFF) is defined (0874) from

$$TFLUX = 4\pi (FBR)^2 \sigma (TEFF)^4$$

where $\sigma = 5.67 \times 10^{-5} = \text{Stephan's Constant.}$

It is the temperature of a black body radiation having the same size as the fireball and which emits the same total power. This temperature is a minimum estimate of the fireball "surface" temperature since the fireball does not have an emissivity of unity.

The code definition of (0873) color temperature (TCOL) uses an estimate of the total emissivity and yields a higher temperature which can be used to describe the spectral character of the radiation escaping from the fireball. The emissivity estimate is based on the Z^+ function

for the zone having the largest λ_c and the radiation temperature for that same zone (0689).

After the fireball becomes transparent in the continuum, the effective and color temperatures are no longer defined since their definitions involve the fireball radius, and by the code's definition, FBR=0 under these circumstances.

At this point (0875), the printout routine calls subroutine PHOTOG (1061). This routine computes an estimate of the photographic brightness as a function of radius. Using an approximate fit (1073) to the absorption coefficient for the "photographic" region of the spectrum, and a Planck function (1083), the emitted intensity is calculated for chord rays which are tangent to the mid-point of each mass zone. Since the spectral band width of the photographic region is unspecified, only relative brightness values are obtained. The brightness scale, however, remains fixed throughout the entire computation. It is clear that only an estimate can be obtained from this computation since the absorption coefficient is not independent of wavelength across the photographic region of the spectrum, and also because the appropriate absorption coefficient data are not available at temperatures above 20 eV. The data is useful, however, in making comparisons with experimental results and in finding the gross brightness variations across the fireball.

The CGSPO routine next makes an estimate of the spectral distribution of the total radiation emitted by the fireball. The code decides (0877) whether the fireball is optically thick or is transparent. If the fireball is transparent (0878), no realistic estimate of the spectral distribution can be made since the spectrum consists of emission lines and a weak

continuum. An extremely crude estimate of the "visible power" (4000-7000 Å) can be made by noting that fireballs tend to form an isothermal region at these late times. Most of the emitted radiation must come from this isothermal region since it is the hottest part of the fireball. These isothermal region temperatures range from 9500°K down to 5000°K as the transparent fireball cools. If it is assumed that the envelope of the emitted spectrum crudely approximates a Planckian distribution, then $37 \pm 3\%$ of the radiation will fall in the "visible" region of the spectrum over this entire range of temperatures. Hence, for the transparent case, the visible power (P47) is taken as 37% of the total power (0878).

If the fireball is optically thick (0888), then the color temperature is used as a basis for division of the total power into broad spectral bands (0889-0939). The formula for the Z^+ function, which very nearly approximates the fractional Planck function in the visible and IR spectrum, was used in place of an accurate fit to $\int_{\lambda}^{\infty} B_{\lambda} d\lambda$ as an analytic fit to this integral was not known to be readily available. The accuracy so achieved is probably better than the physics of the spectral estimation process. The overall results are of a quality comparable to those achieved by assuming the sun to be a 6000°K black body.

The next sequence (0944-0963) performs an energy check by summing the internal and kinetic energy of the current configuration. The sequence computes the internal energy and the kinetic energy zone by zone, and also the internal energy of the volume of space currently occupied by the configuration if there had been no detonation. This "ambient" energy of

the undisturbed air constitutes a significant part of the total energy of the configuration, particularly at late times when the radius of the configuration is large. It must be taken into account in studying the energetics of the model.

The code has no built-in method of forcing energy conservation. The energy check sequence is simply an after-the-fact sampling to see if energy has been conserved. If the difference equations do in fact represent the basic conservation equations, then mass, energy, and momentum will automatically be conserved.

The energy accounting at any one moment can be verified by adding the present model energy due to the detonation and the thermal losses up to the given moment. The quantities TOT ES, EAMB and TYIELD are printed out and are the appropriate numbers to use for this purpose. TOT ES in the printout is the total energy, (DPP(LZ) in the code (0959)), and includes EAMB, the energy content of the cold air before the detonation. TYIELD in the printout, (FLEX in the code (0139)), is the total energy radiated outward across the outer boundary of the model from the time of detonation up to the present time. In general, the code conserves energy to within a fraction of 1%.

Sandwiched in the energy check routine are some operations which concern the printing out of shock parameters. (0955-0958). It should be remarked that the location of shock fronts in a numerical configuration is a difficult problem because of the varying number of shocks and the wide range in their characteristics. Many methods were tried, but with limited success. Shocks are best located by a careful study of density vs. radius

and velocity vs. radius graphs,

The location of a strong shock is determined by the program by finding the largest value of the artificial viscous pressure , with the added requirement that it be larger than the ambient gas pressure at burst altitude. This shock radius is printed, but cannot be relied upon without further inspection to see if a shock really exists at that radius. This simple technique will print out the location of one shock, but it may not select the same shock on consecutive printouts.

The sequence (0978-0991) simply changes units and sets up certain quantities in proper form for printing them out. For example, (0987) computes the effective value of "gamma," while (0984) yields the temperature in electron volts.

The sequence (1001-1016) prints out the main listing, while the sequence (1022-1029) prints out the user magnetic tape for use in continuation computations such as fireball environmental studies.

A.5 Variation of the number of zones in use

It has been said that there are three major problems to be solved in writing a fireball code: the basic physics, the interpretation of the results, and the use of proper zoning. Proper zoning is by far the most difficult of these problems. One simply cannot use a fine mesh throughout the configuration as the computing time increases approximately as the square of the number of zones, i.e. halving a zone halves the time step and doubles the number of computer operations, thereby requiring four times as much computer time.

In the other extreme, if the model is represented by zones of equal size, some of the zones may be too large to properly represent the gradients in physical properties.

Consider, for example, a model where the fireball has a radius of 10^3 cm and may require zones of width 10^{-1} cm at the fireball boundary. Since the computer can accommodate only about 100 zones at a time, the zone obviously cannot be of equal size. Furthermore, use of a 10^{-1} cm zone in the hot isothermal region would slow the computation by at least a factor of a hundred, and perhaps a factor of ten thousand or more.

Ideally, new zones should be created and old zones combined in an optimum manner based on the local physical conditions at each point in the configuration. The subroutines SPLIT (0785) and REZONE (0701) are provided for these purposes.

In the split subroutine, the zone indices for the zones exterior to the zone to be split are first shifted outward (0789-0808) to make room for the new zone.

The zone is then split in half mass-wise (0810-0811). The particle velocity at the new interface is taken as the square root of the average of the squares of the particles velocity at the boundaries of the original zone. The temperature of the two new zones are displaced 10% above and below the temperature of the original zone, (0824-0825) and a similar treatment is accorded the internal energies (0826-0827).

This routine must be considered as only a crude beginning and much work is still being done in developing new techniques. The present routine can only be used before the gradients become large, and even then its use should be discouraged.

The calling sequence for the SPLIT subroutine occurs in the main program (0225-0257). Statements (0228 and 0248) prevent a split more often than each third cycle. Statement (0231) requires a split at any time that a single zone represents more than 8% of the radius of the entire configuration.

The real purpose of zone splitting is to provide very fine zones just ahead of an advancing shock front so that the optical properties will not be too severely distorted. The sequence (0232-0244) attempts to achieve this goal. Optical depth 0.7 from the outside is located (0232) and this zone is tested to see if it is being compressed (0235). Then if the particle velocity is greater than 10^5 cm/sec as is characteristic of optically thick shocks, the five zones immediately exterior are scanned and one per cycle can be split, until a certain minimum zone size is reached. Once the shock has started, the splitting takes place 5 zones ahead of the shock until the shock becomes transparent. The minimum zone size has not yet been formulated in general terms, and must be re-programmed in for each separate run. In the program listing (0240) a zone of 200 cm or more can be split, resulting in a minimum zone size of 100 cm. This is about appropriate for a megaton burst at sea level.

As a final insurance against undesirable zone splitting at high altitudes, statement (0244) prevents splitting at temperatures above 6×10^4 °K.

Subroutine REZONE (0701), which combines two existing zones is on a much more sound basis. Conservation of mass in the zone combining process is trivial (0735), but the conservation of energy and momentum are slightly more complicated. The internal energy of the new zone is taken

as a mass weighted average of the internal energies of the two zones being combined (0733). The conservatism of kinetic energy and momentum for a four zone system (0709-0712), which is collapsed into a 3 zone system, results in two equations for the two unknown particle velocities at the inner and outer edges of the combined zone.

The remainder of the subroutine REZONE consists of a shifting of indices for zones exterior to the fusion, and the addition of a new zone 100 at the outer edge of the configuration.

While this routine works well and quite accurately, some skill is required (but not always attained) in deciding when rezoning should take place.

The calling sequence for rezoning is in the main program (0179-0224). On the basis of optical properties (0182), the outer limit of the region to be scanned (the index NZ TS) and an allowable mass ratio for neighboring zones (PMT) are selected (0181-0202). If at least two cycles have passed since the last rezone (0204), zones 9 through NZTS are tested for size compared to the size of the entire configuration (0205), temperature gradient (0206), density gradient (0207), and mass gradient (0208). If these gradients are less than the allowable arbitrary limits, then rezoning is allowed so long as the zone is not undergoing significant compression (0209).

A.6 Hydrodynamics routine

The hydrodynamics routine (1261) is patterned after the artificial viscosity method of treating shocks (see Chapter 2). In addition to advancing four of the basic equations, this routine also controls the size of the time increments and performs miscellaneous other functions.

At the beginning of the routine, the previous temperature increment is tested (1273) against the temperature, and if the increment is too large, the proposed time step is cut a factor of five (1277). This test serves several purposes depending upon the values of the previous temperature increment that may be stored in the computer at the moment. If a main cycle has been completed satisfactorily, i.e. all temperature increments are less than 10% of their respective temperatures, then no decrease in estimated time step takes place. If, however, a main cycle was completed after three passes of the energy equation, the 10% requirement may not have been satisfied, i.e., the iteration may not have converged. Should this be the case, then the time step is shortened in the hope that a numerical instability can be avoided.

If the main program stability check (0457) is violated, the program returns to the beginning of that master cycle after restoring all data except the temperature increments. Then, since the HYDRO tests are slightly more demanding than are the main program tests, the time step will also be decreased when the main program senses a difficulty.

The equation of motion sequence is carried out in two separate phases which are separated by criteria to choose a new time increment. The particle velocities are first advanced using the previous value of the time step (1289) so that proper time centering of the difference equation (Eq. A.9) is maintained.

A new time increment is then selected (1298-1335). First a time step 30% larger is suggested (1299). This value is then reduced should the Courant criterion, Eq. (2.5-4), demand that a smaller value be used

(1302-1310). The time may be further reduced by a radiative criterion (1314-1326). Gross checks are then imposed, as a safety factor, which demand that the new time step can never exceed the previous one by more than a factor of two, or be less than a given minimum value (DTMIN). The value of DTMIN is continually increased during the computation and is kept a factor of 50 smaller than the largest time step that has been used. Should the speed of computation decrease more than this factor of 50, too large a time step (the value of DTMIN) is forced into use and the computation may become unstable and turn itself off. This feature prevents the waste of computer time should the time step conditions become abnormally critical at some point in the configuration.

Superimposed on these criteria is the mechanism for causing data to be printed out exactly at fixed predetermined times (1333-1335). This criterion may further decrease the time step.

After a new time step has been decided upon, new values of the particle velocity are determined by linear interpolation (or extrapolation) so that proper time centering of the equation of motion is maintained (1337).

The radii (1344) and specific volumes (1362) are then advanced in a straightforward manner. The new radii are tested before adoption (1348) to prevent sudden zone collapse should the estimated hydrodynamic time step be too large. A local recycle with decreased time step is then instituted (1358).

It is perhaps appropriate to again mention that the use of large safety factors in the time step criteria result in the use of large amounts of computer time. Considerable economy is achieved by lowering the safety factors, testing the proposed results before closing a cycle,

and re-cycling when necessary. Using this technique and with a little experience, the code can be kept running at near optimum speed.

The sequence (1372-1385) advances the artificial viscous pressure. A variety of formulae are available in the literature for this purpose. The formulae used here is similar to that given by Richtmyer (see Chapter 8 references). This form appears to give better results when shocks reflect at the center of the sphere than do the "linear" and "quadratic" forms. In the final analysis, the use of an artificial viscosity is an art and an adjustable constant (1374) is available to achieve optimum results for any specific situation. Use of too small a constant causes numerical ripples behind the shock, while use of too large a value spreads the shock-over too large a distance and lowers the shock velocity. According to Richtmyer, choice of the arbitrary constant in a manner so as to spread the shock discontinuity over 3-4 zones results in shock velocities and pressures that agree well with laboratory experiments.

The use of an artificial viscosity causes a fictitious precursor ahead of the shock front. If this precursor is optically thick, the shock radiation rate will be affected. This effect reduces the rate of radiation loss when the shock temperature is large, but numerical testing has shown that it has little effect on the shock energetics.

A.7 Equation of state routine

The equation of state subroutine (1217) is entered with known values of the temperatures and specific volumes for each zone, and values of pressure and internal energy are computed.

The source data for the analytic fit to equation of state are primarily due to Gilmore (1955) and to Hilsenrath and Beckett (1955). This polynomial type of fit, though in principle not as accurate as an iterative routine, is preferred for computational purposes because the derivatives are well behaved. This fit is also self consistent in that the hugoniot are closely satisfied, while some of the piece-wise fits, that are accurate over limited ranges, fail in this regard. No significant inaccuracies are known to have resulted from use of this simple expression.

There is some question as to whether radiation pressure and the radiation energy density should be included in the equations of state (see Chapter 2). The subroutine STATE allows an explicit choice to be made in this regard (1222-3). These effects can only be important at high temperatures. The argument against including these effects is that at the high temperatures the matter and the radiation cannot be in equilibrium according to the local high temperature since the gas is too transparent. The radiation field is characteristic of the lower temperatures where the opacity is higher. To base the radiation pressure on the higher values of temperatures in the interior would thus be an overestimate.

A.8 Radiative properties routine

The radiative properties of the fluid, which are characterized by the S , W , A , and Z functions, Eqs. (A.17) through (A.25), are supplied by subroutine SWABZ (0492-0692). The analytic representations of the Z and A functions, which differ only in that the electron scattering is omitted in the A function, are formulated in terms of λ_H , a radiative mean free path which depends upon the zone temperature, zone specific volume, and the time.

The Z^- function (ZI in the code) is formulated directly as a transmission (0500-0507).^{*} The A function cannot be formulated directly in this fashion since $\ln A$ is needed to define optical distance, and truncation errors would occur as $A \rightarrow 1.0$. Thus λ_H (HMFP in the code, is found (0508-0511), together with a separate high temperature emission term (0512) due to Bremsstrahlung (HMFF in the code). The smaller of these two mean free paths is used for temperatures above 10 eV (0514).

The emission optical depth (0516) then follows immediately from the zone thickness. The A function (0517) at this point in the code is identical with the definitions used in Eqs. (A.21) and (2.5-14). A later sequence (0670-0675) redefines A as (1-A) (an emissivity) as a computational convenience for zones of small emissivity.

The variables BC and BB 91518 and 0526) are used to represent the source function at the zone centers and zone boundaries respectively. It will be noted that the boundary value is determined by linear interpolation of the source function in terms of geometrical rather than optical distance. The two methods yield substantially the same results when the two neighboring zones have comparable optical thicknesses, but the geometrical method gives better values when an optically thick zone occurs next to an optically thin zone. The terms involving the boundary values cancel if both zones are optically thick, while the source function gradient is small for two transparent zones, so that the method of interpolation is not important in these cases.

The sequence (0536-0563) computes the optical depth inward from

* The double subscripting, i.e. $A(K,N)$ has been carried over from an earlier version of the code in which N spectral bands were used.

the outer boundary of the configuration and sets various control variables used by the program at other locations. The index LZR specifies the last zone to be included in the radiative part of the iteration scheme. The fireball radius, FBR, is set as the outer radius of the zone in which the total optical depth as measured from the outside has reached 0.44. Choice of this value has no particular significance. For high air densities the optical depth increases abruptly so that any reasonable test value will result in choosing of the same zone to specify the radius. For rarefied atmospheres, considerable limb darkening takes place and chord integrations would be necessary to find a precise radius. The test value of 0.44 has been found to yield radii satisfactory for the intended applications elsewhere in the code. The index MCP is used to specify the zone in which optical depth unity occurs as measured along the representative ray. (This corresponds to a radial optical depth of $2/3$).

The sequence (0564-0607) computes the wavelength at which the principal spectral absorption edge occurs for each zone. This wavelength depends only upon the physical characteristics of each zone, i.e., its temperature, density, and zone thickness. Zones are first sorted according to temperature to determine whether the spectral transition is due to an atomic species, the nitrogen molecule, or the oxygen molecule.

The transition edges due to atomic species are in the far ultraviolet and a fit will be required only at very high altitudes when the fireball is transparent throughout while the temperatures are high enough so that the Planck function is significant in the ultraviolet. This fit used by the code is therefore very limited in its application.

The nitrogen and oxygen molecular formulations involve a continuum with a relatively sharp long wavelength limit, and an extensive system of molecular bands extending from this limit toward longer wavelengths. The continua are assumed to exist at all times that the molecules have sufficient population, but the band systems, which depend upon the population of the higher vibrational levels, are assumed not to exist until the passage of a vibrational relaxation period.

While in principle the relaxation time should be measured from the time that each zone is first heated (actually the temperature-time history should be taken into account), a satisfactory first approximation is given by use of the time since the detonation. The relaxation time for N_2 at sea level is taken as 5×10^{-7} sec and for O_2 as 3×10^{-7} secs. These times are scaled inversely with the density to obtain the relaxation times at higher altitudes. These times are based on data by Blackman (1956).

The absorption edge and the continuum absorption due to a particular species must fade away as the population is diminished by dissociation. At a given density, the population decreases very rapidly with temperature as soon as kT becomes comparable with the dissociation energy. Due to the finite zoning structure, the population of a particular species will be appreciable in one zone, but negligible in a neighboring hotter zone due to the rapid temperature dependence of the populations. Thus, for the purpose of computing absorption edges, the species can be assumed to exist below a certain temperature and not to exist above that temperature. The dissociation is thus assumed to take place at a temperature rather than over a narrow temperature range. The dissociation temperatures for N_2

and O_2 , as a function of density, are represented in the code by two formulae (1708-1709) and are used in the SWABZ subroutine (0572-0580).

The sequence (0612-0669) computes the Z^+ values (ZO in the code). The Z^+ function depends on λ_c which has been determined above, and the temperature T_R used to describe the spectral distribution of the radiation incident upon the zone. The sequence (0622-0642) selects this temperature for each zone. In the case of an optically thick fireball, this temperature is that of the first zone at optical depth greater than 0.7 from the zone in question (0628). For a transparent fireball, where the radiation comes from a shell rather than from a "surface", the temperature is taken as an optical depth weighted average of the zones interior to the zone in question (0624). This "shell source" sequence is important only at high altitudes where the fireball is transparent, and when the temperatures are still high enough to have radiative flow in the far UV region of the spectrum where the absorption edges occur.

The Z^+ values are corrected for the effects of intervening zones between the source of the radiation and the zone in question (0655).

The sequence (0676-0688) becomes effective at very high altitudes when the configuration is quite thin and thermal radiation plays only a minor part in determining the temperature distribution. Under these circumstances, the series expansion of the source function should not be truncated and derivatives of higher order than the first should be included. But since the radiation is of little importance in this case, the series can be further truncated so that only the zero order term is used and the code automatically switches over to radiative transfer for isothermal optically thin slabs.

The variable EMS (0689) is used as an estimate of the total emissivity. It corresponds to the Z^+ function for that zone having the maximum cut-off wavelength, but without correction for intermediate zones.

A.9 Radiative flux routine

Since all the needed data has been generated elsewhere by the code, the radiative flux routine is particularly simple (1183).

To perform the flux integration a boundary condition is needed. For this purpose, the inward flux incident on the outer boundary of the configuration is chosen as zero (1190).

The inward flux at the boundary, one zone inside, is given by the sum of the transmitted and emitted components (1193) as in Eq. (A.27). The integration continues inward until the spherical central zone is reached. The outward flux for this zone is the sum of the transmitted inward flux and the local emission (1195). The integration then proceeds outward (1197) using Eq. (A.26). One can view this process as an integration starting at one side of the fireball, passing through the center, and then on out the other side. All of the inward and outward fluxes needed to form the radial component of the flux divergences (1211) are generated during this integration.

It should be noted that this subroutine is written again for N spectral bands, and that the total directional flux at a given boundary is obtained by a summation over the spectrum, even though only 1 spectral band is used by the present code. In addition, the A function used in (1193-1198) does not correspond to the transmission function used elsewhere in the text, but to (1-A) as explained in the SWABZ subroutine.

The energy Equation (Eq. (A.5)) is solved by an iterative method as described by Hillendahl (1964). Subroutine COEFF (1395) performs the necessary algebra to form the required derivatives.

The basic approach is to compute the derivatives numerically by a ripple zone technique, rather than to derive and to code explicit formulae for the derivatives. In using this technique, the temperature of a single zone is increased 2%, then formulae identical to those used in subroutine SWABZ are used to calculate those radiative properties which change as a result of this temperature increment (1429-1576). A flux integration is then carried out (1577-1593), the flux derivatives are formed (1614), and the perturbed variables are returned to their normal values (1627) which were saved (1411). This ripple zone process is repeated until all the required derivatives are available. Derivatives with respect to zone temperature more than two zones distant are truncated.

The energy equation derivatives, including both the radiative and hydrodynamic parts, are formed numerically (1647). The data is then available to form a set of linear algebraic equations for the temperature increments of the zones.

This matrix is then solved by direct elimination and back substitution using recursion formulae (1673) and (0447).

This numerical method of solution, involving the ripple zone method of obtaining flux derivatives and the step by step formation of the energy equation derivatives has been found to be both convenient and economical. If details of the radiative properties or flux formulae are changed, duplicates of the new formulae are simply inserted into the coefficient subroutine without the necessity of deriving explicit formulae for the

derivatives, which in some cases, have as many as 40 terms. Such lengthy formulae are difficult to derive and code without errors, and the sorting of terms to avoid arithmetic truncation difficulties is a major task. Since the actual number of operations to be carried out by the computer is approximately equivalent in the two methods, the numerical technique is to be preferred.

A.10 Code listing

The pages following present a complete listing of an actual working radiation-hydrodynamic code which has been described in sections A.1-A.9. No attempt has been made to edit the listing for publication purposes since this practice quite often results in the publication of codes that do not work.


```

*      FORTRAN
CFIRE 1
C      MODIFIED DIMENSION STATEMENT  NSZ=1  ONLY
      DIMENSION  T(101),  TS(100),  TP(100),  TM(100),  TR(100),
2      PA(100),  P(100),  PS(100),  PP(100),  PM(100),  PR(100),
3      DE(100),  E(100),  GM(100),  EP(100),  EM(100),  ER(100),
4      Q(100),  V(100),  VS(100),  RHOZ(100),U(100),  VR(100),
SDR(100),D(1),R(101),  RZ(100),  R2(100),  UA(100),  UR(100),
6      DTM(100),  DTR(100),  DTH(100),  DPT(100),  DET(100),  RR(100),
7      ZMAS(100),DIVFA(100),DIVFR(100),RESDUE(100),FP(100),  FZ(100),
8      FM(100),  FMM(100),  HZ(100),  HP(100),  HPPP(100),HPP(100),
9      DMM(100),  DM(100),  DZ(100),  DP(100),  DPP(100),  BN(100),
1     CN(100),DN(100),EN(100),ETA(100),XS(100),GNU(100),PART(100)
      DIMENSION THETA(100)
C
C      STORAGE FOR RADIATION VARIABLES
C
      DIMENSION  BB(100,10),  DTAU(100,10),  S(100,2),  FO(100,10),
1FOT(100,10),FI(100,10),  FIT(100,10),  ZO(100,10),ZI(100,10)
2.A(100,10),  W(100,10),  BC(101,10),  FIS(100),  FOS(100),
3CWL(100, 2),YM(100),TAU(100, 2)
      COMMON  T,TS,TP, TM, TR,PA,P,PS,PP,PM,PR,DE,E,GM,EP,EM,ER,Q,V,VS,RHO
2Z,U,VR,DR,D,R,RZ,R2,UA,UR,DTM,DTR,DTH,DPT,DET,RR,ZMAS,DIVFA,DIVFR
3,RESDUE,FP,FZ,FM,FMM,HZ,HP,HPPP,HPP,DMM,DM,DZ,DP,DPP,BN,CN,DN,EN
4,ETA,XS,GNU,PART,THETA,KGU,KG
5,BB,DTAU,S,FO,FOT,FI,FIT,ZO,ZI,A,W,BC,FIS,FOS,CWL,YM,TAU,NSZ,
6  NZSS,  LZ,LZM1,LZM2,LZP1,LZP2,BR,RJ,RX,NCW,NMC,NTI,FLOX,FLEX,
7TIME,DT,CS,CR,RS,MCL,MCP,MCW,RM,VD,ZA,NB,NQS,FBR,LZR,DTMIN,NR
8,KZ1,KZ2,KZ3,KZ4,KZ5,KZ6,KZ7,KZ8,KZ,TD02,TDN2,NDP,SCALE,EMS,
9BLANK,AST,TEE,PLUS,PERIOD,DASH,EQUAL,PINUS,FFF,UUU,PPP,NTAPE,TIMEW
6,TFLUX,FLIX,TIMES,P03,P34,P45,P57,P71,P47,Q47,Q71,WKT,YIELD,XYIELD
      KZ6=0
      REWIND 41
      REWIND 31
      REWIND 32
      REWIND 22
      REWIND 42
      REWIND 25
B      BLANK=606060606060
B      AST=545454545454
B      PLUS=2020202020
B      PERIOD=333333333333
      D(1)=0.0
      TIMEW=1.0E-10
40     FORMAT(17HCONTROL DATA RUN 9I4,6X,E10.3,11A1)
41     FORMAT(14HCONSTANTS RUN 12,7H CYCLE 14,1X,1P3E12.5,0P4F4.2)
42     FORMAT(17HDATA CARDS CYCLE 14,10X,10HRUN NUMBER13,10X,5HSET A/
42     1(14,1P5E12.5,1PE11.4,12,13))
43     FORMAT(17HDATA CARDS CYCLE 14,10X,10HRUN NUMBER13,10X,5HSET B/
43     1(14,1P5E12.5,1PE11.4,12,13))

```

```

44  FORMAT(1H ,6H MODE=14/6H NMC=14/6HNZONE=14/6H NQS=14/6H MCL=14/ 0052
44  16H RS=1PE11.4/6H TIME=E11.4/6H DT=E11.4/6H CS=E11.4/6H CR= 0053
44  2E11.4/6H BR=E11.4/7H TIMEL=1PE11.4) 0054
45  FORMAT(1H1,2I4,1PE12.3,15,1P6E12.3/(14,1P12E10.3)) 0055
47  FORMAT(1H ,18HZONE SPLIT AT NMC=14.5X,5HTIME=1PE11.4,5X,5HZONE=14, 0056
47  119) 0057
48  FORMAT(1H1,30X,4HRUN=14,15X,20HLOG POWER (ERGS/SEC)/6H CYCLE,X,4HT 0058
48  2IME,3X,12,13X,12,13X,12,13X,12,13X,12,13X,12,X,11HTOTAL POWER,3X, 0059
48  36HRADIUS/15X,76A1) 0060
49  FORMAT(1H ,15HREZONED AT NMC=14.5X,5HTIME=1PE11.4,5X,5HZONE=14,17) 0061
50  FORMAT(14,1P5E13.5) 0062
    NSZ=1 0063
    REWIND 15 0064
    REWIND 16 0065
    READ INPUT TAPE 5,40,NR,MODE,NMC,NLP,NDD,LZ,NZONE,NQS,MCL,TIMEL 0066
    1,BLANK,AST,TEE,PLUS,PERIOD,DASH,EQUAL,PINUS,FFF,UUU,PPP 0067
    PRINT 8321, MCL,TIMEL 0068
8321  FORMAT(34H NORMAL TERMINATION CONDITION NMC=14,10X,5HTIME=1PE12.3) 0069
    WRITE OUTPUT TAPE 15,12345,NR 0070
12345  FORMAT(1H1//////////1H ,40X, 32HR W HILLEDAHL PALO ALTO 201 0071
123451//1H ,40X,33HPRODUCTION OUTPUT LIST RUN NUMBER14) 0072
    READ INPUT TAPE 5,41,NR,NMC,TIME,DT,FLEX,CS,CR,BR,RS 0073
    NSTART=NMC 0074
    DTMIN=DT 0075
    NEG=NMC 0076
    MCDC=NMC+50 0077
    NMA6=MCDC 0078
    JXC=0 0079
    NMCS=NMC 0080
    TIMES=TIME 0081
    FLIX=FLEX 0082
    NSTOP=0 0083
    NRZ=50 0084
    NB=14 0085
    IPS=0 0086
    LZM1=LZ-1 0087
    LZM2=LZ-2 0088
    IF(MODE-1)1,1,1000 0089
1  CALL ENTRY 0090
    WRITE OUTPUT TAPE 6,44 ,MODE,NMC,NZONE,NQS,MCL,RS,TIME,DT,CS,CR, 0091
    1BR,TIMEL 0092
    FBR=R(100) 0093
    RTEST=R(1) 0094
    NPL=NMC 0095
    GO TO 1036 0096
1000  READ INPUT TAPE 5,42,NMC,NR,(NMC,R(K),U(K),V(K),Q(K),T(K),P(K),NR, 0097
1000  1K,K=1,100) 0098
    READ INPUT TAPE 5,43,NMC,NR,(NMC,RZ(K),R2(K),ZMAS(K),DR(K),RHOZ(K) 0099
    1,TR(K),NR,K,K=1,100) 0100
    READ INPUT TAPE 5,50,NR,TIME,TEE,WKT,TDN2,TD02 0101
    READ INPUT TAPE 5,50,NR,SCALE,EQUAL,Q71,Q47,TIMEW 0102

```

NB=NMC+1	0103
LZ=100	0104
NLP=NLP+25	0105
DTMIN=DT*0.1	0106
CALL REJUST	0107
IPS=0	0108
NPL=NMC	0109
1034 WRITE OUTPUT TAPE 6,1035,DT,DR(1),(K,R(K),RH0Z(K),V(K),T(K),U(K),O	0110
1(K),ZMAS(K),DR(K),K=1,100)	0111
1035 FORMAT(1H1,10HINPUT DATA,10X,3HDT=E12.4,5X,3HDR=E12.4/3H K,2X,4HR	0112
1(L),8X,7HRH0Z(K),5X,4HV(K),8X,4HT(K),8X,4HU(L),8X,4HQ(K),8X,7HZMAS	0113
1(K),5X,5HDR(K) / (14,1P8E12.4))	0114
	0115
WRITE OUTPUT TAPE 6,44 ,MODE,NMC,NZONE,NGS,MCL,RS,TIME,DT,CS,CR,	0116
1BR,TIMEL	0117
FBR=R(100)	0118
RTEST=R(1)	0119
1036 NTAPE=15	0120
GO TO 3000	0121
C MASTER CYCLE RE-ENTRY POINT	0122
2000 TIME=TIME+DT	0123
C ROUTINE TO CHANGE NUMBER OF ZONES IN USE " " LIMIT 100 ZONES	0124
10 DO 14 J=1,100	0125
K=101-J	0126
IF(U(K)-1.0E+02) 11,12,12	0127
IF(T(K)-2.0*T(100)) 14,14,12	0128
11 LZ=K+6	0129
12 GO TO 16	0130
13 CONTINUE	0131
14 LZ=100	0132
15 IF(LZ-100) 18,18,17	0133
16 LZ=100	0134
17 LZM1=LZ-1	0135
18 LZM2=LZ-2	0136
19 LZP1=LZ+1	0137
20 LZP2=LZ+2	0138
21 FLEX=FLEX+FLOX*DT	0139
22 IF(NMC) 33,24,26	0140
23 NTAPE=15	0141
24 CN(LZ)=0.0	0142
TFLUX=FLOX	0143
FLEX=0.0	0144
25 GO TO 732	0145
26 IF(NMC- 3) 27,27,29	0146
27 NTAPE=6	0147
28 GO TO 32	0148
29 IF(TIME-TIMEW) 33,30,30	0149
30 TIMEW=TIMEW*(10.0**((1.0/18.0))	0150
IF(NMC- 4) 31,29,31	0151
31 NTAPE=15	0152
LZP2=N1	0153

32	CN(LZ)=(TIME-TIMES)/FLOATF(NMC-NMCS)	0154
	TFLUX=(FLEX-FLIX)/(TIME-TIMES)	0155
732	CALL CGSP0	0156
	NOP=NOP	0157
	FLIX=FLEX	0158
	NMCS=NMC	0159
	TIMES=TIME	0160
	LZP2=LZ+2	0161
33	CONTINUE	0162
		0163
494	IF(NMC-MCDC) 414.409.409	0164
409	MCDC=MCDC+50	0165
	REWIND 16	0166
	MODE=MODE+1	0167
	WRITE OUTPUT TAPE 16.40.NR.MODE.NMC.NLP.NEG.LZ.NZONE.NQS.MCL.	0168
	ITIMEL.BLANK.AST.TEE.PLUS.PERIOD.DASH.EQUAL.PINUS.FFF.UUU.PPP	0169
	WRITE OUTPUT TAPE 16.41.NR.NMC.TIME.DT.FLEX.CS.CR.BR.RS	0170
	WRITE OUTPUT TAPE 16.42.NMC.NR.(NMC.R(K),UCK),V(K),Q(K),T(K).	0171
	IP(K),NR,K,K=1,100)	0172
	WRITE OUTPUT TAPE 16.43.NMC.NR.(NMC.RZ(K),R2(K),ZMAS(K),DR(K).	0173
	IRHOZ(K),TR(K),NR,K,K=1,100)	0174
	WRITE OUTPUT TAPE 16.50.NR.TIME.TEE.WKT.TDN2.TD02	0175
	WRITE OUTPUT TAPE 16.50.NR.SCALE.EQUAL.Q71.Q47.TIMEW	0176
	MODE=MODE-1	0177
		0178
		0179
C	REZONE SWITCH	
414	RTEST=R(LZ-5)	0180
	NZTS=LZ-11	0181
	IF(MCP-3) 415.415.4150	0182
C	4150 ALL OPTICALLY THICK CASES	0183
4150	NZTS=MCP-4	0184
	PMT=2.55	0185
4153	IF(NZTS-9) 427.417.417	0186
C	415 ALL TRANSPARENT CASES	0187
415	IF(T(4)-2.0*TDN2) 4170.4170.416	0188
C	416 HIGH ALTITUDE EARLY PHASE	0189
416	DO 4161 L=9,LZ	0190
	IF(T(L)-1.5*TDN2) 4160.4161.4161	0191
4160	NZTS=L-1	0192
	PMT=1.5	0193
	IF(NZTS-9) 427.417.417	0194
4161	CONTINUE	0195
C	4170 LATE TIME TRANSPARENT CASE	0196
4170	DO 4140 J=11,LZ	0197
	IF(R(J)-W(1.9)) 4140.4141.4141	0198
4141	NZTS=J-5	0199
	PMT=2.8	0200
	IF(NZTS-9) 427.417.417	0201
4140	CONTINUE	0202
417	DO 426 K=9,NZTS	0203
4013	IF(NMC-NRZ) 427.427.419	0204

419	IF((R(K)-R(K-2))-0.08*RTEST)	422,422,426	0205
422	IF(ABSF(T(K)-T(K-1))-0.30*T(K))	423,423,426	0206
423	IF(ABSF(V(K)-V(K-1))-0.7*V(K))	424,424,426	0207
424	IF(ZMAS(K)+ZMAS(K-1)-PMT*ZMAS(K-2))	425,425,426	0208
425	IF(Q(K)-0.05*P(K))	9425,9425,426	0209
9425	LZP2=K		0210
	NRZ=NMC		0211
	JXC=JXC+1		0212
	WRITE OUTPUT TAPE 22,49,NMC,TIME,LZP2 ,JXC		0213
	WRITE OUTPUT TAPE 6,49,NMC,TIME,LZP2 ,JXC		0214
	CALL REZONE		0215
	LZ=LZ-1		0216
	LZM2=LZ-2		0217
	LZM1=LZ-1		0218
	LZP1=LZ+1		0219
	LZR=LZR-2		0220
	LZP2=LZ+2		0221
	NRZ=NMC+2		0222
	GO TO 427		0223
426	CONTINUE		0224
C	OPTICAL SPLIT TEST		0225
427	NS=LZ-5		0226
	KS=0		0227
	IF(NMSP-NMC)	428,428,448	0228
428	DO 440 J=3,NS		0229
429	K=LZ-J		0230
	IF((R(K)-R(K-1))-0.08*R(LZ))	430,430,442	0231
430	IF(TAU(K,1)-1.7)	440,440,431	0232
431	KS=KS+1		0233
432	IF(KS-1)	448,433,448	0234
433	IF(Q(K)-P(K))	448,434,434	0235
434	IF(U(K)-1.0E+05)	448,435,435	0236
435	KST=K		0237
	KSP=K+5		0238
	DO 436 J=KST,KSP		0239
	IF((R(J)-R(J-1))-200.0)	436,436,437	0240
436	CONTINUE		0241
	GO TO 448		0242
437	KZ2=J		0243
	IF(T(J)-6.0E+04)	443,448,448	0244
440	CONTINUE		0245
441	GO TO 448		0246
442	KZ2=K		0247
443	NMSP=NMC+3		0248
	JXD=JXD+1		0249
444	CALL SPLIT		0250
	WRITE OUTPUT TAPE 6,47,NMC,TIME,KZ2,JXD		0251
	WRITE OUTPUT TAPE 22,47,NMC,TIME,KZ2,JXD		0252
	LZ=LZ+1		0253
	LZM1=LZ-1		0254
	LZP1=LZ+1		0255

	LZP2=LZ+2	0256
	LZM2=LZ-2	0257
		0258
448	IF(NMC-NSTART) 449,451,449	0259
449	IF(NMC-NSTART-1) 450,451,450	0260
450	IF(NMC-NDD) 453,451,453	0261
451	KZ2=-451	0262
452	CALL DIAGNS	0263
453	NMC=NMC+1	0264
		0265
C		0266
	IF(NSTOP) 35,35,36	0267
35	IF(TIME-6.0) 34,52,52	0268
34	IF(SENSE SWITCH 1) 52,65	0269
52	MODE=MODE+1	0270
	NSTOP=1	0271
	MCL=MCL+3000	0272
	CALL DIAGNS	0273
	GO TO 28	0274
36	PUNCH 40, NR, MODE, NMC, NLP, NEG, LZ, NZONE, NQS, MCL, TIMEL	0275
	1, BLANK, AST, TEE, PLUS, PERIOD, DASH, EQUAL, PINUS, FFF, UUU, PPP	0276
	PUNCH 41, NR, NMC, TIME, DT, FLEX, CS, CR, BR, RS	0277
	PUNCH 42, NMC, NR, (NMC, R(K), U(K), V(K), Q(K), T(K), P(K), NR, K, K=1, 100)	0278
	PUNCH 43, NMC, NR, (NMC, RZ(K), R2(K), ZMAS(K), DR(K), RHOZ(K)	0279
	1, TR(K), NR, K, K=1, 100)	0280
	PUNCH 50, NR, TIME, TEE, WKT, TDN2, TDO2	0281
	PUNCH 50, NR, SCALE, EQUAL, Q71, Q47, TIMEW	0282
	END FILE 15	0283
	END FILE 25	0284
	REWIND 25	0285
	CALL COPY (25, 15)	0286
	END FILE 15	0287
	END FILE 22	0288
	REWIND 22	0289
	CALL COPY(22, 15)	0290
	END FILE 15	0291
	WRITE OUTPUT TAPE 6, 37, JXC	0292
37	FORMAT(1H ,13HREZONE CALLED14.6H TIMES)	0293
	REWIND 16	0294
	NR=9999	0295
	WRITE OUTPUT TAPE 41, 1499, NR, KZ6	0296
	WRITE TAPE 31, NR, KZ6	0297
1499	FORMAT(214)	0298
	WRITE OUTPUT TAPE 32, 45, NR, NMC, TIME, LZ, P(99), T(99), RHOZ(99), POWER	0299
	2, P47, FBR, (K, R(K), U(K), P(K), UR(K), T(K), FOS(K), FIS(K), DM(K), Q(K),	0300
	3FZ(K), E(K), HPPP(K), K=1, LZ)	0301
	IF(NMC-NMA6) 1502, 1502, 1501	0302
1501	READ INPUT TAPE 16, 40, NR, MODE, NMC, NLP, NEG, LZ, NZONE, NQS, MCL,	0303
	1TIMEL, BLANK, AST, TEE, PLUS, PERIOD, DASH, EQUAL, PINUS, FFF, UUU, PPP	0304
	READ INPUT TAPE 16, 41, NR, NMC, TIME, DT, FLEX, CS, CR, BR, RS	0305
	READ INPUT TAPE 16, 42, NMC, NR, (NMC, R(K), U(K), V(K), Q(K), T(K),	0306

	1P(K),NR,K,K=1,100)	0307
	READ INPUT TAPE 16,43,NMC,NR,(NMC,RZ(K),R2(K),ZMAS(K),DR(K),	0308
	1RHOZ(K),TR(K),NR,K,K=1,100)	0309
	READ INPUT TAPE16,50,NR,TIME,TEE,WKT,TDN2,TD02	0310
	READ INPUT TAPE16,50,NR,SCALE,EQUAL,Q71,Q47,TIMEW	0311
	PUNCH 40,NR,MODE,NMC,NLP,NEG,LZ,NZONE,NQS,MCL,TIMEL	0312
	1,BLANK,AST,TEE,PLUS,PERIOD,DASH,EQUAL,MINUS,FFF,UUU,PPP	0313
	PUNCH 41,NR,NMC,TIME,DT,FLEX,CS,CR,BR,RS	0314
	PUNCH 42,NMC,NR,(NMC,R(K),U(K),V(K),Q(K),T(K),P(K),NR,K,K=1,100)	0315
	PUNCH 43,NMC,NR,(NMC,RZ(K),R2(K),ZMAS(K),DR(K),RHOZ(K)	0316
	1,TR(K),NR,K,K=1,100)	0317
	PUNCH 50,NR,TIME,TEE,WKT,TDN2,TD02	0318
	PUNCH 50,NR,SCALE,EQUAL,Q71,Q47,TIMEW	0319
	END FILE 16	0320
1502	CALL UNLOAD(16)	0321
	CEASE=1.0E+29	0322
	END FILE 32	0323
	END FILE 42	0324
	REWIND 42	0325
	CALL COPY(42,32)	0326
	CALL UNLOAD(42)	0327
		0328
C	EXTRA COPY OF USER TAPE 32 INFO COPIED AS FILE 2 OF TAPE 15	0329
	END FILE 32	0330
	REWIND 32	0331
	CALL COPY(32,15)	0332
	END FILE 15	0333
	CALL COPY (32,15)	0334
	END FILE 15	0335
	CALL UNLOAD(15)	0336
	CALL UNLOAD(32)	0337
	END FILE 41	0338
	CALL UNLOAD(41)	0339
	END FILE 31	0340
	CALL UNLOAD(31)	0341
1500	CALL EXIT	0342
65	NTI=0	0343
	IF(NMC-MCL) 64,64,52	0344
64	IF(TIME-TIMEL) 66,66,52	0345
C SET	RETARDED VARIABLES	0346
66	DO 71 K=1,100	0347
67	VR(K)=V(K)	0348
68	ER(K)=E(K)	0349
69	PR(K)=P(K)	0350
70	W(K,4)=T(K)	0351
	W(K,6)=V(K)	0352
	W(K,7)=P(K)	0353
	W(K,8)=Q(K)	0354
	W(K,9)=E(K)	0355
71	DIVFR(K)=DIVFA(K)	0356
	KRT=0	0357

72	IF(DT-50.0*DTMIN) 74,74,73	0358
73	DTMIN=DT/50.0	0359
74	CALL HYDRO	0360
	KZ4=KZ4	0361
	IF(U(99)-1.0E+03) 290,290,52	0362
	C INITIAL TEMPERATURE EXTRAPOLATION	0363
290	CONTINUE	0364
	C ITERATION CYCLE RE-ENTRY POINT	0365
	C DERIVATIVES WITH RESPECT TO TEMP OP DE	0366
3000	DO 301 K=1,LZ	0367
3001	IF(T(K)) 3002,3002,300	0368
3002	KZ2=-3000	0369
	CALL DIAGNS	0370
	GO TO 52	0371
300	TP(K)=1.02*T(K)	0372
301	TS(K)=TP(K)	0373
303	CALL STATE	0374
304	DO 310 K=1,LZ	0375
305	PP(K)=P(K)	0376
306	EP(K)=E(K)	0377
309	TM(K)=0.98*T(K)	0378
310	TS(K)=TM(K)	0379
311	CALL STATE	0380
312	DO 318 K=1,LZ	0381
313	PM(K)=P(K)	0382
314	EM(K)=E(K)	0383
315	DPT(K)=(PP(K)-PM(K))/(TP(K)-TM(K))	0384
316	DET(K)=(EP(K)-EM(K))/(TP(K)-TM(K))	0385
318	TS(K)=T(K)	0386
320	CALL STATE	0387
	C CALL RADIATIVE PROPERTIES ROUTINE	0388
	CALL SWABZ	0389
501	LZR=LZR	0390
	MCP=MCP	0391
	KZ1=KZ1	0392
	KZ2=KZ2	0393
	KZ3=KZ3	0394
	KZ8=KZ8	0395
	KZ9=KZ9	0396
321	NCW=NCW	0397
322	DTAU(LZP1,1)=0.0	0398
		0399
	C INTENSITY INTEGRATION	0400
500	CALL FLUXS	0401
502	IF(IPS) 503,503,530	0402
503	IPS=IPS+1	0403
504	TIME=TIME-DT	0404
505	GO TO 2000	0405
	C TEMPERATURE TEST BYPASS ON FIRST GUESS	0406
530	IF(NTI) 540,540,532	0407
	C TEMPERATURE TEST	0408

532	DO 536 K=1,LZ	0409
533	IF(ABS(DTM(K)/T(K))-0.1) 536,536,540	0410
536	CONTINUE	0411
C	MAIN CYCLE COMPLETED -- RETURN TO 2000	0412
537	GO TO 2000	0413
540	NTI=NTI+1	0414
C	ENERGY EQUATION BLOCK 600	0415
600	IF(NTI-3) 601,601,2000	0416
601	DO 617 K=1,LZ	0417
602	L=K	0418
603	N=110+K	0419
613	DE(K)=(E(K)-ER(K))/DT	0420
614	PA(K)=(PR(K)+P(K))/2.0	0421
615	RESQDE(K)=DE(K)+(PA(K)+Q(K))*(V(K)-VR(K))/DT	0422
625	1+(DIVFA(K)+DIVFR(K))/2.0	0423
617	CONTINUE	0424
C	TEMPERATURE ITERATION OF ENERGY EQUATION	0425
700	IF(LZR-4) 703,703,701	0426
701	CALL COEFF	0427
702	GO TO 829	0428
C	NO ITERATION OF RADIATION	0429
703	DO 704 K=1,LZ	0430
704	DTM(K)=-RESQDE(K)/((DET(K)/DT)+(DPT(K)/(2.0*DT))*(V(K)-VR(K)))	0431
705	IF(NMC-NLP) 906,706,906	0432
706	NLP=NLP+50	0433
	PRINT 707,NMC,TIME,DT,LZ	0434
707	FORMAT(23H PROGRESS REPORT NMC=14, 5X,5HTIME=1PE12.3,5X,11HTIME	0435
707	1 STEP=1PE12.3,10X,5HRADHYDRO14///)	0436
708	GO TO 906	0437
		0438
C	RADIATIVE ITERATION	0439
829	CONTINUE	0440
830	IF(NMC-NLP) 987,831,987	0441
831	NLP=NLP+50	0442
	PRINT 832,NMC,TIME,DT,LZ	0443
832	FORMAT(23H PROGRESS REPORT NMC=14, 5X,5HTIME=1PE12.3,5X,11HTIME	0444
832	1 STEP=1PE12.3,10X,8HRADHYDRO14///)	0445
C		0446
C	COEFFICIENTS NOW KNOWN-SOLUTION FOR DTM(K)	0447
987	LZJ=LZR+1	0448
	DO988 K=LZJ,LZ	0449
988	DTM(K)=-RESQDE(K)/((DET(K)/DT)+(DPT(K)/(2.0*DT))*(V(K)-VR(K)))	0450
900	DTM(LZR)=(EN(LZR)-EN(LZR-1))/(CN(LZR)-CN(LZR-1))	0451
902	DTM(LZR-1)=(EN(LZR-1)-CN(LZR-1)*DTM(LZR))	0452
	DO 905 J=3,LZR	0453
	K=LZJ-J	0454
905	DTM(K)=EN(K)-DN(K)*DTM(K+2)-CN(K)*DTM(K+1)	0455
906	CONTINUE	0456
C	STABILITY CHECK	0457
907	DO 930 K=1,LZ	0458
908	IF(DTM(K)) 909,930,910	0459

909	IF(ABSF(DTM(K))-0.5*T(K))	930.930.918	0460
910	IF(T(K)-2.0E+05)	912.911.911	0461
911	IF(ABSF(DTM(K))-0.9*T(K))	930.930.918	0462
912	IF(ABSF(DTM(K))-5.0*T(K))	930.930.918	0463
918	KZ2=-920		0464
919	KZ5=K		0465
920	CALL DIAGNS		0466
921	KRT=KRT+1		0467
922	IF(KRT-3)	923.933.933	0468
923	DO 927 L=1,LZ		0469
	U(L)=W(L,3)		0470
	T(L)=W(L,4)		0471
	R(L)=W(L,5)		0472
	V(L)=W(L,6)		0473
	P(L)=W(L,7)		0474
	Q(L)=W(L,8)		0475
	E(L)=W(L,9)		0476
	R2(L)=R(L)**2		0477
927	CONTINUE		0478
928	WRITE OUTPUT TAPE 6,929,NMC,KRT,K		0479
	PRINT 929,NMC,KRT,K		0480
929	FORMAT(418)		0481
	NTI=0		0482
	GO TO 74		0483
930	CONTINUE		0484
C	MODIFY TEMPERATURE		0485
933	DO 934 K=1,LZ		0486
934	T(K)=T(K)+DTM(K)		0487
935	GO TO 3000		0488
936	END		0489
*	FORTRAN		0490
CF1SWZ			0491
	SUBROUTINE SWABZ		0492
C	STANDARD DIMENSION AND COMMON STATEMENTS AS IN MAIN PROGRAM		0493
	D(1)=0.0		0494
			0495
	DO 126 K=1,LZ		0496
	DO 135 N=1,NSZ		0497
	TS(K)=TS(K)/11606.5		0498
	ETA(K)=1.293E-03*V(K)		0499
	ALPHA=9.0*EXPF(-TIME/1.0E-03*(ETA(K)**2))		0500
	BETA=((6.0E-18*V(K)**0.5)*(TS(K)**0.1)		0501
300	ZI(K,1)=EXPF(-1.5*(R(K)-R(K-1)) /((ETA(K)**1.5)/((TS(K)**ALPHA)		0502
300	2+BETA) +0.2*(ETA(K)**1.91)/(TS(K)**2.73)		0503
300	3+0.023*(ETA(K)**1.8)*(TS(K)**0.25)+1.0E-07*(ETA(K)**2.0)/		0504
300	4((TS(K)**(-5.0))+4.0E-14*V(K)))		0505
	ZI(K,1)=ZI(K,1)*0.99999998		0506
	ZI(K,2)=ZI(K,1)		0507
	HMFP=(ETA(K)**1.5)/((TS(K)**ALPHA)+BETA)		0508
	1+0.2*(ETA(K)**1.91)/(TS(K)**2.73)		0509
	2+0.023*(ETA(K)**1.8)*(TS(K)**0.25)		0510

	3+1.0E-07*(ETA(K)**2.0)*(TS(K)**5.00)	0511
	HMFF=9.3E-06*(ETA(K)**2.0)*(TS(K)**3.5)	0512
	IF(TS(K)-10.0) 301,298,298	0513
298	IF(HMFF-HMFP) 299,301,301	0514
299	HMFP=HMFF	0515
301	DTAU(K,1)=1.5*(R(K)-R(K-1))/HMFP	0516
302	A(K,N)=EXP(-DTAU(K,N))	0517
312	BC(K,N)=5.67E-05*(T(K)**4)	0518
	TS(K)=TS(K)*11606.5	0519
135	CONTINUE	0520
126	CONTINUE	0521
C	SOURCE FUNCTION INTERPOLATION	0522
	DO 201 K=1,LZ	0524
	DO 202 N=1,NSZ	0525
311	BB(K,N)=((((R(K+1)-R(K))*T(K)**4)+((R(K)-R(K-1))*T(K+1)**4))/	0526
311	1(R(K+1)-R(K-1))))*5.67E-05	0527
	BB(K,2)=BB(K,1)	0528
506	S(K,N)=(BC(K,N)-BC(K+1,N))/(DTAU(K,N)+DTAU(K+1,N))	0529
507	W(K,N)=1.0-A(K,N)-A(K,N)*DTAU(K,N)	0530
508	IF(W(K,N)-1.0E-04) 509,202,202	0531
509	W(K,N)=0.5*(DTAU(K,N)**2)	0532
202	CONTINUE	0533
201	CONTINUE	0534
		0535
C	SET OPTICAL INDICES	0536
	KM=0	0537
501	KD=0	0538
502	KN=0	0539
503	TAU(LZ,1)=DTAU(LZ,1)	0540
511	DO 522 J=1,LZM1	0541
512	K=LZ-J	0542
513	TAU(K,1)=TAU(K+1,1)+DTAU(K,1)	0543
514	IF(TAU(K,1)-5.0E-06) 522,515,515	0544
515	KN=KN+1	0545
516	IF(KN-1) 518,517,518	0546
517	LZR=K+3	0547
518	IF(TAU(K,1)-.44) 522,519,519	0548
519	KD=KD+1	0549
520	IF(KD-1) 622,523,622	0550
523	FBR=R(K)	0551
622	IF(TAU(K,1)-1.0) 522,623,623	0552
623	KM=KM+1	0553
624	IF(KM-1) 522,625,522	0554
625	MCP=K	0555
522	CONTINUE	0556
525	IF(LZR-LZ+1) 530,530,529	0557
529	LZR=LZ-1	0558
530	CONTINUE	0559
	IF(KD) 521,521,524	0560
521	FBR=0.0	0561

	MCP=0	0562
524	CONTINUE	0563
C	SET CUTOFF WAVELENGTH CWL(K)	0564
	CWMAX=0.0	0565
	KCWMAX=0	0566
	CWL(MCP.1)=0.0	0567
	NCW=MCP	0568
	TR(MCP)=T(MCP)	0569
		0570
540	DO 565 K=1,LZ	0571
541	IF(T(K)-TDN2) 546,542,542	0572
		0573
C	OPACITY DUE TO ATOMIC SPECIES	0574
542	CWL(K.1)= 700.0*EXPF(-0.36*(T(K)-11606.5)/11606.5)	0575
B544	DTH(K)=2121212121	0576
	IF(CWL(K.1)-275.0) 545,560,560	0577
545	CWL(K.1)=275.0	0578
	GO TO 560	0579
546	IF(T(K)-TD02) 551,547,547	0580
		0581
C	OPACITY DUE TO N2 MOLECULE	0582
B 547	DTH(K)=454545454545	0583
	TCN2=5.0E-07*1.293E-03*V(K)	0584
549	CWL(K.1)=1140.0*((R(K)-R(K-1))/(V(K)*1.293E-03))**0.11)	0585
	1*(1.0-EXPF(-TIME/TCN2))	0586
	IF(CWL(K.1)-1000.0) 550,560,560	0587
550	CWL(K.1)=1000.0	0588
	GO TO 560	0589
		0590
C	OPACITY DUE TO O2 MOLECULE	0591
551	TC=4250.0-271.0*LOGF(1.293E-03* V(K))	0592
	TC02=3.0E-07*1.293E-03*V(K)	0593
B 552	DTH(K)=676767676767	0594
553	IF(T(K)-TC)554,554,556	0595
554	CWL(K.1)=1500.0+TS(K)*(0.163+0.0745*LOGF(DR(K)*RHOZ(K)/1.293E-03))	0596
554	1*(1.0-EXPF(-TIME/TC02))	0597
555	GO TO 557	0598
556	TSB=TS(K)*(0.0647*LOGF(R(K)-R(K-1))-0.25-.109*LOGF(1.293E-03*V(K)))	0599
	CWL(K.1)=3500.0+TSB-(2000.0+TSB)*EXPF(-TIME/TC02)	0600
557	IF(CWL(K.1)-1500.0) 558,560,560	0601
558	CWL(K.1)=1500.0	0602
560	IF(K-MCP) 565,565,561	0603
561	IF(CWL(K.1)-CWMAX) 565,565,563	0604
563	CWMAX=CWL(K.1)	0605
564	KCWMAX=K	0606
565	CONTINUE	0607
566	NCW=KCWMAX	0608
		0609
	IF(LZR-NCW) 603,603,604	0610
603	LZR=NCW+1	0611
C	CALCULATE Z0 VALUES	0612

604	Z0(1,1)=Z1(1,1)	0613
	KD=0	0614
605	DO 670 L=2,LZ	0615
	TR(L)=T(L)	0616
	IF(T(L)-8.0E+04) 607,668,668	0617
607	KD=KD+1	0618
	IF(KD-1) 608,608,609	0619
608	MS=L-1	0620
609	IF(DTAU(L,1)-1.0) 610,668,668	0621
C	SELECT TR(L)= TEMPERATURE OF RADIATION TRAVERSING ZONE L	0622
610	LIM=L-1	0623
611	TAUSUM=0.0	0624
615	DO 630 NN=1,LIM	0625
616	M=L-NN	0626
617	TAUSUM=TAUSUM+DTAU(M,1)	0627
620	IF(TAUSUM-0.7) 630,627,627	0628
627	TR(L)=T(M)	0629
628	IF(M-2) 630,630,638	0630
630	CONTINUE	0631
	IF(T(L)-2500.0) 631,632,632	0632
631	TR(L)=TR(L-1)	0633
	GO TO 637	0634
632	EPTSUM=0.0	0635
	EPSUM=0.0	0636
	DO 635 K=3,LIM	0637
	EPSUM=EPSUM+DTAU(K,1)	0638
	EPTSUM=EPTSUM+T(K)*DTAU(K,1)	0639
	IF(T(K)-2500.0) 636,636,635	0640
635	CONTINUE	0641
636	TR(L)=EPTSUM/EPSUM	0642
637	M=2	0643
638	IZ=M+1	0644
639	DO 646 I=IZ,L	0645
640	IF(TR(L)*CWL(1,1)-2.0E+08) 641,641,644	0646
641	ZI(1,2)= EXPF((-3.41E-08*CWL(1,1)*TR(L)+2.5E-25*((CWL(1,1)*TR(L	0647
641	2))*3))*EXPF(-3.07E+13/((CWL(1,1)*TR(L))*1.8)))	0648
642	GO TO 646	0649
644	ZI(1,2)=7.61E+22/((CWL(1,1)*TR(L))*3)	0650
646	CONTINUE	0651
	ZMAX=ZI(M+1,2)	0652
	Z0(L,1)=ZI(M+1,2)	0653
647	IF(L-M-1) 668,663,650	0654
C	CORRECTION FOR INTERMEDIATE ZONES	0655
650	IZ=M+2	0656
651	CWLTST=CWL(M+1,1)	0657
652	DO 660 NZ=IZ,L	0658
653	IF(CWL(NZ,1)-CWLTST) 654,654,657	0659
654	IF(NZ-L) 660,655,668	0660
655	Z0(L,1)=1.0	0661
656	GO TO 660	0662
657	Z0(L,1)=ZI(NZ,2)/ZMAX	0663

658	CWLTST=CWL(NZ,1)	0664
659	ZMAX=ZI(NZ,2)	0665
660	CONTINUE	0666
663	IF(ZO(L,1)-ZI(L,1)) 670,668,668	0667
668	ZO(L,1)=ZI(L,1)	0668
670	CONTINUE	0669
671	DO 676 K=1,LZ	0670
672	IF(DTAU(K,1)-1.0E-04) 673,675,675	0671
673	A(K,1)=DTAU(K,1)	0672
674	GO TO 676	0673
675	A(K,1)=1.0-A(K,1)	0674
676	CONTINUE	0675
	DO 699 K=1,LZ	0676
	IF(S(K,1)-1.69E+38) 767,767,677	0677
767	HZ(K)=BB(K,1)*A(K+1,1)	0678
	DZ(K)=2.0*S(K,1)*W(K+1,1)	0679
	HP(K)=BC(K+1,1)*A(K+1,1)	0680
	IF(HZ(K)-DZ(K)-HP(K)*0.01) 677,677,699	0681
677	S(K,1)=0.0	0682
678	BB(K,1)=BC(K+1,1)	0683
679	BB(K,2)=BC(K,1)	0684
699	CONTINUE	0685
900	IF(BC(1,1)-BC(2,1)) 915,916,916	0686
915	BB(1,2)=BC(1,1)	0687
916	CONTINUE	0688
	EMS=ZI(NCW,2)	0689
179	RETURN	0690
	END	0691
		0692
*	FORTRAN	0693
CF1RJST		0694
	SUBROUTINE REJUST	0695
C	STANDARD DIMENSION AND COMMON STATEMENTS AS IN MAIN PROGRAM	0696
	TD02=7100.0*EXP((0.43429*LOGF(RHOZ(99)/1.293E-03))/5.3)	0697
	TDN2=15000.0*EXP((0.43429*LOGF(RHOZ(99)/1.293E-03))/4.8)	0698
	RETURN	0699
	END	0700
*	FORTRAN	0701
CF1RZNE		0702
	SUBROUTINE REZONE	0703
C	STANDARD DIMENSION AND COMMON STATEMENTS AS IN MAIN PROGRAM	0704
		0705
I	M=LZP2	0706
	ZETA=(T(M-1)+T(M))/(E(M-1)+E(M))	0707
C	ROUTINE TO COMBINE ZONES M AND M-1	0708
	FKE=(ZMAS(M-2)*(U(M-2)**2)+ZMAS(M-1)*((U(M-1)**2)+(U(M-2)**2)	0709
	2)+ZMAS(M)*((U(M-1)**2)+(U(M)**2))+ZMAS(M+1)*(U(M)**2))	0710
	FMV=(ZMAS(M-2)*U(M-2)+ZMAS(M-1)*(U(M-1)+U(M-2))+ZMAS(M)*(U(M-1)	0711
	2+U(M))+ZMAS(M+1)*U(M))	0712
	FKA=ZMAS(M-2)+ZMAS(M-1)+ZMAS(M)	0713
	FKB=ZMAS(M-1)+ZMAS(M)+ZMAS(M+1)	0714

	FKB=FKB/FKA	0715
	FKE=FKE/FKA	0716
	FMV=FMV/FKA	0717
	FSR=(FKE*FKB)*(FKB+1.0)-FKB*(FMV**2)	0718
	IF(FSR) 7700,7701,7701	0719
7700	U(M-2)=U(M-2)	0720
	U(M-1)=U(M)	0721
	GO TO 7733	0722
7701	FSR=(FSR**0.5)/FKB	0723
	UPLUS=(FMV+FSR)/(FKB+1.0)	0724
	UMINS=(FMV-FSR)/(FKB+1.0)	0725
	IF(U(M-2)-U(M)) 7722,7711,7711	0726
7711	U(M-2)=UPLUS	0727
	U(M-1)=UMINS	0728
	GO TO 7733	0729
7722	U(M-2)=UMINS	0730
	U(M-1)=UPLUS	0731
7733	CONTINUE	0732
2	E(M-1)=(ZMAS(M-1)*E(M-1)+ZMAS(M)*E(M))/(ZMAS(M-1)+ZMAS(M))	0733
3	T(M-1)=(E(M-1) *ZETA)	0734
4	ZMAS(M-1)=ZMAS(M-1)+ZMAS(M)	0735
5	DIVFA(M-1)=(R2(M)/ZMAS(M-1))*(FOS(M)-FIS(M))	0736
5	1-(R2(M-2)/ZMAS(M-1))*(FOS(M-2)-FIS(M-2))	0737
7	R(M-1)=R(M)	0738
8	RZ(M-1)=RZ(M)	0739
9	R2(M-1)=R2(M)	0740
10	DR(M-1)=DR(M-1)+DR(M)	0741
11	RR(M-1)=RR(M)	0742
13	TR(M-1)=TR(M)	0743
14	V(M-1)=(R(M-1)**3-R(M-2)**3)/(3.0*ZMAS(M-1))	0744
15	P(M-1)=(P(M-1)+P(M))/2.0	0745
16	Q(M-1)=(Q(M-1)+Q(M))/2.0	0746
	DTM(M-1)=0.0	0747
		0748
C	SHIFT IN EXTERIOR ZONES	0749
20	DO 50 K=M,99	0750
21	V(K)=V(K+1)	0751
22	T(K)=T(K+1)	0752
23	RHOZ(K)=RHOZ(K+1)	0753
24	U(K)=U(K+1)	0754
25	P(K)=P(K+1)	0755
26	R(K)=R(K+1)	0756
27	R2(K)=R2(K+1)	0757
28	RZ(K)=RZ(K+1)	0758
29	DR(K)=DR(K+1)	0759
30	Q(K)=Q(K+1)	0760
31	E(K)=E(K+1)	0761
32	DIVFA(K)=DIVFA(K+1)	0762
33	UR(K)=UR(K+1)	0763
34	ZMAS(K)=ZMAS(K+1)	0764
35	RR(K)=RR(K+1)	0765

	DTM(K)=DTM(K+1)	0766
50	TR(K)=TR(K+1)	0767
		0768
C	ADDITION OF NEW ZONE 100	0769
51	R(100)=R(99)+DR(99)	0770
52	R2(100)=R(100)**2	0771
53	RZ(100)=R(100)	0772
54	RHOZ(100)=RHOZ(99)	0773
55	RR(100)=1.0	0774
56	DR(100)=DR(99)	0775
57	ZMAS(100)=(RHOZ(100)/3.0)*((RZ(100)**3)-(RZ(99)**3))	0776
58	U(100)=0.0	0777
59	T(100)=T(99)	0778
60	V(100)=V(99)	0779
62	Q(100)=0.0	0780
		0781
	T(101)=T(100)	0782
	RETURN	0783
	END	0784
*	FORTRAN	0785
	SUBROUTINE SPLIT	0786
C	STANDARD DIMENSION AND COMMON STATEMENTS AS IN MAIN PROGRAM	0787
	M=100-KZ2	0788
	DO 30 J=1,M	0789
	K=101-J	0790
	R(K)=R(K-1)	0791
	DR(K)=DR(K-1)	0792
	RR(K)=RR(K-1)	0793
	RHOZ(K)=RHOZ(K-1)	0794
	RZ(K)=RZ(K-1)	0795
	R2(K)=R2(K-1)	0796
	U(K)=U(K-1)	0797
	RR(K)=RR(K-1)	0798
	TR(K)=TR(K-1)	0799
	V(K)=V(K-1)	0800
	P(K)=P(K-1)	0801
	ZMAS(K)=ZMAS(K-1)	0802
	Q(K)=Q(K-1)	0803
	T(K)=T(K-1)	0804
	E(K)=E(K-1)	0805
	DIVFA(K)=DIVFA(K-1)	0806
	UR(K)=UR(K-1)	0807
30	CONTINUE	0808
C	ADD ZONE JUST OUTSIDE K=KZ2	0809
	ZMAS(KZ2)=ZMAS(KZ2)/2.0	0810
	ZMAS(KZ2+1)=ZMAS(KZ2)	0811
	V(KZ2+1)=V(KZ2)	0812
	RHOZ(KZ2+1)=RHOZ(KZ2)	0813
	R(KZ2)=((R(KZ2+1)**3)-(3.0*ZMAS(KZ2+1)* V(KZ2+1)))* (1.0/3.0)	0814
	RZ(KZ2)=((RZ(KZ2+1)**3)-(3.0*ZMAS(KZ2+1)/RHOZ(KZ2+1)))* (1.0/3.0)	0815
	RR(KZ2)=R(KZ2)/RZ(KZ2)	0816


```

DR(KZ2+1)=R(KZ2+1)-R(KZ2)                                0817
DR(KZ2)=R(KZ2)-R(KZ2-1)                                  0818
R2(KZ2)=R(KZ2)**2                                         0819
U(KZ2)=(((U(KZ2-1)**2)+(U(KZ2+1)**2))/2.0)**0.5         0820
TR(KZ2+1)=TR(KZ2)                                         0821
P(KZ2+1)=P(KZ2)                                           0822
Q(KZ2+1)=Q(KZ2)                                           0823
T(KZ2+1)=0.9*T(KZ2)                                       0824
T(KZ2)=1.1*T(KZ2)                                         0825
E(KZ2+1)=0.85*E(KZ2)                                      0826
E(KZ2)=1.15*E(KZ2)                                       0827
DIVFA(KZ2+1)=DIVFA(KZ2)                                   0828
UR(KZ2)=0.5*(UR(KZ2-1)+UR(KZ2+1))                       0829
RETURN                                                     0830
END                                                         0831
* FORTRAN                                                 0832
CF1CGSP0 CGS PRINT OUT PACKAGE FIRE 1                   0833
SUBROUTINE CGSP0                                         0834
C STANDARD DIMENSION AND COMMON STATEMENTS AS IN MAIN PROGRAM 0835
45 FORMAT(1H1//39H AT COMPLETION OF MASTER CYCLE NUMBER 14.25X,15. 0836
45 240X,3HSE=0PF10.3//6H TIME=1PE10.3,21X,6HPOWER=1PE10.3,2X,5HWATTS, 0837
45 313X,10HTIME STEP=1PE10.3,20X,14HPASSES ENG EQ 14// 0838
45 43H K,2X,6HRADIUS,5X,8HPART VEL,2X,4HPRES,6X,3HQ/P,3X,3HTEV,4X,3HR 0839
45 5H0,7X,3HE/G,7X,4HFOUT,5X,5HF1/F0,2X,4HDIVF,5X,4HTEMP,4X,5HGAMMA, 0840
45 6X,4HPART,X,1HC,2X,3HTAU,5X,4HDTAU//((14,1PE10.3,1P2E10.2,0P2F6.2, 0841
45 71P3E10.2,0PF6.2,1P2E10.2,0PF5.2,0PF6.2,1A1,0PF7.2,1A1,1PE9.2)) 0842
46 FORMAT(1H /8H T PART=1PE12.4,9H FRACT ,5X,6HDTHYD=1PE12.4,8H SEC 0843
46 1S ,5X,6HPOW03=1PE12.4,8H WATTS ,5X,5HTEFF=0PF6.0,8H DEG K ,5X, 0844
46 24HLZR=14/8H TYIELD=1PE12.4,9H ERGS ,5X,6HDTRAD=1PE12.4,8H SECS 0845
46 3 ,5X,6HPOW34=1PE12.4,8H WATTS ,5X,5HTCOL=0PF6.0,8H DEG K ,5X, 0846
46 44HNCW=14/8H IN ENG=1PE12.4,9H ERGS ,5X,6HDTMIN=1PE12.4,8H SECS 0847
46 5 ,5X,6HPOW45=1PE12.4,8H WATTS ,5X,5HWLMX=0PF6.0,8H ANG ,5X, 0848
46 64H0D1=14/8H KN ENG=1PE12.4,9H ERGS ,5X,6HDTLST=1PE12.4,8H SECS 0849
46 7 ,5X,6HPOW57=1PE12.4,8H WATTS ,5X,5HTY41=0PF7.2,7HKT ,5X, 0850
46 8.4HEMS=0PF5.4) 0851
36 FORMAT(8H TOT ES=1PE12.4,9H ERGS 5X,6HFBRAD=1PE12.4,8H CM , 0852
36 25X,6HPOW71=1PE12.4,8H WATTS ,5X,5HTY71=0PF7.2,7HKT ,5X, 0853
36 34HNSZ=14/8H E AMBT=1PE12.4,9H ERGS 5X,6HSHRAD=1PE12.4,8H CM 0854
36 4 ,5X,6HPOW47=1PE12.4,8H WATTS ,5X,5HTY47=0PF7.2,7HKT ,5X, 0855
36 56HD1589-12) 0856
47 FORMAT(1H1//, 0857
47 43H K,2X,6HRADIUS,5X,8HPART VEL,2X,4HPRES,6X,3HQ/P,3X,3HTEV,4X,3HR 0858
47 5H0,7X,3HE/G,7X,4HFOUT,5X,5HF1/F0,2X,4HDIVF,5X,4HTEMP,4X,5HGAMMA, 0859
47 6X,4HPART,X,1HC,2X,3HTAU,5X,4HDTAU//((14,1PE10.3,1P2E10.2,0P2F6.2, 0860
47 71P3E10.2,0PF6.2,1P2E10.2,0PF5.2,0PF6.2,1A1,0PF7.2,1A1,1PE9.2)) 0861
YIELD=EQUAL 0862
DO 1000 K=4,LZ 0863
IF(T(K-1)-0.6*T(K)) 1002,1002,1000 0864
1002 KZ2=0 0865
CALL DIAGNS 0866
1000 CONTINUE 0867

```

```

RSHOCK=0.0                                0868
SAVE1=DT                                    0869
DT=CN(LZ)                                    0870
STX=P(LZ)                                    0871
POWER=TFLUX*1.0E-07                         0872
TCOL=(TFLUX/( EMS *12.56*5.67E-05*(FBR**2)))*0.25 0873
TEFF=(TFLUX/(12.56*5.67E-05*(FBR**2)))*0.25 0874
CALL PHOTOG                                  0875
C ESTIMATE OF OBSERVED SPECTRAL DISTRIBUTION 0876
IF(FBR) 1059,1059.1061                       0877
1059 P47=0.37*POWER                          0878
      Q47=Q47+P47*(TIME-TIMES)/4.186E+12    0879
      Q41=0.0                                 0880
      P03=0.0                                 0881
      P34=0.0                                 0882
      P45=0.0                                 0883
      P57=0.0                                 0884
      P71=0.0                                 0885
      Q71=0.0                                 0886
1060 GO TO 1600                               0887
1061 SAVET=T(MCP)                             0888
1062 T(MCP)=TCOL                              0889
1064 IF( T(MCP)*CWLM -2.0E+08) 1065,1065.1068 0890
1063 CWLM=CWL(NCW,1)                          0891
1065 FLM = EXPF((-3.41E-08*CWLM * T(MCP)+2.5E-25*((CWLM * T(MCP))**3) 0892
1065 1)*EXPF(-3.07E+13/((CWLM * T(MCP))**1.8))) 0893
1067 GO TO 1164                               0894
1068 FLM =7.61E+22/((CWLM *T(MCP))**3)       0895
1164 IF( T(MCP)*3000.0-2.0E+08) 1165,1165.1168 0896
1165 F3 = EXPF((-3.41E-08*3000.0* T(MCP)+2.5E-25*((3000.0* T(MCP))**3) 0897
1165 1)*EXPF(-3.07E+13/((3000.0* T(MCP))**1.8))) 0898
1167 GO TO 1264                               0899
1168 F3 =7.61E+22/((3000.0*T(MCP))**3)       0900
1264 IF( T(MCP)*4000.0-2.0E+08) 1265,1265.1268 0901
1265 F4 = EXPF((-3.41E-08*4000.0* T(MCP)+2.5E-25*((4000.0* T(MCP))**3) 0902
1265 1)*EXPF(-3.07E+13/((4000.0* T(MCP))**1.8))) 0903
1267 GO TO 1364                               0904
1268 F4 =7.61E+22/((4000.0*T(MCP))**3)       0905
1364 IF( T(MCP)*5000.0-2.0E+08) 1365,1365.1368 0906
1365 F5 = EXPF((-3.41E-08*5000.0* T(MCP)+2.5E-25*((5000.0* T(MCP))**3) 0907
1365 1)*EXPF(-3.07E+13/((5000.0* T(MCP))**1.8))) 0908
1367 GO TO 1464                               0909
1368 F5 =7.61E+22/((5000.0*T(MCP))**3)       0910
1464 IF( T(MCP)*7000.0-2.0E+08) 1465,1465.1468 0911
1465 F7 = EXPF((-3.41E-08*7000.0* T(MCP)+2.5E-25*((7000.0* T(MCP))**3) 0912
1465 1)*EXPF(-3.07E+13/((7000.0* T(MCP))**1.8))) 0913
1467 GO TO 1564                               0914
1468 F7 =7.61E+22/((7000.0*T(MCP))**3)       0915
1564 IF( T(MCP)*10000.0-2.0E+08) 1565,1565.1568 0916
1565 F1= EXPF((-3.41E-08*10000.0* T(MCP)+2.5E-25*((10000.0* T(MCP))**3) 0917
1565 1)*EXPF(-3.07E+13/((10000.0* T(MCP))**1.8))) 0918

```

1567	GO TO 1580	0919
1568	F1 =7.61E+22/((10000.0*T(MCP))**3)	0920
1580	CONTINUE	0921
	T(MCP)=SAVET	0922
1581	IF(CWLM-3000.0) 1583,1583,1582	0923
1582	F3=FLM	0924
1583	IF(CWLM-4000.0) 1585,1585,1584	0925
1584	F4=FLM	0926
1585	IF(CWLM-5000.0) 1587,1587,1586	0927
1586	F5=FLM	0928
1587	IF(CWLM-7000.0) 1589,1589,1588	0929
1588	F7=FLM	0930
1589	IF(CWLM-10000.0) 1591,1591,1590	0931
1590	F1=FLM	0932
1591	CONTINUE	0933
	P03=POWER*(FLM-F3)/FLM	0934
	P34=POWER*(F3-F4)/FLM	0935
	P45=POWER*(F4-F5)/FLM	0936
	P57=POWER*(F5-F7)/FLM	0937
	P71=POWER*(F7-F1)/FLM	0938
	P47=POWER*(F4-F7)/FLM	0939
	Q71=Q71+P71*(TIME-TIMES)/4.186E+12	0940
	Q47=Q47+P47*(TIME-TIMES)/4.186E+12	0941
	Q41=Q47+Q71	0942
		0943
1600	EN(1)=4.189*(R(1)**3)*(E(1)/V(1))	0944
	BN(1)=EN(1)	0945
	CN(1)=3.14159*(U(1)**2)*ZMAS(1)	0946
	DN(1)=CN(1)	0947
	DPP(1)=BN(1)+DN(1)	0948
	DO 490 K=2,LZ	0949
	EN(K)=4.189*((R(K)**3)-(R(K-1)**3))*(E(K)/V(K))	0950
	CN(K)=3.14159*(U(K)**2+U(K-1)**2)*ZMAS(K)	0951
	BN(K)=BN(K-1)+EN(K)	0952
	DN(K)=DN(K-1)+CN(K)	0953
B	THETA(K)=2121212121	0954
	IF(Q(K)-STX) 490,490,488	0955
488	STX=Q(K)	0956
	J3=K-3	0957
489	RSHOCK=R(K)	0958
490	DPP(K)=BN(K)+DN(K)	0959
	EAMB=4.189*(R(LZ)**3)*E(99)/V(99)	0960
	ESYSM=DPP(LZ)-EAMB	0961
	ETOTAL=ESYSM/4.186E+19	0962
	PARTT=FLEX/YIELD	0963
491	IF(NMC) 493,492,493	0964
492	YIELD=ESYSM	0965
	EQUAL=YIELD	0966
493	CONTINUE	0967
	WRITE OUTPUT TAPE22,495,NR,NMC,TIME,EAMB,NCW,MCP,DPP(NCW),DPP(MCP)	0968
	1,TR(NCW),TR(MCP),(K,EN(K),BN(K),CN(K),DN(K),DPP(K),A(K,1),Z0(K,1)).	0969

```

2Z1(K,1),TR(K),K=1,LZ)
495  FORMAT(1H1,13H ENERGY CHECK,10X,4HRUN=14.5X,4HNMC=14.5X,5HTIME=1PE 0970
495  210.3,5X,6HE AMB=1PE10.3//5H NCW=14.5X,4HMCP=14.5X,9HDPP(NCW)=1PE12 0971
495  3.4,5X, 9HDPP(MCP)=1PE12.4,5X,8HTR(NCW)=1PE10.3,5X,8HTR(MCP)=1PE10 0972
495  4.3//5H ZONE,3X,2HDE,10X,4HSUME,6X,3HOKE,7X,5HSUMKE,5X,9HSUMTOTALE. 0973
495  511X,1HA,11X,2HZ0,10X,2HZ1,10X,2HTR//((15,1P5E12.4,3X,1P4E12.4)) 0974
B494  THETA(1)=646464646464 0975
B      THETA(2)=232323232323 0976
      DO 29 K=1,LZ 0977
      HZ(K)=DTAU(K,1)/1.5 0978
      DMM(K)=DTAU(K,1)/(R(K)-R(K-1)) 0979
      FZ(K)=4.28 E-08*(E(K)+P(K)*V(K)) 0980
      DZ(K)=TAU(K,1)/1.5 0981
      DP(K)=Q(K)/P(K) 0982
      FM(K)=T(K)/11606.5 0983
      HP(K)=FOS(K)*1.0E-07 0984
      HPP(K)=ABS(FIS(K)/FOS(K)) 0985
      GM(K)=1.0+(P(K)*V(K)/E(K)) 0986
      UR(K)=1.0/V(K) 0987
      IF(PART(K)-4.0) 29,28,28 0988
      DTH(K)=313131313131 0989
B28    CONTINUE 0990
29     SHVEL=U(J3)*(1.0+GM(J3))/2.0 0991
      PSHK=(2.0/(GM(J3)+1.0))*RH(Z(LZ))*(SHVEL**2) 0992
      ESHK=0.5*((2.0*SHVEL/(1.0+GM(J3)))**2) 0993
      TRSHK=T(J3)*ESHK/E(J3) 0994
      ETOE=(5.67E-05*(TRSHK**4)/(RHOZ(LZ)*SHVEL))+E(LZ) 0995
      TTOE=ETOE*T(LZ)/E(LZ) 0996
      POWSK=12.56*(R(J3+2)**2)*5.67E-05*(TRSHK**4)*FLM 0997
      WRITE OUTPUT TAPE 6,496,NR,NMC,TIME,SHVEL,PSHK,TRSHK,TTOE 0998
      PUNCH 496, NR,NMC,TIME,SHVEL,PSHK,TRSHK,TTOE 0999
496    FORMAT(2I4,1P5E12.4) 1000
80     IF(LZ-40) 30,30,81 1001
81     WRITE OUTPUT TAPE NTAPE,45,NMC,LZ,ETOTAL,TIME,POWER,DT,NT1, 1002
81     1(K,R(K),U(K),P(K),DP(K),FM(K),UR(K),E(K),HP(K),HPP(K),DIVFA(K),T(K 1003
81     2),GM(K),PART(K),THETA(K),DZ(K),DTH(K),HZ(K),K=1,40) 1004
82     WRITE OUTPUT TAPE NTAPE,47, 1005
82     1(K,R(K),U(K),P(K),DP(K),FM(K),UR(K),E(K),HP(K),HPP(K),DIVFA(K),T(K 1006
82     2),GM(K),PART(K),THETA(K),DZ(K),DTH(K),HZ(K),K=41,LZ) 1007
83     GO TO 85 1008
30     WRITE OUTPUT TAPE NTAPE,45,NMC,LZ,ETOTAL,TIME,POWER,DT,NT1, 1009
30     1(K,R(K),U(K),P(K),DP(K),FM(K),UR(K),E(K),HP(K),HPP(K),DIVFA(K),T(K 1010
30     2),GM(K),PART(K),THETA(K),DZ(K),DTH(K),HZ(K),K=1,LZ) 1011
85     WRITE OUTPUT TAPE NTAPE,46,PARTT,RJ,P03,TEFF,LZR,FLEX,RX,P34,TCOL, 1012
85     2NCW,8N(LZ),DTMIN,P45,CWL(NCW,1),MCP,ON(LZ),SAVE1,P57,Q41,EMS 1013
      WRITE OUTPUT TAPE NTAPE,36,DPP(LZ),FBR,P71,Q71,NSZ,EAMB,RSHOCK,P47 1014
      1,Q47,NR 1015
      W(1,9)=RSHOCK 1016
      DT=SAVE1 1017
      IF(NMC-1) 403,400,400 1018
400    IF(NMC-10) 411,411,403 1019
      1020

```

403	CONTINUE	1021
C	USER TAPE PRINT OUT	1022
	WRITE OUTPUT TAPE 32,300,NR,NMC,TIME,LZ,P(99),T(99),RHOZ(99),POWER	1023
	2,P47,FBR,(K,R(K),U(K),P(K),UR(K),T(K),FOS(K),FIS(K),DMM(K),Q(K),	1024
	3FZ(K),E(K),HPPP(K),K=1,LZ)	1025
300	FORMAT(1H1,2I4,1PE12.3,15,1P6E12.3/(14,1P12E10.3))	1026
	WRITE OUTPUT TAPE 42,437,NR,NMC,TIME,T(1),TCOL,TEFF,ETOTAL,PARTT,	1027
	1BN(LZ),DN(LZ),ESYSM,EAMB,FLEX,Q41,Q47,Q71,P03,P34,P45,P57,P71,P47,	1028
	2FBR,RSHOCK	1029
437	FORMAT(1H,2I4,1P10E11.3/1P12E11.4///)	1030
410	IF(NMC) 500,420,411	1031
411	IF(TIME-6.82E-05) 500,412,412	1032
412	NSIX=NSIX+1	1033
413	IF(NSIX-3) 500,420,500	1034
420	NSIX=0	1035
421	CALL SIXDPO	1036
500	RETURN	1037
	END	1038
*	FORTRAN	1039
CFISIXD		1040
	SUBROUTINE SIXDPO	1041
C	STANDARD DIMENSION AND COMMON STATEMENTS AS IN MAIN PROGRAM	1042
	FLAG=1.0E+31	1043
	SOUNDS=SQRTF(1.4*P(99)/RHOZ(99))	1044
	DO 10 K=1,LZ	1045
	BN(K)=P(K)/P(99)	1046
	CN(K)=V(99)/V(K)	1047
	DN(K)=T(K)/T(99)	1048
	EN(K)=U(K)/SOUNDS	1049
C	AVERAGE ZONE RADIUS IN FEET	1050
10	OP(K)=(R(K)+R(K-1))/60.96	1051
	WRITE TAPE 31,NR,TIME,LZ,(OP(K),BN(K),CN(K),DN(K),EN(K),GM(K),	1052
	1K=1,LZ),FLAG	1053
	WRITE OUTPUT TAPE 41,50,NR,TIME,LZ,(OP(K),BN(K),CN(K),DN(K),EN(K),	1054
	1GM(K),K=1,LZ)	1055
50	FORMAT(1H1/I4,X,27H SIXDPL0T DIAGNOSTICS TIME=1PE10.3,5X,3HLZ=14	1056
50	2///(1P6E16.4))	1057
	KZ6=KZ6+1	1058
20	RETURN	1059
	END	1060
*	FORTRAN	1061
CF1PHOTOG	PHOTOGRAPHIC BRIGHTNESS ROUTINE	1062
	SUBROUTINE PHOTOG	1063
C	STANDARD DIMENSION AND COMMON STATEMENTS AS IN MAIN PROGRAM	1064
	IF(NMC) 32,30,32	1065
30	JTAPE=25	1066
31	GO TO 40	1067
32	IF(NMC-3) 33,33,30	1068
33	JTAPE=6	1069
40	CONTINUE	1070
C	SOURCE FUNCTION EM(K) AND ABSORPTION COEFF BN(K)	1071

```

DO 5 K=1,LZ                                1072
BN(K)=(V(K)/((16.5*((1.293E-03*V(K))**1.15)/(((T(K)/11606.5)**8.0)+2.6E-12*V(K))
16.5*((1.293E-03*V(K))**1.15)/(((T(K)/11606.5)**8.0)+2.6E-12*V(K)) 1073
2+0.180*((1.293E-03*V(K))**1.91)/((T(K)/11606.5)**(3.5)) 1074
4+6.00E-05*((1.293E-03*V(K))**2.0)*((T(K)/11606.5)**0.59) 1075
5+1.00E-09*((1.293E-03*V(K))**2.0)*((T(K)/11606.5)**4.00))) 1076
6*(1.0-EXPF(-3.2E+04/T(K))) 1077
TEA=3.956E+04/T(K) 1079
IF(TEA-80.0) 1,1,2 1080
2 EM(K)=0.0 1081
3 GO TO 5 1082
1 EM(K)=1.0E+05/(EXPF(3.956E+04/T(K))-1.0) 1083
5 CONTINUE 1084
C OPTICAL DEPTHS 1085
DO 200 K=1,LZ 1086
DM(K)=0.0 1087
DZ(K)=0.0 1088
DP(K)=(R(K)+R(K-1))/2.0 1089
LS=K 1090
DO 100 L=LS,LZ 1091
300 IF(L-K) 320,310,320 1092
310 DZ(L)=SQRTF(R(L)**2-DP(K)**2) 1093
311 DM(L)=DZ(L) 1094
313 GO TO 100 1095
320 DZ(L)=SQRTF(R(L)**2-DP(K)**2)-DM(L-1) 1096
324 DM(L)=DM(L-1)+DZ(L) 1097
100 HZ(L)=EXPF(-BN(L)*DZ(L)/V(L)) 1098
C BRIGHTNESS INTEGRATION 1099
HP(LZ)=0.0 1100
LS=LZ-K+1 1101
DO 7 J=1,LS 1102
M=LZ-J 1103
7 HP(M)=HP(M+1)*HZ(M+1)+((1.0-HZ(M+1))*EM(M+1)) 1104
LS=K 1105
DO 6 J=LS,LZ 1106
6 HP(J)=HP(J-1)*HZ(J)+((1.0-HZ(J))*EM(J)) 1107
HPP(K)=HP(LZ) 1108
IF(K-3) 155,150,155 1109
150 HNORM=HPP(3) 1110
IF(NMC) 155,151,155 1111
151 SCALE=HPP(3)*10.0 1112
155 CONTINUE 1113
199 HPPP(K)=HPP(K)/SCALE 1114
200 HPP(K)=HPP(K)/HNORM 1115
210 WRITE OUTPUT TAPE JTape,201,NMC,TIME,(K,DP(K),HPPP(K),HPP(K),K=1, 1116
210 1LZ) 1117
201 FORMAT(1H1,6HPHOTO6,14,10X,5HTIME=1PE10.3//5H ZONE,3X,6HMEAN R,4X, 1118
201 25HABS B,5X,5HREL B//((16,1P3E10.3)) 1119
280 RETURN 1120
END 1121

```

•	FORTTRAN	1123
	CFIDIAG	1124
	SUBROUTINE DIAGNS	1125
C	STANDARD DIMENSION AND COMMON STATEMENTS AS IN MAIN PROGRAM	1126
35	FORMAT(1H1,4HNMC=14.5X,4HNTI=14.5X,4HKZ2=15.5X,5HZONE=14.5X,4HRUN=	1127
	214/)	1128
	M=KZ5	1129
	IF(KZ2) 5,10,15	1130
5	WRITE OUTPUT TAPE 6,6,KZ2	1131
6	FORMAT(1H1,21HDIAG CALLED FROM MAINIS)	1132
	GO TO 20	1133
10	WRITE OUTPUT TAPE 6,11,KZ2	1134
11	FORMAT(1H1,22HDIAG CALLED FROM CGSP015)	1135
	GO TO 20	1136
15	WRITE OUTPUT TAPE 6,16,KZ2	1137
16	FORMAT(1H1,22HDIAG CALLED FROM HYDRO15)	1138
20	WRITE OUTPUT TAPE 6,21,NMC,NTI,LZ,LZR,MCP,MCL,TIME,DT,CS,CR,BR,RS,	1139
20	1(K,V(K),VR(K),E(K),ER(K),RESQUE(K),PA(K),DIVFA(K),DIVFR(K),K=1,LZ)	1140
21	FORMAT(1H ,4HNMC=14,2X,4HNTI=14,2X,3HLZ=14,2X,4HLZR=14,2X,4HMCP=14	1141
21	1,2X,4HMCL=14/6H TIME=1PE12.4,2X,3HDT=1PE12.4,2X,3HCS=OPF5.2,2X,	1142
21	23HCR=OPF5.2,2X,3HBR=OPF5.2,2X,3HRS=OPF5.2//3H K,6X,1HV,13X,2HVR,	1143
21	312X,1HE,13X,2HER,12X,6HRESQUE,8X,2HPA,12X,5HDIVFA,9X,5HDIVFR//	1144
21	4(14,1P8E14.7))	1145
22	WRITE OUTPUT TAPE 6,23,NMC,NTI,DTMIN,YIELD,SCALE,TFLUX,FBR,TIMEW,	1146
22	1(K,T(K),DTM(K),DET(K),DPT(K),BN(K),CN(K),DN(K),EN(K),K=1,LZ)	1147
23	FORMAT(1H1,4HNMC=14,2X,4HNTI=14,2X,6HDTMIN=1PE12.4,2X,6HYIELD=1PE1	1148
23	12.4,2X,6HSCALE=1PE12.4,2X/7H TFLUX=1PE12.4,2X,4HFBR=1PE12.4,2X,6HT	1149
23	2IMEW=1PE12.4//3H K,6X,1HT,13X,3HDTM,11X,3HDET,11X,3HDPT,11X,2HBN,	1150
23	312X,2HCN,12X,2HDN,12X,2HEN//(14,1P8E14.7))	1151
	WRITE OUTPUT TAPE 6,35,NMC,NTI,KZ2,M,NR	1152
24	WRITE OUTPUT TAPE 6,25,(K,FOS(K),FIS(K),BB(K,1),BC(K,1),R(K),	1153
24	1Z0(K,1),A(K,1),ZI(K,1),K=1,LZ)	1154
25	FORMAT(1H /3H K,6X,2HF0,12X,2HF1,12X,2HBB,12X,2HBC,12X,1HR,13X,	1155
25	12HZ0,12X,1HA,13X,2HZ1/(14,1P8E14.7))	1156
	WRITE OUTPUT TAPE 6,35,NMC,NTI,KZ2,M,NR	1157
26	WRITE OUTPUT TAPE 6,27,(K,S(K,1),W(K,1),DTAU(K,1),R2(K), ZMAS(K),	1158
26	1TAU(K,1),CWL(K,1),TR(K),K=1,LZ)	1159
27	FORMAT(1H /3H K,6X,1HS,13X,1HW,13X,4HDTAU,10X,2HR2,12X,4HZMAS,10X	1160
27	1,3HTAU,11X,3HCWL,11X,2HTR/(14,1P8E14.7))	1161
	WRITE OUTPUT TAPE 6,35,NMC,NTI,KZ2,M,NR	1162
28	WRITE OUTPUT TAPE 6,29,(K,DMM(K),DM(K),DZ(K),DP(K),DPP(K),Q(K),	1163
28	1FO(K,2),FI(K,2),K=1,LZ)	1164
29	FORMAT(1H /3H K,6X,3HDM,11X,2HDM,12X,2HDZ,12X,2HDP,12X,3HOPP,11X	1165
29	1,1HQ,13X,5HFOTJZ,9X,5HFITJZ/(14,1P8E14.7))	1166
	WRITE OUTPUT TAPE 6,35,NMC,NTI,KZ2,M,NR	1167
30	WRITE OUTPUT TAPE 6,31,(K,FMM(K),FM(K),FZ(K),HZ(K),FP(K),HP(K),	1168
30	1HPP(K),HPPP(K),K=1,LZ)	1169
31	FORMAT(1H /3H K,6X,3HFMM,11X,2HFMM,12X,2HFZ,12X,2HHZ,12X,2HFP,12X,	1170
31	12HHP,12X,3HPPP,11X,4HHPPP/(14,1P8E14.7))	1171
	WRITE OUTPUT TAPE 6,35,NMC,NTI,KZ2,M,NR	1172
32	WRITE OUTPUT TAPE 6,33,TON2,TOO2,TIMES,Q47,Q71,FLIX,FLOX,FLEX,	1173

```

32 1RM,RX,RJ.(K,FO(K,3),DTR(K),RZ(K),P(K),DE(K),RR(K),RHOZ(K), U(K),      1174
32 2K=1.100)                                                                    1175
33  FORMAT(1H ,2X,5HTDN2=1PE12.4,2X,5HTD02=1PE12.4,2X,6HTIMES=1PE12.4,      1176
33 12X,4HQ47=1PE12.4,2X,4HQ71=1PE12.4,2X/6H FLIX=1PE12.4,2X,5HFLOX=1PE      1177
33 212.4,2X,5HFLEX=1PE12.4,2X,3HRM=1PE12.4,2X,3HRX=1PE12.4,2X,3HRJ=1PE      1178
33 312.4//3H K,6X,3HOTH,11X,3HOTR,11X,2HRZ,12X,1HP,13X,2HOE,12X,2HRR,      1179
33 412X,4HRHOZ,10X,2HU /([14.1P8E14.7])                                         1180
      RETURN                                                                    1181
      END                                                                        1182
*   FORTRAN                                                                    1183
CF1FLUX                                                                    1184
      SUBROUTINE FLUXS                                                            1185
C   STANDARD DIMENSION AND COMMON STATEMENTS AS IN MAIN PROGRAM              1186
500  LZMI=LZ-1                                                                    1187
      DO 530 N=1,NSZ                                                            1188
C   BOUNDARY CONDITION NO INWARD FLUX AT OUTER BOUNDARY                    1189
      FI(LZ,N)=0.0                                                              1190
510  DO 512 J=1,LZMI                                                            1191
511  K=LZ-J                                                                      1192
512  FI(K,N)=FI(K+1,N)*ZI(K+1,N)+BB(K,1)*(A(K+1,N))-2.0*S(K,N)*W(K+      1193
512  1,N)                                                                        1194
520  FO(1,N)=FI(1,N)*ZI(1,N)+BB(1,2)*(A(1,N))+2.0*S(1,N)*W(1,N)            1195
522  DO 525 K=2,LZ                                                            1196
525  FO(K,N)=FO(K-1,N)*(R2(K-1)/R2(K))*Z0(K,N)                                1197
525  2+BB(K,2)*(A(K,N))+2.0*S(K,N)*W(K,N)                                       1198
525  3+(1.0-(R2(K-1)/R2(K)))*FI(K,N)*ZI(K,N)                                    1199
530  CONTINUE                                                                    1200
549  DO 555 K=1,LZ                                                            1201
      FIS(K)=0.0                                                                1202
      FOS(K)=0.0                                                                1203
      DO 550 N=1,NSZ                                                            1204
      FIS(K)=FIS(K)+FI(K,N)                                                    1205
550  FOS(K)=FOS(K)+FO(K,N)                                                    1206
551  IF(K-1) 552,552,554                                                       1207
552  D1=0.0                                                                      1208
553  GO TO 555                                                                  1209
554  D1=1.0                                                                      1210
555  DIVFA(K)=(R2(K)/ZMAS(K))*(FOS(K)-FIS(K))                                   1211
555  1-D1*(R2(K-1)/ZMAS(K))*(FOS(K-1)-FIS(K-1))                               1212
541  FLOX=12.56*R2(LZ-3)*FOS(LZ-3)                                             1213
590  RETURN                                                                      1214
591  END                                                                        1215
*   FORTRAN                                                                    1217
CF1STE                                                                    1218
      SUBROUTINE STATE                                                            1219
C   STANDARD DIMENSION AND COMMON STATEMENTS AS IN MAIN PROGRAM              1220
C   STEFAN =2.514E-09 TO INCLUDE RADIATION ENERGY AND PRESSURE              1221
C   STEFAN =0.00 TO DELETE RADIATION ENERGY AND PRESSURE                   1222
      STEFAN=0.0                                                                1223
      STEFAN=0.0                                                                1224

```



```

100 DO 126 K=1,LZ 1225
101 ETA(K)=1.0/(1.293E-03* V(K)) 1226
102 TS(K)=TS(K)*1.0E-04 1227
103 XS(K)=1.0E+04*TS(K)/( ETA(K)**0.086) 1228
104 GNU(K)=LOGF(XS(K)/2000.0)/LOGF(1250.0) 1229
105 IF(XS(K)-2000.0) 106,106,108 1230
106 PART(K)=1.0 1231
107 GO TO 112 1232
108 IF(XS(K)-2.5E+06) 109,111,111 1233
109 PART(K)=1.0+15.4*( GNU(K)**3)*(4.0-3.0* GNU(K)) 1234
110 GO TO 112 1235
111 PART(K)=16.4 1236
112 P(K)= (2.881*(TS(K)/ V(K))* PART(K)+STEFAN*(TS(K)**4))*1.0E+10 1237
113 Y=0.0784/(2.881*TS(K)* PART(K)) 1238
114 UZ=1.0+(27.0*Y+3.0)/(5.0*Y+1.0)+861.0*(1.0-Y)*Y/(3000.0*(Y**2)+1.0 1239
114 1)+(2356.0*(1.0-Y)*Y)/(9.0E+04*(Y**2)+1.0)+( 41000.0*(1.0-Y)*Y)/ 1240
114 2(12.0E+06*(Y**2)+1.0)+(2.15E+05*(1.0-Y)*Y)/(1.5E+18*(Y**4)+1.0) 1241
115 UT=(24.0*(Y**2)+4.0E-10)/(4.*(Y**2)+1.E-10)-(0.0970*(Y**2)*(1.0-Y) 1242
115 1)/(2.0E-06+Y**3)+(4.18E-05*(Y**3)*(1.0-Y))/(1.14E-11+Y**6) 1243
116 UC=UZ-0.09*(UZ-UT)*LOGF( ETA(K)) 1244
117 E(K)= (0.03920*(UC-1.0)/Y+3.0*STEFAN*(TS(K)**4)* V(K))*1.0E+10 1245
126 TS(K)=TS(K)*1.0E+04 1246
TS(2)=TS(2)*1.0E-04 1247
TS(1)=TS(1)*1.0E-04 1248
P(1)=(0.538E+10*TS(1)**1.5)/V(1) 1249
E(1)=2.53E+10*(((V(1)**0.25)+10.0)/(3.0*V(1)**0.5+10.0))* 1250
1((V(1)**0.25)+0.13)*(TS(1)**1.5+.02722/V(1)**1.5) 1251
P(2)=36.18*TS(2)*1.0E+10*(920.0+TS(2)**2)/(V(2)*(TS(2)**2+1.08E+04 1252
1)) 1253
E(2)=((649.0+TS(2)**2)/(100.0+TS(2))) 1254
1*((82.7*TS(2)*1.0E+10)/(116.0/(V(2)**0.25)+TS(2)*(1.0+0.12/(V(2)** 1255
20.25)))) 1256
TS(1)=TS(1)*1.0E+04 1257
TS(2)=TS(2)*1.0E+04 1258
176 RETURN 1259
177 END 1260
* FORTRAN 1261
CF1HYDO 1262
SUBROUTINE HYDRO 1263
C STANDARD DIMENSION AND COMMON STATEMENTS AS IN MAIN PROGRAM 1264
KHR=0 1265
KRS=1 1266
KZ4=0 1267
C TEST FOR IMPROPER CONVERGENCE 1268
DO 195 K=1,LZ 1269
IF(DTM(K)) 192,195,191 1270
191 IF(T(K)-2.0E+05) 188,188,189 1271
188 IF(ABSF(DTM(K))-4.99*T(K)) 195,195,193 1272
189 IF(ABSF(DTM(K))-0.80*T(K)) 195,195,193 1273
192 IF(ABSF(DTM(K))-0.25*T(K)) 195,195,193 1274
1275

```

193	KZ2=193	1276
	RQX=RQX*0.2	1277
	RM=RQX*1.3	1278
	CALL DIAGNS	1279
194	GO TO 198	1280
195	CONTINUE	1281
198	IF(RQX) 199,199,200	1282
199	RQX=DTMIN	1283
	C RICHTMYER - VON NEUMANN HYDRODYNAMIC SCHEME	1284
	C ADVANCE VELOCITY - - CHOOSE TIME STEP	1285
200	DO 207 K=1,LZ	1286
201	W(K,3)=U(K)	1287
202	UR(K)=U(K)	1288
203	U(K)= U(K)-2.0*((RZ(K) *DT)/(ZMAS(K)+ZMAS(K+1)))*(P(K+1)+Q(K+1))	1289
204	1-P(K)-Q(K))	1290
206	IF(U(K)-1.0E+11) 207,210,210	1291
207	CONTINUE	1292
208	U(LZ)=0.0	1293
209	GO TO 217	1294
210	KZ2=210	1295
	CALL DIAGNS	1296
213	GO TO 52	1297
	C HYDRODYNAMIC TIME STEP - - COURANT CRITERION	1298
217	RM=RQX*1.3	1299
218	IF(RM-0.070*TIME) 222,222,219	1300
219	RM=0.070*TIME	1301
222	DO 227 K=1,LZ	1302
224	DTH(K)=DR(K)/(RS*SQRTF(P(K)/(V(K)*(RHOZ(K)**2))))	1303
	DTH(K)=DTH(K)*((RZ(K)/R(K))**2)	1304
	FQ(K,3)=DTH(K)	1305
225	IF(RM-DTH(K)) 227,226,226	1306
226	RM=DTH(K)	1307
	KZ4=K	1308
227	CONTINUE	1309
228	RJ=RM	1310
		1311
	C RADIATION LIMITED TIME STEP	1312
229	RX=RM	1313
230	DO 242 K=KRS,LZ	1314
	IF(K-1) 233,233,223	1315
223	IF(R(K)-FBR) 231,231,233	1316
231	AR=BR	1317
232	GO TO 234	1318
233	AR=BR*2.0	1319
234	CONTINUE	1320
235	DTR(K)=ABSF(AR*E(K)/DIVFA(K))	1321
238	IF(DTR(K)-DTMIN) 242,242,239	1322
239	IF(DTR(K)-RX) 240,240,242	1323
240	RX=DTR(K)	1324
241	KZ4=K	1325
242	CONTINUE	1326

243	RM=RX		1327
244	IF(RM-2.0*DT)	246,246,245	1328
245	RM=2.0*DT		1329
246	IF(RM-DTMIN)	247,248,248	1330
247	RM=DTMIN		1331
248	RQX=RM		1332
249	IF((TIME+RM)-TIMEW)	252,252,250	1333
250	IF(NMC-4)	252,252,251	1334
251	RM=TIMEW-TIME		1335
252	DO 255 L=1,LZM1		1336
253	UA(L)=(U(L)/2.0)+(UR(L)/2.0)+(U(L)*RM)/(2.0*DT)-(UR(L)*RM)/(2.*DT)		1337
254	UR(L)=(U(L)/2.0)+(UR(L)/2.0)-(U(L)*RM)/(2.0*DT)+(UR(L)*RM)/(2.*DT)		1338
255	U(L)=UA(L)		1339
256	DT=RM		1340
C	ADVANCE RADIUS ALL L		1341
260	DO 263 L=1,LZ		1342
	W(L,5)=R(L)		1343
261	R(L)=R(L)+DT*U(L)		1344
262	RR(L)=R(L)/RZ(L)		1345
263	R2(L)=R(L)**2		1346
	DO 269 K=2,LZ		1347
	IF((R(K)-R(K-1))-0.15)	264,264,269	1348
264	KHR=KHR+1		1349
	IF(KHR-3)	265,265,270	1350
265	KZ2=266		1351
266	CALL DIAGNS		1352
	DO 268 L=1,LZ		1353
	U(L)=W(L,3)		1354
	R(L)=W(L,5)		1355
268	CONTINUE		1356
	RQX=DT*0.2		1357
	GO TO 200		1358
269	CONTINUE		1359
C	ADVANCE SPECIFIC VOLUME		1360
270	V(1)=((R(1)**3)/(RZ(1)**3))/RHOZ(1)		1361
271	DO 277 K=2,LZ		1362
273	V(K)=((1.0/RHOZ(K))*(((R(K)/DR(1))**3)-((R(K-1)/DR(1))**3)))/		1363
274	1(((RZ(K)/DR(1))**3)-((RZ(K-1)/DR(1))**3))		1364
275	IF(V(K)-1.0E+20)	276,279,279	1365
276	IF(V(K))	279,279,277	1366
277	CONTINUE		1367
278	GO TO 283		1368
279	KZ2=279		1369
	CALL DIAGNS		1370
282	GO TO 52		1371
C	ADVANCE ARTIFICIAL VISCOSITY		1372
283	IF(NMC-NQS)	284,284,286	1373
284	VD=CS		1374
285	GO TO 287		1375
286	VD=CR		1376
287	DO 295 K=1,LZ		1377

	IF(V(K)-VR(K)) 293,2942,2942	1378
293	Q(K)=(VD*((ZMAS(K)/R(K)**2)**2)/(V(K)+VR(K)))*(((V(K)-VR(K))/DT)**	1379
	12)	1380
294	IF(Q(K)-1.0E+22) 2941,298,298	1381
2941	IF(Q(K)) 2942,295,295	1382
2942	Q(K)=0.0	1383
295	CONTINUE	1384
296	Q(LZ)=0.0	1385
297	RETURN	1386
298	KZ2=298	1387
	CALL DIAGNS	1388
52	WRITE OUTPUT TAPE 6,43,T(1)	1389
43	FORMAT(1H,15HEXIT FROM HYDRO,5X,5HT(1)=1PE13.6)	1390
	T(1)=0.000000	1391
1500	GO TO 297	1392
	END	1393
		1394
*	FORTRAN	1395
CFIC0EF		1396
	SUBROUTINE COEFF	1397
C	STANDARD DIMENSION AND COMMON STATEMENTS AS IN MAIN PROGRAM	1398
700	LZR=LZR	1399
C	SET FLUX DERIVATIVES NEAR OUTER BOUNDARY OF RADIATIVE REGION	1400
701	FP(LZR)=0.0	1401
702	HP(LZR)=0.0	1402
703	HPP(LZR)=0.0	1403
704	HPPP(LZR)=0.0	1404
705	HPP(LZR-1)=0.0	1405
706	HPPP(LZR-1)=0.0	1406
707	HPPP(LZR-2)=0.0	1407
	DO 769 J=1,LZR	1408
C	SET RIPPLE ZONE PARAMETERS	1409
	DO 514 N=1,NSZ	1410
	SAVE1=BB(J,N)	1411
	SAVE2=BB(J-1,N)	1412
	SAVE3=S(J,N)	1413
	SAVE4=S(J-1,N)	1414
	SAVE5=DTAU(J,N)	1415
	SAVE6=A(J,N)	1416
	SAVE7=W(J,N)	1417
	SAVE8=ZI(J,N)	1418
	SAVE9=ZI(J-1,N)	1419
	SAVE10=ZO(J,N)	1420
	SAVE11=ZO(J+1,N)	1421
	SAVE12=BC(J,N)	1422
	SAVE14=T(J)	1423
	SAVE13=TS(J)	1424
	SAVE15=CWL(J,1)	1425
	SAVE16=ZO(J+2,N)	1426
	SAVE17=BB(J,2)	1427
	SAVE18=BB(J-1,2)	1428

```

311  BB(J,N)=((((R(J+1)-R(J))*TP(J)**4)+((R(J)-R(J-1))*T (J+1)**4))/ 1429
311  1(R(J+1)-R(J-1))))*5.67E-05 1430
    BB(J-1,N)=((((R(J)-R(J-1))*T(J-1)**4)+((R(J-1)-R(J-2))*TP(J)**4)) 1431
    1/(R(J)-R(J-2))))*5.67E-05 1432
    BB(J-1,2)=BB(J-1,1) 1433
    BB(J,2)=BB(J,1) 1434
312  BC(J,N)=5.67E-05*(TP(J)**4) 1435
    TS(J)=TP(J)/11606.5 1436
    T(J)=TP(J) 1437
    ETA(J)=1.293E-03*V(J) 1438
    ALPHA=9.0+EXPF(-TIME/1.0E-03*(ETA(J)**2)) 1439
    BETA=((6.0E-18*V(J)**0.5)*(TS(J)**0.1) 1440
    ZI(J,1)=EXPF(-1.5*(R(J)-R(J-1)) /((ETA(J)**1.5)/((TS(J)**ALPHA) 1441
300  2+BETA) +0.2*(ETA(J)**1.91)/(TS(J)**2.73) 1442
300  3+0.023*(ETA(J)**1.8)*(TS(J)**0.25)+1.0E-07*(ETA(J)**2.0)/ 1443
300  4((TS(J)**(-5.0))+4.0E-14*V(J)))) 1444
    ZI(J,1)=ZI(J,1)*0.99999998 1445
    ZI(J,2)=ZI(J,1) 1446
    HMFP=(ETA(J)**1.5)/((TS(J)**ALPHA)+BETA) 1447
    1+0.2*(ETA(J)**1.91)/(TS(J)**2.73) 1448
    2+0.023*(ETA(J)**1.8)*(TS(J)**0.25) 1449
    3+1.0E-07*(ETA(J)**2.0)*(TS(J)**5.00) 1450
    HMFF=9.3E-06*(ETA(J)**2.0)*(TS(J)**3.5) 1451
    IF(TS(J)-10.0) 301,298,298 1452
298  IF(HMFF-HMFP) 299,301,301 1453
299  HMFP=HMFF 1454
301  DTAU(J,1)=1.5*(R(J)-R(J-1))/HMFP 1455
302  A(J,N)=EXPF(-DTAU(J,N)) 1456
305  TS(J)=TP(J) 1457
506  S(J,N)=(BC(J,N)-BC(J+1,N))/(DTAU(J,N)+DTAU(J+1,N)) 1458
    S(J-1,N)=(BC(J-1,N)-BC(J,N))/(DTAU(J-1,N)+DTAU(J,N)) 1459
507  W(J,N)=1.0-A(J,N)-A(J,N)*DTAU(J,N) 1460
508  IF(W(J,N)-1.0E-04) 509,514,514 1461
509  W(J,N)=0.5*(DTAU(J,N)**2) 1462
514  CONTINUE 1463
    1464
C SET CUTOFF WAVELENGTHS 1465
540  I=J 1466
541  IF(T(I)-TDN2) 546,542,542 1467
    1468
C OPACITY DUE TO ATOMIC SPECIES 1469
542  CWL(I,1)= 700.0*EXPF(-0.36*(T(I)-11606.5)/11606.5) 1470
    IF(CWL(I,1)-275.0) 545,560,560 1471
545  CWL(I,1)=275.0 1472
    GO TO 560 1473
546  IF(T(I)-TD02) 551,547,547 1474
    1475
C OPACITY DUE TO N2 MOLECULE 1476
547  TCN2=5.0E-07*1.293E-03*V(I) 1477
    CWL(I,1)=1140.0*(((R(I)-R(I-1))/(V(I)*1.293E-03))**0.11) 1478
    1*(1.0-EXPF(-TIME/TCN2)) 1479

```

	IF(CWL(I,1)-1000.0) 550.560.560	1480
550	CWL(I,1)=1000.0	1481
	GO TO 560	1482
		1483
C	OPACITY DUE TO O2 MOLECULE	1484
551	TC=4250.0-271.0*LOGF(1.293E-03* V(I))	1485
	TCO2=3.0E-07*1.293E-03*V(I)	1486
553	IF(T(I)-TC)554.554.556	1487
554	CWL(I,1)=1500.0+TS(I)*(0.163+0.0745*LOGF(DR(I)*RHOZ(I)/1.293E-03))	1488
554	1*(1.0-EXP(-TIME/TCO2))	1489
555	GO TO 557	1490
556	TSB=TS(I)*(0.0647*LOGF(R(I)-R(I-1))-0.25-.109*LOGF(1.293E-03*V(I)))	1491
	CWL(I,1)=3500.0+TSB-(2000.0+TSB)*EXP(-TIME/TCO2)	1492
557	IF(CWL(I,1)-1500.0) 558.560.560	1493
558	CWL(I,1)=1500.0	1494
560	CONTINUE	1495
		1496
C	CALCULATE Z0 VALUES	1497
	Z0(I,1)=Z1(I,1)	1498
604	JSTR=J+2	1499
	KD=0	1500
605	DO 670 L=J,JSTR	1501
	TR(L)=T(L)	1502
	IF(T(L)-8.0E+04) 607.668.668	1503
607	KD=KD+1	1504
	IF(KD-1) 608.608.609	1505
608	MS=L-1	1506
609	IF(DTAU(L,1)-1.0) 610.668.668	1507
C	SELECT TR(L)= TEMPERATURE OF RADIATION TRAVERSING ZONE L	1508
610	LIM=L-1	1509
611	TAUSUM=0.0	1510
615	DO 630 NN=1,LIM	1511
616	M=L-NN	1512
617	TAUSUM=TAUSUM+DTAU(M,1)	1513
620	IF(TAUSUM-0.7) 630.627.627	1514
627	TR(L)=T(M)	1515
628	IF(M-2) 630.630.638	1516
630	CONTINUE	1517
	IF(T(L)-2500.0) 631.632.632	1518
631	TR(L)=TR(L-1)	1519
	GO TO 637	1520
632	EPTSUM=0.0	1521
	EPSUM=0.0	1522
	DO 635 I=3,LIM	1523
	EPTSUM=EPTSUM+T(I)*DTAU(I,1)	1524
	EPSUM=EPSUM+DTAU(I,1)	1525
	IF(T(I)-2500.0) 636.636.635	1526
635	CONTINUE	1527
636	TR(L)=EPTSUM/EPSUM	1528
637	M=2	1529
638	IZ=M+1	1530

639	DO 646	I=IZ,L	1531
640	IF(TR(L)*CWL(I,1)-2.0E+08)	641,641,644	1532
641	ZI(I,2)= EXPF((-3.41E-08*CWL(I,1)*TR(L)+2.5E-25*((CWL(I,1)*TR(L		1533
641	2))*3))*EXPF(-3.07E+13/((CWL(I,1)*TR(L))*1.8))		1534
642	GO TO 646		1535
644	ZI(I,2)=7.61E+22/((CWL(I,1)*TR(L))*3)		1536
646	CONTINUE		1537
	ZMAX=ZI(M+1,2)		1538
	ZO(L,1)=ZI(M+1,2)		1539
647	IF(L-M-1) 668,663,650		1540
C	CORRECTION FOR INTERMEDIATE ZONES		1541
650	IZ=M+2		1542
651	CWLTST=CWL(M+1,1)		1543
652	DO 660 NZ=IZ,L		1544
653	IF(CWL(NZ,1)-CWLTST) 654,654,657		1545
654	IF(NZ-L) 660,655,668		1546
655	ZO(L,1)=1.0		1547
656	GO TO 660		1548
657	ZO(L,1)=ZI(NZ,2)/ZMAX		1549
658	CWLTST=CWL(NZ,1)		1550
659	ZMAX=ZI(NZ,2)		1551
660	CONTINUE		1552
663	IF(ZO(L,1)-ZI(L,1)) 670,668,668		1553
668	ZO(L,1)=ZI(L,1)		1554
670	CONTINUE		1555
671	IF(DTAU(J,1)-1.0E-04) 672,674,674		1556
672	A(J,1)=DTAU(J,1)		1557
673	GO TO 675		1558
674	A(J,1)=1.0-A(J,1)		1559
675	IF(S(J,1)-1.69E+38) 8675,8675,677		1560
8675	IF((BB(J,1)*A(J+1,1)-2.0*S(J,1)*W(J+1,1))-BC(J+1,1)*A(J+1,1)*0.01)		1561
8675	I 677,680,680		1562
677	S(J,1)=0.0		1563
678	BB(J,1)=BC(J+1,1)		1564
679	BB(J,2)=BC(J,1)		1565
680	IF(S(J-1,1)-1.69E+38) 8680,8680,681		1566
8680	IF((BB(J-1,1)*A(J,1)-2.0*S(J-1,1)*W(J,1))-BC(J,1)*A(J,1)*0.01)		1567
8680	I 681,684,684		1568
681	S(J-1,1)=0.0		1569
682	BB(J-1,1)=BC(J,1)		1570
683	BB(J-1,2)=BC(J-1,1)		1571
684	IF(J-2) 900,900,916		1572
900	IF(BC(1,1)-BC(2,1)) 915,916,916		1573
915	BB(1,2)=BC(1,1)		1574
916	T(J)=SAVE14		1575
	CWL(J,1)=SAVE15		1576
C	CALCULATE TEMPORARY FLUXS		1577
831	JSTR=J+2		1578
832	IF(JSTR-LZR) 834,834,833		1579
833	JSTR=LZR		1580
834	DO 842 N=1,NSZ		1581

835	FIT(JSTR+1,N)=FI(JSTR+1,N)	1582
836	DO 838 L=1,JSTR	1583
837	K=JSTR-L+1	1584
838	FIT(K,N)=FIT(K+1,N)* ZI(K+1,N)+BB(K,1)*(A(K+1,N))-2.0* S(K,N)	1585
838	2* W(K+1,N)	1586
839	FOT(1,N)=FIT(1,N)* ZI(1,N)+BB(1,2)*(A(1,N))+2.0* S(1,N)	1587
839	2* W(1,N)	1588
840	DO 841 K=2,JSTR	1589
841	FOT(K,N)=FOT(K-1,N)*(R2(K-1)/R2(K))* Z0(K,N)	1590
841	2+BB(K,2)*(A(K,N))+2.0* S(K,N)* W(K,N)	1591
841	3+(1.0-(R2(K-1)/R2(K)))*FIT(K,N)* ZI(K,N)	1592
842	CONTINUE	1593
C	SPECTRAL SUMMATION	1594
726	FOTJP2=0.0	1595
727	FOTJP1=0.0	1596
728	FOTJZ=0.0	1597
729	FOTJM1=0.0	1598
730	FITJZ=0.0	1599
731	FITJM1=0.0	1600
732	FITJM2=0.0	1601
733	FITJM3=0.0	1602
734	DO 742 N=1,NSZ	1603
735	FOTJP2=FOTJP2 + FOT(J+2,N)	1604
736	FOTJP1=FOTJP1 + FOT(J+1,N)	1605
737	FOTJZ=FOTJZ + FOT(J,N)	1606
738	FOTJM1=FOTJM1 + FOT(J-1,N)	1607
739	FITJZ=FITJZ + FIT(J,N)	1608
740	FITJM1=FITJM1 + FIT(J-1,N)	1609
741	FITJM2=FITJM2 + FIT(J-2,N)	1610
742	FITJM3=FITJM3 + FIT(J-3,N)	1611
	F0(J,2)=FOTJZ	1612
	FI(J,2)=FITJZ	1613
C	CALCULATE FLUX DERIVATIVES	1614
743	IF(J-LZR+1) 744,745,746	1615
744	FMM(J+2)=(FOTJP2 -FOS(J+2))/(TP(J)-T(J))	1616
745	FM(J+1)=(FOTJP1 -FOS(J+1))/(TP(J)-T(J))	1617
746	FZ(J)=(FOTJZ-FOS(J))/(TP(J)-T(J))	1618
747	HZ(J)=(FITJZ-FIS(J))/(TP(J)-T(J))	1619
748	IF(J-1) 755,755,749	1620
749	FP(J-1)=(FOTJM1 -FOS(J-1))/(TP(J)-T(J))	1621
750	HP(J-1)=(FITJM1-FIS(J-1))/(TP(J)-T(J))	1622
751	IF(J-2) 755,755,752	1623
752	HPP(J-2)=(FITJM2-FIS(J-2))/(TP(J)-T(J))	1624
753	IF(J-3) 755,755,754	1625
754	HPPP(J-3)=(FITJM3-FIS(J-3))/(TP(J)-T(J))	1626
C	RETURN RIPPLE ZONE PARAMETERS TO NORMAL VALUES	1627
755	DO 768 N=1,NSZ	1628
	BB(J,N)=SAVE1	1629
	BB(J-1,N)=SAVE2	1630
	S(J,N)=SAVE3	1631
	S(J-1,N)=SAVE4	1632

	DTAU(J,N)=SAVE5	1633
	A(J,N)=SAVE6	1634
	W(J,N)=SAVE7	1635
	ZI(J,N)=SAVE8	1636
	ZI(J-1,N)=SAVE9	1637
	ZO(J,N)=SAVE10	1638
	ZO(J+1,N)=SAVE11	1639
	BC(J,N)=SAVE12	1640
	TS(J)=SAVE13	1641
	ZO(J+2,N)=SAVE16	1642
	BB(J,2)=SAVE17	1643
	BB(J-1,2)=SAVE18	1644
768	CONTINUE	1645
769	CONTINUE	1646
C	GENERALIZED COEFFICIENT ROUTINE DEC 6.1963	1647
770	DO 789 K=1,LZR	1648
771	IF(K-1) 772,772,775	1649
772	DMM(1)=0.0	1650
	D1=0.0	1651
773	DM(1)=0.0	1652
774	GO TO 780	1653
775	D1=1.0	1654
	IF(K-2) 777,776,778	1655
776	DMM(2)=0.0	1656
777	GO TO 779	1657
778	DMM(K)=(0.5*R2(K)/ZMAS(K))*FMM(K)	1658
778	1-D1*(0.5*R2(K-1)/ZMAS(K))*FM(K-1)	1659
779	DM(K)=(0.5*R2(K)/ZMAS(K))*FM(K)	1660
779	1-D1*(0.5*R2(K-1)/ZMAS(K))*(FZ(K-1)-HZ(K-1))	1661
780	DZ(K)=(0.5*R2(K)/ZMAS(K))*(FZ(K)-HZ(K))	1662
780	1-D1*(0.5*R2(K-1)/ZMAS(K))*(FP(K-1)-HP(K-1))	1663
780	2+(DET(K)/DT)+(DPT(K)/(2.*DT))*(V(K)-VR(K))	1664
781	DP(K)=(0.5*R2(K)/ZMAS(K))*(FP(K)-HP(K))	1665
781	1-D1*(0.5*R2(K-1)/ZMAS(K))*(-HPP(K))	1666
782	DPP(K)=(0.5*R2(K)/ZMAS(K))*(-HPP(K))	1667
782	1-D1*(0.5*R2(K-1)/ZMAS(K))*(-HPPP(K-1))	1668
789	CONTINUE	1669
790	DPP(LZR-1)=0.0	1670
791	DP(LZR)=0.0	1671
792	DPP(LZR)=0.0	1672
C	BLOCK 800 SOLUTION OF MATRIX	1673
800	CN(1)=DP(1)/DZ(1)	1674
801	DN(1)=DPP(1)/DZ(1)	1675
802	EN(1)=-RESDUE(1)/DZ(1)	1676
803	BN(2)=DZ(2)-DM(2)*CN(1)	1677
804	CN(2)=(DP(2)-DM(2)*DN(1))/BN(2)	1678
805	DN(2)=DPP(2)/BN(2)	1679
806	EN(2)=-RESDUE(2)+DM(2)*EN(1))/BN(2)	1680
807	DO 811 K=3,LZR	1681
808	BN(K)=(DZ(K)-DM(K)*CN(K-1)-DMM(K)*DN(K-2)+DMM(K)*CN(K-2)*CN(K-1))	1682
809	CN(K)=(DP(K)-DM(K)*DN(K-1)+DMM(K)*CN(K-2)*DN(K-1))/BN(K)	1683

```

810  DN(K)=DPP(K)/BN(K) 1684
811  EN(K)=-((RESDUE(K)+DM(K)*EN(K-1)-DMM(K)*CN(K-2)*EN(K-1)+DMM(K)*EN(K 1685
811  1-2))/BN(K) 1686
812  DN(LZR-1)=0.0 1687
813  BN(LZR)=DM(LZR)-DMM(LZR)*CN(LZR-2) 1688
814  CN(LZR)=(DZ(LZR)-DMM(LZR)*DN(LZR-2))/BN(LZR) 1689
815  DN(LZR)=0.0 1690
816  EN(LZR)=-((RESDUE(LZR)+DMM(LZR)*EN(LZR-2))/BN(LZR) 1691
819  RETURN 1692
820  END 1693
C 1694
VERSION C ENTRY ROUTINE 1694
STARTING MODEL IS READ IN FROM DATA CARDS GENERATED 1695
BY THE X-RAY DEPOSIT ROUTINE ON UNIVAC 1107 1696
* 1697
SUBROUTINE ENTRY 1698
C STANDARD DIMENSION AND COMMON STATEMENTS AS IN MAIN PROGRAM 1699
2 1700
D(1)=0.0 1700
TEE=3.0E+04 1701
READ INPUT TAPE 5, 9277,RUNID1,RUNID2,TR(NN1),TR(NN2),ENERGY,TIME, 1702
1FX,(K,R(K),DR(K),T(K),RHOZ(K),U(K),E(K),RUNID1,RUNID2,K=1,100) 1703
9277 FORMAT(2A6,1P5E13.3/(14,1P6E11.3,2A5)) 1704
LZ=100 1705
VD=CS 1706
WKT=ENERGY/4.18E+19 1707
TD02=7100.0*EXPF((0.43429*LOGF(RHOZ(99)/1.293E-03))/5.3) 1708
TON2=15000.0*EXPF((0.43429*LOGF(RHOZ(99)/1.293E-03))/4.8) 1709
1019 DO 1033 K=1,100 1710
1026 V(K)=1.0/RHOZ(K) 1711
VR(K)=V(K) 1712
1027 L=K 1713
TS(K)=T(K) 1714
RZ(L)=R(L)**2 1715
1029 RZ(L)=R(L) 1716
1030 RR(L)=1.0 1717
TR(K)=T(K) 1718
ZMAS(K)=(RHOZ(K)/3.0)*((RZ(L)**3)-(RZ(L-1)**3)) 1719
DU=U(L)-U(L-1) 1720
Q(K)=-((VD/(2.0*V(K)))*DU*ABSF(DU) 1721
Q(1)=-((VD/(2.0*V(1)))*U(1)*ABSF(U(1))) 1722
IF(Q(K)) 2233,1033,1033 1723
2233 Q(K)=0.0 1724
1033 CONTINUE 1725
ZMAS(1)=RHOZ(1)*(R(1)**3)/3.0 1726
1034 WRITE OUTPUT TAPE 6,1035,TON2,TD02,RN2,R02,WKT ,(K,R(K),RHOZ(K), 1727
1034 1V(K),T(K),U(K),Q(K),ZMAS(K),DR(K),DPP(K),DTAU(K,1),TAU(K,1),K=1, 1728
1100) 1729
1035 FORMAT(1H,10HINPUT DATA,10X,5HTON2=0PF7.1,10X,5HTD02=0PF6.1,5X, 1730
1035 14HRN2=1PE9.2,5X,4HR02=1PE9.2,5X,4HWKT=0PF7.2//4H K,2X,4HR(L) 1731
1,7X,7HRHOZ(K),4X,4HV(K),7X,4HT(K),7X,4HU(L),7X,4HQ(K),7X,7HZMAS 1732
1(K),4X,5HDR(K),7X,6HENG(K),5X,7HDTAU(K),4X,3HTAU//((14,1P11E11.4)) 1733
T(101)=T(100) 1734
1000 RETURN 1735
END 1736

```

References

- Blackman, V., Vibrational Relaxation in Oxygen and Nitrogen, Jour. Fluid Mech. 1, p. 61, 1956.
- Brode, H., B. Whittaker, private communications, 1965.
- Gilmore, F.R., Equilibrium Composition and Thermodynamic Properties of Air to 24,000°K, RAND Corp. RM-1543, 1955.
- Hillendahl, R.W., Approximation Techniques for Radiation-Hydrodynamics Computations, Lockheed Report 3-27-64-1, DASA 1522, 1964.
- Hilsenrath, J. and C.W. Beckett, Thermodynamic Properties of Argon-Free Air, N.B.S. Report 3991, 1955.

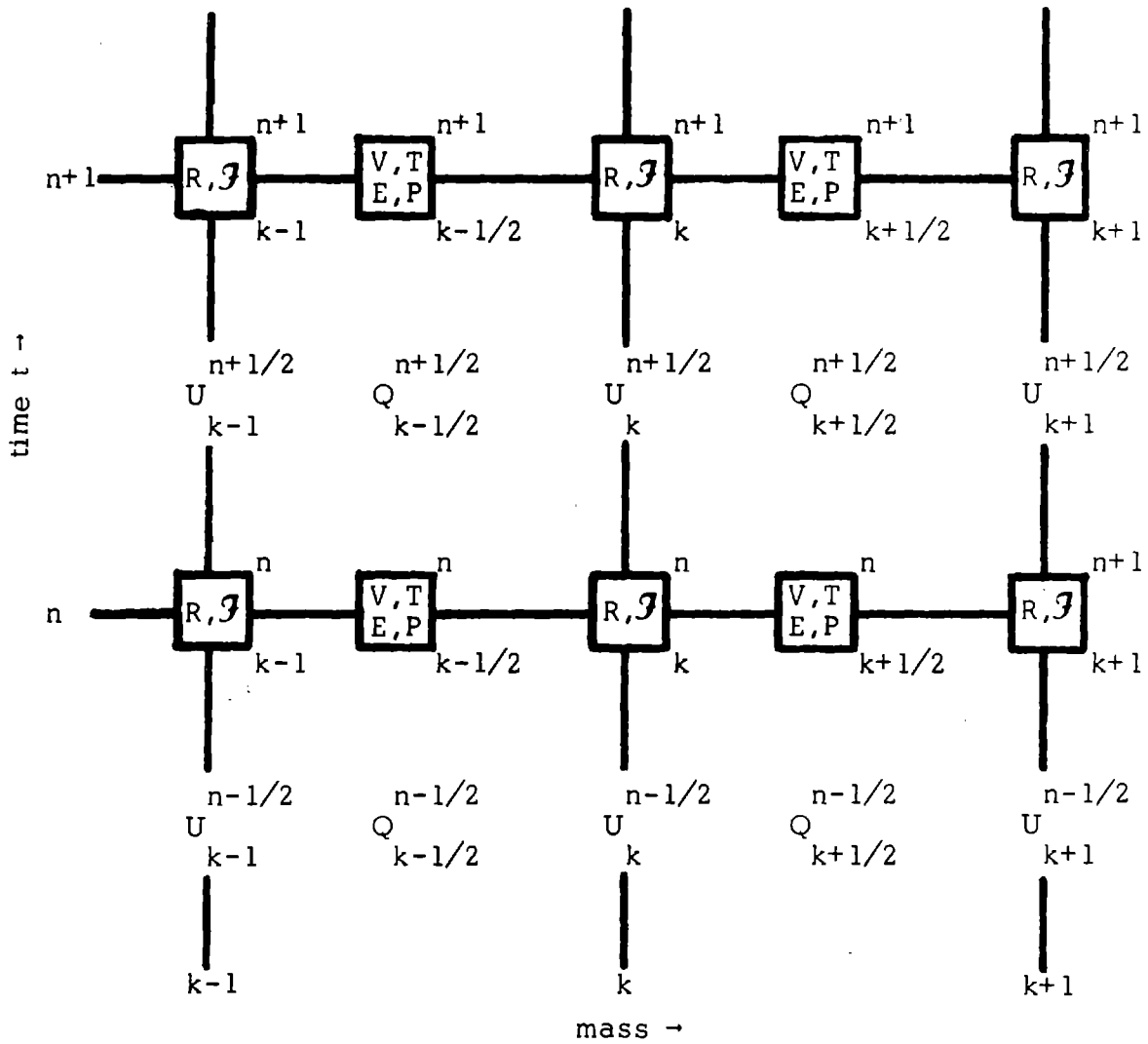


FIG. A-1 FINITE DIFFERENCE GRID

DISTRIBUTION LIST

No of Cys

Department of Defense:

Commander in Chief, Strategic Air Command, Offutt AFB, Nebraska 68113	1
Administrator, Defense Documentation Center, Cameron Station- Building 5, ATTN: Document Control, Alexandria, Virginia 22314	20
Director, Defense Atomic Support Agency, Washington, D. C. 20305	2
Director of Defense Research & Engineering, ATTN: Tech Library, Washington, D. C. 20301	1
Director, Defense Intelligence Agency, Washington, D. C. 20301	1

Department of the Army:

Commanding General, Army Munitions Command, Picatinny Arsenal, ATTN: Technical Library, Dover, New Jersey 07801	1
Commanding Officer, Army Nuclear Defense Laboratory, ATTN: AMXND-NT, Edgewood Arsenal, Maryland 21010	1
Commanding Officer, Harry Diamond Laboratories, Connecticut Avenue & Van Ness Street, N. W., ATTN: Technical Reference Branch, Washington, D. C. 20438	1
Commanding General, Army Missile Command, Redstone Arsenal, Alabama 35809	1
Commanding General, Army Electronics Command, ATTN: AMSEL/SMA, Fort Monmouth, New Jersey 07703	1
Commanding Officer, U. S. Army Ballistic Research Laboratories, ATTN: Mr. Baicy, Aberdeen Proving Ground, Maryland 21005	1
Commanding Officer, Army Combat Developments Command, Institute of Nuclear Studies, Fort Bliss, Texas 79916	1
Chief of Research and Development, Department of the Army, ATTN: Nuclear, Chemical-Biological Division, Washington, D. C. 20310	1
Commanding General, U. S. Army Materiel Command, ATTN: Nuclear Branch, Washington, D. C. 20315	1
Commanding Officer, Frankford Arsenal, Bridge and Tacony Streets, ATTN: Mr. A. Britten, Philadelphia, Pennsylvania 19137	1
Office of the Secretary of the Army, Director of Civil Defense, ATTN: Research Director, Washington, D. C. 20310	1

Department of the Navy:

Commanding Officer and Director, Naval Radiological Defense Laboratory, ATTN: Code 222A, Technical Information Division, San Francisco, California 94135	1
--	---

Commander, Naval Ordnance Laboratory-White Oak, 1
 ATTN: Dr. Rudlin, Silver Spring, Maryland 20910
 Commander, Naval Ships Systems Command, Department of the 1
 Navy, ATTN: Code 03541, Mr. L. Sieffert, Washington,
 D. C. 20360
 Commanding Officer and Director, Naval Applied Science 1
 Laboratory, Flushing and Washington Avenues,
 ATTN: Mr. W. Derksen, Brooklyn, New York 11251
 Chief of Naval Research, Department of the Navy, 1
 ATTN: Code 811, Washington, D. C. 20360
 Director, Naval Research Laboratory, ATTN: Code 2029, 1
 Washington, D. C. 20390
 Director, Special Projects Office, Department of the Navy, 1
 ATTN: SP-42, Washington, D. C. 20360
 Commanding Officer and Director, Naval Civil Engineering 1
 Laboratory, ATTN: Code L31, Port Hueneme, California
 93041

Department of the Air Force:

Commander, Air Force Weapons Laboratory, ATTN: 1
 WLL-Technical Library, Kirtland AFB, New Mexico
 87117
 Headquarters, USAF, TEMPO-BLDG-8, ATTN: AFTAC/SDP-R, 1
 Washington, D. C. 20333
 School of Aerospace Medicine, ATTN: Mr. E. Richey, 1
 Brooks AFB, Texas 78235
 Commander, Space and Missile Systems Organization, 1
 Air Force Unit Post Office, ATTN: Capt Dickison,
 Los Angeles, California 90045
 Director, Air University Library, Maxwell AFB, Alabama 1
 36112
 Commander, Air Force Cambridge Research Laboratories, 1
 ATTN: CROR and CRZC, L. G. Hanscom Field, Bedford,
 Massachusetts 07130
 Commander, Electronic Systems Division, L. G. Hanscom 1
 Field, Bedford, Massachusetts 01730

AEC:

Los Alamos Scientific Laboratory, P. O. Box 1663, 1
 Los Alamos, New Mexico 87544 ATTN: Document Control For-
 Technical Library
 University of California, Lawrence Radiation Laboratory, 1
 Technical Information Division, P. O. Box 808,
 Livermore, California 94550 ATTN: Dr. Gilbert
 Assistant General Manager for Military Application, 1
 U. S. Atomic Energy Commission, Washington, D. C. 20545
 ATTN: Library

Sandia Corporation, P. O. Box 5800, Albuquerque, New Mexico 87116 1
 Sandia Corporation, Livermore Laboratory, P. O. Box 969, Livermore, California 94550 1
 ATTN: Document Control For Technical Library

Civilian:

RAND Corporation, 1700 Main Street, Santa Monica, California 90406 ATTN: Library 1
 Aerospace Corporation, 1111 E. Mill Street, San Bernardino, California 92402 1
 Lockheed Missiles & Space Company, Division of Lockheed Aircraft Corporation, 3251 Hanover Street, Palo Alto, California 94304 ATTN: Dr. R. Meyerott 1
 Boeing Company, P. O. Box 3707, Seattle, Washington 98124 ATTN: Mr. Ed York 1
 IIT Research Institute, 10 West 35th Street, Chicago, Illinois 60616 ATTN: Dr. W. Christian 1
 General Electric Company, TEMPO-Center for Advanced Studies, 816 State Street, Santa Barbara, California 93101 ATTN: DASIAC, Mr. Warren Chan 1
 American Science & Engineering, Inc., 11 Carleton Street, Cambridge, Massachusetts 02138 ATTN: Dr. Jack Carpenter 1
 Kaman Corporation, Kaman Nuclear Division, Garden of the Gods Road, Colorado Springs, Colorado 80907 ATTN: Dr. F. Shelton 1
 EG&G, Inc., P. O. Box 227, Bedford, Massachusetts 01730 Technical Operations, Inc., South Avenue, Burlington, Massachusetts 01804 ATTN: Dr. I. Kofsky 1
 AVCO Everett Research Laboratory, 2385 Revere Beach Parkway, Everett, Massachusetts 02140 ATTN: Library 1
 AVCO Missiles, Space & Electronics Group Missile & Space Systems Division, 201 Lowell Street, Wilmington, Massachusetts 01887 1
 GCA Corporation, Burlington Road, Bedford, Massachusetts 01730 ATTN: Library 1
 Stanford Research Institute, 333 Ravenswood Avenue, Menlo Park, California 94025 ATTN: Document Custodian, FOR: Library 1
 General Dynamics/Convair, 5001 Kearny Villa Road, P. O. Box 1128, San Diego, California 92112 1
 Martin Company, Division of Martin-Marietta Corporation, Orlando Division, P. O. Box 5837, Orlando, Florida 32805 1
 Douglas Aircraft Company, Division of McDonnell-Douglas Corporation, 3000 Ocean Park Boulevard, Santa Monica, California 90405 1
 Systems, Science and Software, 3347 Industrial Court, Sorrento Valley Industrial Park, San Diego, California 92121 ATTN: Dr. B. Freeman 1

Mt. Auburn Research Associates, Inc., 12 Norfolk Street, 1
 Cambridge, Massachusetts 02139

Electro-Optical Systems, Inc., 300 North Halstead Street, 1
 Pasadena, California 91107

EG&G, Inc., Santa Barbara Division, P. O. Box 98, Goleta, 1
 California 93017

General Electric Company, ReEntry Space Systems Department, 1
 3198 Chestnut Street, Philadelphia, Pennsylvania 19101

Physics International, 2700 Merced Street, San Leandro, 1
 California 94577

Bell Telephone Laboratories, Inc., Whippany Road, Whippany, 1
 New Jersey 07981 ATTN: Mr. McAffey

GRC, Inc., 6300 Hollister Avenue, Goleta, California 93105 1

Union Carbide Corporation, Nuclear Division, Oak Ridge National 1
 Laboratory, P. O. Box X, Oak Ridge, Tennessee 37830

Applied Physics Laboratory, John Hopkins University, 1
 8621 Georgia Avenue, Silver Springs, Maryland 20910
 ATTN: Library

The Dikewood Corporation, 1009 Bradbury Drive, S. E., 1
 University Research Park, Albuquerque, New Mexico 87106

Mitre Corporation, Rt. 62 & Middlesex Turnpike, 1
 Bedford, Massachusetts

TRW Systems Group, 1 Space Park, Redondo Beach, California 1
 90278

URS Corporation, 1811 Trousdale Drive, Burlingame, 1
 California 94011

Heliodyne Corporation, 11689 Sorrento Valley Road, San Diego
 Division, San Diego, California 92121 ATTN: Dr. J. W. Bond, Jr. 1

2

1

1

DOCUMENT CONTROL DATA - R&D		
<i>(Security classification of title, body of abstract and indexing annotation must be entered when the overall report is classified)</i>		
1. ORIGINATING ACTIVITY (Corporate author) Lockheed Missiles & Space Company		2a. REPORT SECURITY CLASSIFICATION Unclassified 2b. GROUP
3. REPORT TITLE THERMAL RADIATION PHENOMENA VOL. 5 RADIATION HYDRODYNAMICS OF HIGH TEMPERATURE AIR		
4. DESCRIPTIVE NOTES (Type of report and inclusive dates) Final Report, 5th out of a series of 6		
5. AUTHOR(S) (Last name, first name, initial) Harold L. Brode; Richard W. Hillendahl; Rolf K. Landshoff		
6. REPORT DATE November, 1967	7a. TOTAL NO. OF PAGES 165	7b. NO. OF REFS 22
8a. CONTRACT OR GRANT NO. DA-49-146-XZ-198 b. PROJECT NO.	8a. ORIGINATOR'S REPORT NUMBER(S) DASA-1917-5	
c. d.	9b. OTHER REPORT NO(S) (Any other numbers that may be assigned this report) 3-27-67-1 Vol. 5	
10. AVAILABILITY/LIMITATION NOTICES This document has been approved for public release and sale; its distribution is unlimited.		
11. SUPPLEMENTARY NOTES		12. SPONSORING MILITARY ACTIVITY Defense Atomic Support Agency Washington, D.C. 20305
13. ABSTRACT This report introduces the reader to radiation hydrodynamics (RH) and discusses its application to fireballs in the atmosphere. After formulating the basic equations of RH, special attention is given to the radiative transfer problem. Several methods for solving the equations of transfer are touched upon but special emphasis is placed on the two stream method with a frequency averaging procedure, which is specifically designed for use with finite zone sizes. A version of the FIREBALL code which utilizes this approach is described. The physics of fireballs is illustrated with the example of a one kiloton detonation at sea level density and without interference from the ground. Some remarks are made on scaling procedures for extending the result to higher yields and altitudes. Estimates are made of the validity of the models. () ↑		

14. KEY WORDS	LINK A		LINK B		LINK C	
	ROLE	WT	ROLE	WT	ROLE	WT
Radiation hydrodynamics						
High temperature air						
Radiative transport						
Strong shocks						
Nuclear fireball						
Local thermodynamic equilibrium						

INSTRUCTIONS

1. **ORIGINATING ACTIVITY:** Enter the name and address of the contractor, subcontractor, grantee, Department of Defense activity or other organization (*corporate author*) issuing the report.

2a. **REPORT SECURITY CLASSIFICATION:** Enter the overall security classification of the report. Indicate whether "Restricted Data" is included. Marking is to be in accordance with appropriate security regulations.

2b. **GROUP:** Automatic downgrading is specified in DoD Directive 5200.10 and Armed Forces Industrial Manual. Enter the group number. Also, when applicable, show that optional markings have been used for Group 3 and Group 4 as authorized.

3. **REPORT TITLE:** Enter the complete report title in all capital letters. Titles in all cases should be unclassified. If a meaningful title cannot be selected without classification, show title classification in all capitals in parenthesis immediately following the title.

4. **DESCRIPTIVE NOTES:** If appropriate, enter the type of report, e.g., interim, progress, summary, annual, or final. Give the inclusive dates when a specific reporting period is covered.

5. **AUTHOR(S):** Enter the name(s) of author(s) as shown on or in the report. Enter last name, first name, middle initial. If military, show rank and branch of service. The name of the principal author is an absolute minimum requirement.

6. **REPORT DATE:** Enter the date of the report as day, month, year, or month, year. If more than one date appears on the report, use date of publication.

7a. **TOTAL NUMBER OF PAGES:** The total page count should follow normal pagination procedures, i.e., enter the number of pages containing information.

7b. **NUMBER OF REFERENCES:** Enter the total number of references cited in the report.

8a. **CONTRACT OR GRANT NUMBER:** If appropriate, enter the applicable number of the contract or grant under which the report was written.

8b, 8c, & 8d. **PROJECT NUMBER:** Enter the appropriate military department identification, such as project number, subproject number, system numbers, task number, etc.

9a. **ORIGINATOR'S REPORT NUMBER(S):** Enter the official report number by which the document will be identified and controlled by the originating activity. This number must be unique to this report.

9b. **OTHER REPORT NUMBER(S):** If the report has been assigned any other report numbers (*either by the originator or by the sponsor*), also enter this number(s).

10. **AVAILABILITY/LIMITATION NOTICES:** Enter any limitations on further dissemination of the report, other than those

imposed by security classification, using standard statements such as:

- (1) "Qualified requesters may obtain copies of this report from DDC."
- (2) "Foreign announcement and dissemination of this report by DDC is not authorized."
- (3) "U. S. Government agencies may obtain copies of this report directly from DDC. Other qualified DDC users shall request through _____."
- (4) "U. S. military agencies may obtain copies of this report directly from DDC. Other qualified users shall request through _____."
- (5) "All distribution of this report is controlled. Qualified DDC users shall request through _____."

If the report has been furnished to the Office of Technical Services, Department of Commerce, for sale to the public, indicate this fact and enter the price, if known.

11. **SUPPLEMENTARY NOTES:** Use for additional explanatory notes.

12. **SPONSORING MILITARY ACTIVITY:** Enter the name of the departmental project office or laboratory sponsoring (*paying for*) the research and development. Include address.

13. **ABSTRACT:** Enter an abstract giving a brief and factual summary of the document indicative of the report, even though it may also appear elsewhere in the body of the technical report. If additional space is required, a continuation sheet shall be attached.

It is highly desirable that the abstract of classified reports be unclassified. Each paragraph of the abstract shall end with an indication of the military security classification of the information in the paragraph, represented as (TS), (S), (C), or (U).

There is no limitation on the length of the abstract. However, the suggested length is from 150 to 225 words.

14. **KEY WORDS:** Key words are technically meaningful terms or short phrases that characterize a report and may be used as index entries for cataloging the report. Key words must be selected so that no security classification is required. Identifiers, such as equipment model designation, trade name, military project code name, geographic location, may be used as key words but will be followed by an indication of technical context. The assignment of links, rules, and weights is optional.